UNIVERSITÉ DU LUXEMBOURG

PhD-FSTM-2021-082
The Faculty of Sciences, Technology and Medicine

DISSERTATION

Defence held on 11/11/2021 in Luxembourg

to obtain the degree of

DOCTEUR DE L'UNIVERSITÉ DU LUXEMBOURG

EN SCIENCES DE L'INGÉNIEUR

by

Khachatur TORCHYAN
Born on 1 January 1990 in Yerevan, (Armenia)

ENHANCING PHOTOVOLTAIC HOSTING CAPACITY IN DISTRIBUTION GRID VIA GRID RECONFIGURATIONS, PV DROOPS AND BATTERY INVERTER CONTROL

Dissertation defence committee

Dr Juergen SACHAU, Dissertation supervisor
Professor, Dr.-Ing., Université du Luxembourg

Dr Thomas ENGEL, Chairman
Professor, Dr.-Rer. nat., Université du Luxembourg

Dr Jean-Régis HADJI-MINAGLOU, Vice Chairman
Professor, Dr.-Ing., Université du Luxembourg

Dr Stijn STEVENS
CTO, Dr.-Ir., Meteocontrol, Berlin

Dr Surena NESHVAD
Co-Founder, Dr.-Ing., Zorvan sarl, Luxembourg

Declaration of Authorship

I, Khachatur TORCHYAN, declare that this thesis titled, “Distribution Grid Hosting Capacity Enhancement via Grid Reconfiguration, Inverter Control and Battery Energy Storage Integration” and the work presented in it are my own. I confirm that:

- This work was done wholly or mainly while in candidature for a research degree at this University.
- Where any part of this thesis has previously been submitted for a degree or any other qualification at this University or any other institution, this has been clearly stated.
- Where I have consulted the published work of others, this is always clearly attributed.
- Where I have quoted from the work of others, the source is always given. With the exception of such quotations, this thesis is entirely my own work.
- I have acknowledged all main sources of help.
- Where the thesis is based on work done by myself jointly with others, I have made clear exactly what was done by others and what I have contributed myself.

Signed:

_____

Date:

_____

Abstract

The EU 2030 climate and energy framework has set a mandatory goal to achieve a renewable energy share in the final energy demand of 32% by 2030. Moreover, in the final National Energy and Climate Plan (NECP) Luxembourg has defined its renewable generation share goal at 25% by 2030. Between 2018 and 2019, three times more photovoltaic (PV) panels were installed than in the previous years. To achieve the NECP target and to ensure further smooth integration of PV systems, the PV hosting capacity (HC) of the grid should be enhanced.

This thesis discusses the common issues and current developments of HC enhancement and presents three HC enhancement techniques: grid reconfiguration and grid-code modification, extended current droop control and transformer loading control.

First, the thesis analyzes the potential of grid reconfiguration in HC enhancement. For the analysis the grid configurations are divided into meshed and radial subsets. The grid reconfiguration analysis and HC calculation are done using pandapower and NetworkX library. The cross-influence and the location of DG are considered while determining the HC of the grid. The analysis shows that proper grid configuration selection is important as it can substantially increase the HC and decrease the average loading in the lines.

Second, the impact of extended current droops on HC enhancement is investigated. In the designed extended current droops ($I_d(V), I_q(V)$), extra reactive power reserve is made available by changing the droop gain of the reactive current droop when the overvoltage is not cleared by the existing reactive power reserve. The simulations proved that the extended current droops are a viable grid reinforcement strategy which can not only regulate the voltage at the point of common coupling (PCC), but also relax the transformer loading and improve overall voltage and frequency stability. Additionally, oversizing of the inverter increases the reactive power reserve, which in turn lowers the voltage profile and decreases the amount of curtailed active power.

Finally, two novel communication-less transformer overloading protection strategies based on a battery energy storage (BES): transformer protection droops (TPD) and direct loading control (DLC), are designed and compared. Both strategies force the PV inverters to curtail their active power output without relying on communication. The strategies have been tested on detailed models, where the total installed PV power varies between 0.9 to 2 times the

transformer rating. The static and dynamic performance of the DLC is superior to the TPD control strategy. DLC is a robust control strategy. It can reduce the transformer loading by 41%, compared to the grid configuration without BES and bring the system to the steady-state within 700ms in the worst-case scenario. It also ensures to keep the system voltages within safe operational limits. It can be used as a backup active power curtailment solution in the cases of communication failure in centralized control.

Acknowledgements

I would like to thank my supervisor *Prof. Juergen Sachau*, whose advices, open-mindedness and constructive criticism guided me through this research work. Besides his professional support, I would like to thank him for being such a patient and kind person. It has been a great pleasure working with him.

Many thanks are due to my thesis supervision committee, *Prof. Jean-Regis Hadji-Minaglou* and *Dr. Stijn Stevens* for the valuable remarks and comments provided during these years. Their expertise and knowledge have been of importance for accomplishing the results shown in this thesis.

I would like to thank my colleagues *Dr. Surena Neshvad* for being my mentor during the first year of PhD, *Dr. Patrick Kobou Ngani* for his readiness to help and to discuss my work, *Dr. Sasan Rafii-Tabrizi* and *Dr. Steffen Betchel* for their friendly cooperation and discussions.

A particular mention goes to my friends *Valentino*, my chess companion, and *Seif*, my housemate and a friend who has always been supportive, with whom I have enjoyed my lunch breaks and most of my free time in Luxembourg.

Also, I would like to express my immense gratitude to my mother *Nelli*, my father *Alexander*, my sisters *Tamara* and *Irina* and my late uncle *Albert* whose encouragement and support throughout my life made it all possible. Finally, I would like to separately mention my beloved wife *Piruza*, who joined me here in Luxembourg, helped and supported me during my PhD journey.

Khachatur Torchyan
Luxembourg, November 2021

Contents

Declaration of Authorship iii

Abstract v

Acknowledgements vii

1 Introduction 1
- 1.1 Motivation . . . 1
- 1.2 Thesis Objectives and Scope of the Work . . . 3
- 1.3 Outline of the Thesis . . . 5

2 State of the Art 7
- 2.1 Hosting Capacity . . . 7
  - 2.1.1 Limiting indices . . . 7
    - Overvoltage . . . 8
    - Overloading . . . 9
    - Power quality and Protection . . . 10
  - 2.1.2 HC calculation techniques . . . 11
  - 2.1.3 HC enhancement techniques . . . 11
    - Reactive power control . . . 12
    - Active power control . . . 12
    - Energy storage . . . 13
    - Network reconfiguration . . . 14
    - OLTC control and harmonic mitigation . . . 14
- 2.2 Conclusion . . . 15

3 Modeling and control 17
- 3.1 Modeling of the grid . . . 17
  - 3.1.1 Static modeling . . . 18
  - 3.1.2 Dynamic modeling . . . 19
- 3.2 Modeling and control of the PV plant . . . 19
  - 3.2.1 PV plant . . . 20
  - 3.2.2 Photovoltaic modules . . . 20

3.2.3 DC-DC Converter and MPPT 21
3.2.4 DC-AC Grid-Tied Converter and Control 22

4 Grid Reconfiguration Analysis 25
4.1 Introduction 25
4.2 Subset Sorting and Hosting Capacity Calculation 26
4.3 Representative System Case Study 29
4.3.1 Test Network 29
4.3.2 Assumptions 30
4.3.3 Limiting indices 31
4.3.4 Case scenarios 31
Base case 31
Current grid code case 31
Improved grid code case 31
4.4 Results 32
4.5 Conclusion 40

5 Extended Current Droop Control of PV Plants 43
5.1 Droop control 43
5.2 Extended current droops 44
5.3 Test grid structure and simulation setup 46
5.4 Simulation results 48
5.5 Conclusion 50

6 Overloading Control of Substation Transformer 57
6.1 Transformer overloading protection 57
6.1.1 Transformer protection droops 58
6.1.2 Direct loading control 59
6.2 Test grid structure and simulation setup 59
6.3 Simulation results discussion 61
6.3.1 Static analysis 61
Full load case 62
Partial load case 1 62
Partial load case 2 63
No load case 69
6.3.2 Dynamic analysis 74
6.4 Conclusions 78

7 Conclusion **81**
7.1 Summary 81
7.2 Outlook 83

Bibliography **85**

List of Figures

1.1 PV power evolution in Luxembourg since 2010 2
1.2 Overview of the thesis structure 6

3.1 Base test grid structure. 18
3.2 Typical PV plant consisting of two converters and intermediate DC link. 20
3.3 I-V curve of the SunPower SPR-305E-WHT-D at a constant cell temperature of 25 ℃. 21
3.4 I-V curve of the SunPower SPR-305E-WHT-D module at a constant sun irradiance of $1KW/m^2$. 22
3.5 Schematics of the DC-DC converter including the PV array and boost converter topology. 22
3.6 Control diagram of the DC-AC converter. 24

4.1 Subset sorting overview 27
4.2 HC calculation algorithm 28
4.3 Test grid structure 30
4.4 Case studies 32
4.5 HC for each configuration of the meshed subset 33
4.6 HC for each configuration of the radial subset 34
4.7 Sorted HC distribution for the meshed subset 35
4.8 Sorted HC distribution for the radial subset 35
4.9 Transformer Tr1 loading for the meshed subset 37
4.10 Transformer Tr1 loading for the radial subset 38
4.11 Transformer Tr2 loading for the meshed subset 38
4.12 Transformer Tr2 loading for the radial subset 38
4.13 Line loading for the meshed subset 39
4.14 Line loading for the radial subset 39
4.15 Reconfiguration degree of freedom for the meshed subset . . . 39
4.16 Reconfiguration degree of freedom for the radial subset 40

5.1 Reactive power capability requirement for PV inverters: a - VDE-AR 4110:2018, b - proposed for normal operation, c - proposed for contingencies 44
5.2 Extended reactive and active current droops 46
5.3 Test grid model with only one transformer at reduced nominal power 48
5.4 Voltages at the PV PCC and transformer secondary 51
5.5 Active power outputs of PVs 52
5.6 Reactive power outputs of PVs 53
5.7 Active power at the transformer secondary 54
5.8 Reactive power at the transformer secondary 54
5.9 Transformer loading 54
5.10 Frequency at the PV PCCs and transformer secondary 55

6.1 DLC control structure 59
6.2 Test grid model 60
6.3 Transformer loading and power flow at full load 63
6.4 Transformer loading and power flow at partial load1 64
6.5 Transformer loading and power flow at partial load2 65
6.6 The reactive power output of BES at partial load2 66
6.7 The voltages at the PV plants and transformer secondary at partial load2 67
6.8 The active power outputs of PV plants at partial load2 68
6.9 The reactive power outputs of PV plants at partial load2 69
6.10 Transformer loading and power flow at no load 70
6.11 The reactive power output of BES at no load 71
6.12 The voltages at PV PCCs at no load 72
6.13 The active power outputs of PV plants at no load 73
6.14 The reactive power outputs of PV plants at no load 74
6.15 The dynamic response of the system to the load change without BES 75
6.16 The dynamic response of the system to the load change with TPD 77
6.17 The dynamic response of the system to the load change with DLC 79
6.18 Comparison of TPD and DLC dynamic responses 80

List of Tables

3.1 SunPower SPR-305E-WHT-D module data 21

4.1 Grid subset analysis summary 33
4.2 Sorted radial group switch configurations and HC for the third case 34
4.3 Sorted meshed group switch configurations and HC for the third case 35

5.1 Tie-switch combination 47
5.2 Load and PV data 47

6.1 Tie-switch configuration 60
6.2 Load and generator data 61
6.3 Loading scenarios 61

List of Abbreviations

AC	Alternating Current
ADN	Active Distribution Network
APC	Active Power Curtailment
BES	Battery Energy Storage
CIGRE	Conseil international des grands réseaux électriques
DC	Direct Current
DG	Distributed Generation
DLC	Direct Loading Control
DSO	Distribution System Operator
EC	European Commission
EU	European Union
FACTS	Flexible Alternating Current Transmission System
FNR	Fonds National de la Recherche
GHG	Greenhouse Gas
HC	Hosting Capacity
HV	High Voltage
IDCL	Intermediate DC Link
LV	Low Voltage
MPPT	Maximum Power Point Tracker
MV	Medium Voltage
OLTC	On-Load Tap Changer
PV	Photovoltaic
PCC	Point of Common Coupling
PLL	Phase Locked Loop
PVFEC	PV Front-End Converter
RES	Renewable Energy Sources
SSSC	Static Synchronous Series Compensator
STATCOM	Static Synchronous Compensator
SVC	Static VAR Compensator
TPD	Transformer Protection Droops
VDE	Verband der Elektrotechnik, Elektronik und Informationstechnik
VSI	Voltage Source Inverter

Chapter 1

Introduction

This chapter presents the motivation behind this thesis and lists the objectives of the work. The scope and structure of the thesis are also presented in this chapter.

1.1 Motivation

Climate change mitigation is undeniably one of humanity's most pressing problems today. To avert global warming in a sustainable manner, a comprehensive reduction in greenhouse gas emissions (GHG) is needed. In 2017, 30% of the European Union's (EU) total GHG emissions were caused by the energy supply sector [1]. Hence, reorganization of the electrical power system from conventional, fossil fuel-based energy generation towards renewable energy generation can help to reduce GHG emissions significantly. To accelerate the reorganization process, in October 2014, the European Council (EC) agreed on the 2030 climate and energy framework for the EU, setting a mandatory goal to achieve a renewable energy share in the final energy demand of at least 27% by 2030 [2]. Later in September 2020, this goal was revised and increased to 32% by 2030 [3]. In the final National Energy and Climate Plan (NECP) Luxembourg has defined its goal for the renewables share at 25% by 2030 [4]. The relatively high feed-in prices and decreasing system costs for photovoltaic (PV) power generation ([5], [6]) resulted in increased installation rates over the last decade (Figure 1.1). In 2019, the total installed solar power capacity in Luxembourg reached 160MW. Between 2018 and 2019, three times more photovoltaic panels were installed than in previous years. In 2019, a total of 762 photovoltaic installations were connected to the grid.

A notable feature of PV installations is the voltage level of their point of common coupling (PCC). Even though the majority of the PV systems in

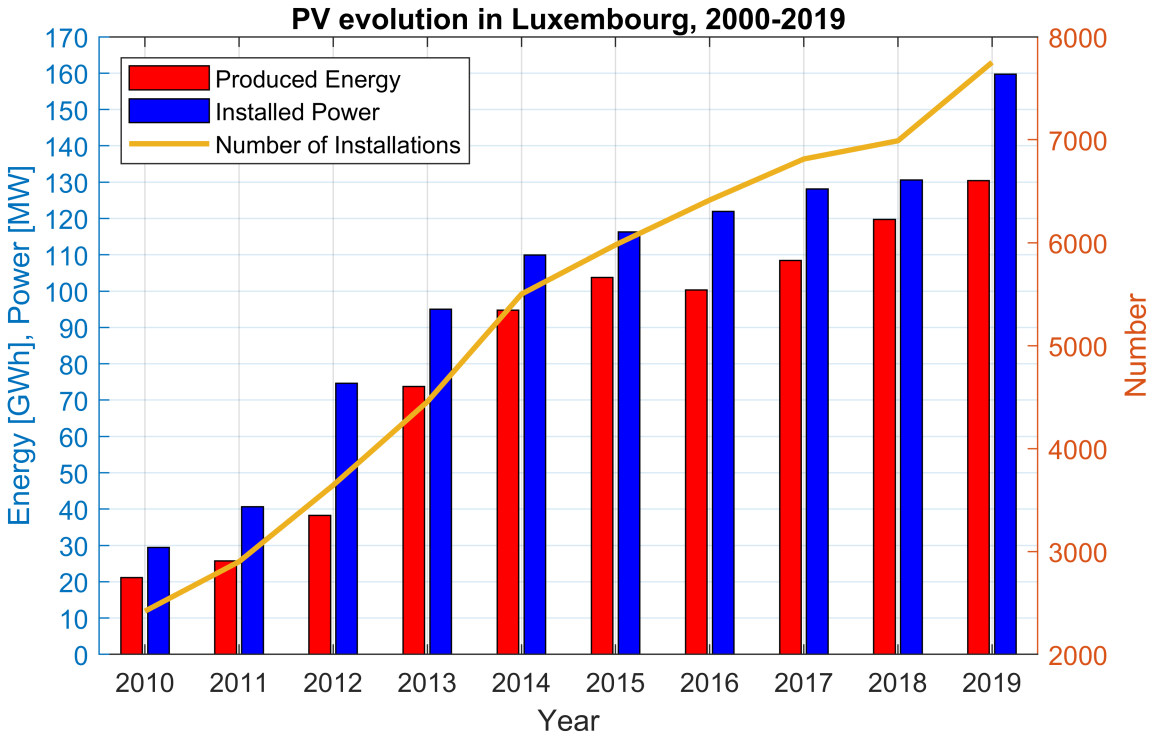

FIGURE 1.1: PV power evolution in Luxembourg since 2010

Luxembourg are directly connected to the low voltage (LV) level, the medium voltage (MV) connections are gaining momentum. Since 2018, the Ministry of Energy and Regional Planning decided to launch calls for tenders for the construction and operation of new large-scale photovoltaic electricity production plants: 14 MW in 2018, 30 MW in 2019, 40 MW planned for 2020 [7]. Thus, a transformation of the power system is on the way.

This transformation process presents new challenges for the distribution system operator (DSO), who, according to the grid codes, is responsible to provide a certain quality of electricity supply to its customers. Reverse power flows towards the higher voltage levels, during high PV peaks and low loads, lead to voltage profile rise along the MV feeders as well as possible temporary equipment overloading, which can lead to a violation of the technical constraints. The basic challenge regarding the grid integration of renewable energy sources can be synthesized as follows:

- How to keep acceptable voltage levels for all consumers connected to the power systems?
- How to protect the system elements from overloading?

Unlike the system frequency, which is the same throughout the grid, voltages at different nodes of the grid are different and form a voltage profile, which is related to the local generation and demand of reactive power at

a certain time. Reactive power flow can cause significant voltage changes across the system, which makes necessary to maintain the reactive power balance between the generation units and the demand points on a zonal basis. As the reactive power flow causes additional losses in the lines, and is not easy to transfer over long distances, it has to be generated as near to the load as it is possible.

According to the grid codes and regulations, the DSOs are requested to increase the hosting capacity (HC) of the connection point on their own cost or at the cost of the energy provider, in order to accommodate new PV connections. Usually, the most popular choice of HC improvement are the traditional measures, such as installation of new transformers and cablings. The main disadvantages of this approach are the cost intensiveness and difficulty to predict in advance the further development of PV connections. Based on the grid development plan of Germany, published in 2012, the necessary grid reinforcement costs for further renewable energy sources (RES) deployment in the German grid approximate to 27.5 bln. EUR until 2030 [8]. Based on their findings, 41.5% of the total costs are linked to grid reinforcement measures at LV and MV levels, where most of the total PV capacity is currently installed.

Innovative grid planning and operation strategies are needed to keep the total extent of grid reinforcement steps as minimal as possible. For example, the PV plants and battery energy storages (BES) can provide ancillary services, such as local voltage support, by using the control capabilities of their inverters. These additional functionalities can help to reduce the total costs of PV grid integration in the near future by increasing local hosting capability for additional generation capacity.

This thesis leads to the discussion of, whether grid-reconfiguration and local, communication-less voltage control strategies, implemented via PV inverters and BES are a technically effective alternative to enhance the hosting capacity of distribution grids for additional PV installations.

1.2 Thesis Objectives and Scope of the Work

In the previous section, the necessity for alternative technical solutions to traditional grid reinforcement measures is supported with the background of steadily increasing PV grid integration costs. The overall research goal of this thesis is derived out of this general need and summarized below:

Without involving additional communication technologies, the scope of technical solutions can be narrowed down to local voltage control strategies, provided by PV inverters and battery storage systems. The investigations are carried out for a three-phase balanced MV grid under the consideration of the current regulatory framework conditions in Germany [9]

The PV plants considered in this thesis are connected over transformers to the distribution grid at MV level. The work includes design of recommendations for DSOs for grid planning, local voltage control and infrastructure protection strategy for PV hosting capacity increase. The main aim of the work is to design a control system which will increase the HC of the grid and will ensure the steady-state and transient voltage stability of the grid and enhance the grid voltage profile, by controlling the PV plants and BES.

As the load is always varying, the impedance of the system is changing continuously. Thus, to fulfill the requirements of the grid codes the controller needs to be designed for the worst-case scenario.

Another characteristic of solar power plants, that needs to be taken into consideration, is their intermittent and volatile nature. The power production of these plants varies over the time, and mostly is below rated power. This intermittency can be used to benefit the system voltage, by extracting more reactive power when the generation units are not working at the rated values. The control system should use this characteristic to enhance the reactive power support capability of the renewable energy generations.

Voltage collapse and islanding phenomenon are not considered in this study. But, briefly said, the source of voltage collapse is the lack of reactive power, linked to the active power flow, and this occurs mainly when the system experiences a heavy load [10]. And the islanding phenomenon is more related to the protection systems, rather than control.

The protection schemes are also out of the scope of this work. For sure, it is very important to have fast, reliable and well-coordinated protection in the network, collector bus, and also within the PV plants. Furthermore, these protection systems have to deal not only with primary system fault currents, but also abnormal conditions, such as high or low voltage, high or low frequency, out of synchronism, islanded operation, etc. According to appropriate grid codes, solar power plants have to be able to handle the most common types of grid faults without being tripped or damaged [11]–[13]. Thus, the protection system is considered to be properly designed to avoid any damage in the grid.

Additionally, the frequency of the grid is considered to be stable and the

curtailment of active power outputs of the PV plants doesn't affect the frequency stability of the grid.

1.3 Outline of the Thesis

The thesis is organized into 7 chapters. An overview of the structure is given in Figure 1.2.

- *Chapter 1. Introduction*: This chapter presents the motivation behind this thesis, defines the problem and the possible solution of the problem. The scope and the structure of the thesis are also presented in this chapter.
- *Chapter 2. State of the Art*: This chapter discusses the state of the art on current grid codes, droop control and hosting capacity improvement. Review of current droop control strategies and common hosting capacity enhancement measures is presented. The chapter concludes by defining the research problem and the proposed solutions to solve them.
- *Chapter 3. Modeling and Control*: This chapter focuses on the power system and PV plant modeling and control. The choice of the modeling and simulation environments is presented. The selected grid model is presented in details and the assumptions made for further investigation are justified. The modeling of the PV plant is described in details as well as the control of the PV inverters.
- *Chapter 4. Grid Reconfiguration Analysis*: In this chapter an assessment of HC improvement by grid reconfiguration and grid code improvement in a MV grid with meshing possibilities is completed. The grid reconfiguration analysis is performed for all the possible switch configurations. First the grid is transformed into a graph, after which graph analysis tools are used to assess the configuration. To assess the cross-influence of DGs and the influence of DG location, four PV plants connected at different parts of the grid are considered. Also, to assess the impact of grid code modification on the HC, several PV control case scenarios are considered. The chapter concludes with a grid reconfiguration summary showing the connection between the configuration number, tie-switch configuration and the distribution of HC. This summary provides the grid operators a reconfiguration degree of freedom to

safely reconfigure the system in cases of system contingencies, while keeping the HC within a certain range.

- *Chapter 5. Extended Current Droop Control of PV Plants*: This chapter presents the extended active and reactive current droops developed for controlling the output of the PV plants connected in a meshed MV grid. To assess the load sharing capability, the cross-influence of DGs and the influence of DG location, four PV plants connected at different parts of the grid are considered. The static and dynamic performance of the droops is analyzed. For the assessment of the dynamic performance abrupt load variation is performed to show the superiority of the proposed droop control over the traditional droops during voltage fluctuations in the grid.

- *Chapter 6. Overloading Control of Substation Transformer*: This chapter presents a novel substation transformer overloading prevention strategy. The strategy is meant to protect the transformer during the high PV/ low load situations via reactive power control using a battery energy storage connected at the MV side of the substation transformer. The proposed direct loading control strategy does not depend on any communication means and is connection failsafe. The proposed strategy is tested on the same meshed network used in the previous chapter and the performance is compared to the no curtailment case. Additionally, the influence of the substation transformer power rating on the system stability and curtailment is analyzed.

- *Chapter 7. Conclusions and Outlook*: This chapter summarizes the main achievements of the thesis and discusses possible advances on the topic.

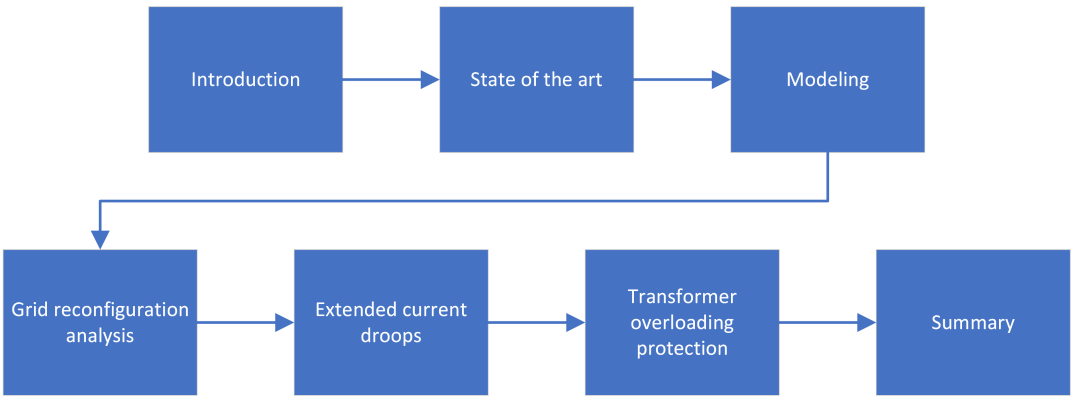

FIGURE 1.2: Overview of the thesis structure

Chapter 2

State of the Art

This chapter discusses the state of the art on grid PV hosting capacity (HC) enhancement. The definition of hosting capacity and the review of common hosting capacity determination and enhancement measures is presented. The chapter concludes by defining the research problem and the proposed solutions to solve them.

2.1 Hosting Capacity

The concept of HC was first introduced in 2005 by Bollen et al. [14] to specify the impacts of increasing DG share in the energy generation mix on the power grid. Later, Bollen and Hasan [15] defined the HC as the maximum total installed power of DG that can be accommodated by the grid, above which the performance of the grid becomes unacceptable. The HC determination is not a fixed calculation with only one possible result. It depends on many factors such as the location of the DG [16]–[18], number of DGs [19], [20], etc. Several limiting indices should be taken into consideration when calculating the HC. In [15] the HC determination criterion is described using the limiting index based on which it has been calculated. Etherden et al. [21] discussed the importance of HC for DSOs and highlighted that the HC should be calculated for several limiting indices and the lowest HC value should be chosen as the system HC.

2.1.1 Limiting indices

The negative impacts of high DG penetration levels on the grid have been studied in many researches [22]–[28]. Here, the main HC limiting indices are discussed.

The limiting indices of HC, such as overloading, overvoltages, protection and power quality issues are discussed in [15], [26], [29]. When the DG unit

power output is higher than the load demand, the excess power is being injected back to the grid. Because of the resulting reverse active power flows, an overvoltage may happen at the connection bus of the DG in a more resistive grid. In contrary, in more inductive grids, the reverse active power flows will not affect the voltage levels in the grid as much as the loading of the lines and transformers, resulting in overloading issues, especially when combined with the reactive power flow.

Overvoltage

In [24], Shayani et al. examined the impact of high PV penetration on the grid. The study concluded that the voltage limitations and the continuous maximum current of the grid components were the main indices that violate the permissible operational limits during high share of PV production. Based on the simulations, the authors suggest that PV installations up to twice the total load power are permissible. They also proposed practical general guidelines on determination of maximum HC based on the specified limiting indices by the operator. Furthermore, the authors suggested that the voltage drop without a PV injection and the voltage rise with maximum DG penetration will have approximately the same value, as presented in the Eq. 2.1.

$$|\Delta V_{drop}| \cong |\Delta V_{rise}| \tag{2.1}$$

In [30] Bertini et al. propose a systematic methodology that calculates the HC, while taking into account the steady state voltage violations and fast voltage variations. They have tested their approach on a real Italian distribution network using simplified reconfigurable models where several parameters like transformer rating, system loading and feeder cross section and length can be altered. Degner et al. [31] investigates the high PV penetration in the German LV distribution network while focusing on the overvoltage problems. The article underlines that the upper voltage limit is usually reached faster than the thermal loading limits of the distribution system. The authors concluded that the application of appropriate reactive power control strategy can increase the system HC by 1,5 to more than 2 times. In [32], Monfredini et al. investigated the impact of large scale DG integration into distribution networks at MV level. They underlined that it impacts the voltage profile of the feeders and increases the risks of overvoltages at the DG connection bus. The authors also discussed possible voltage improvement techniques and their impact on the HC.

In [33], Alalamat investigates the impact of DG penetration on the voltage profile of the network. The voltage rise at different buses is approximated by the Eq. 2.2.

$$\Delta V_{rise} \cong \frac{(P * R) + (Q * X)}{|V_n|} \tag{2.2}$$

From Eq. 2.2 we can see that the amount of voltage rise depends on two terms, $(P*R)$ and $(Q*X)$. The method selection for reducing the voltage rise depends on which term is more dominant at the connection bus. $|V_n|$ is the nominal voltage at the connection bus and is defined by the system operator. It can be adjusted by controlling the tap position of the OLTC transformer connected upstream. R and X are the resistance and the reactance at the connection point and are depending on the characterstics of the grid. As the voltage rise depends on the R and X, one way to reduce the voltage rise is to reduce the values of R and X. This is done by reinforcing the cables. However, this solution is not always an economically feasible solution. The (X/R) ratio is a constant that depends on the characteristics of the grid and describes the restiveness of the grid. High (X/R) ratio means that the grid is more inductive and the $(Q * X)$ term is dominant in Eq. 2.2. Thus, to lower the voltage rise a reactive power control strategy could be a solution. On the contrary, low (X/R) ratio means that the network is more resistive and the $(P * R)$ term is dominant in Eq. 2.2. In this case, to lower the voltage rise an active power control strategy could be a solution. In [34], Collins et al. studied the influence of active and reactive power control strategies on the reduction of overvoltage caused by high PV penetration. In [35], Seguin et al discusses the different impacts of high PV penetration to the planning of the grid by system operators. They concluded that the overvoltage and fast voltage variation problems are more frequent and significant when large amount of PV is connected at the end of a lightly loaded feeders.

Overloading

The overloading of grid components is the next limiting index for DG integration [36]. With high DG penetration the DG output power can be higher than the load power at the connected bus, $P_{DG} > P_{load}$. This leads to reverse power flows to the upstream network, which may lead to exceeding the thermal limits of transformers and feeders. Although the grid components are designed to withstand 100% loading for long periods, DSOs from different countries have different limitations for the total DG amount connected to

the grid [37]. The overloading of the components with high DG penetration depends on several factors such as the DG location, the loading of the bus etc. Correct DG connection location selection reduces the feeder losses and decreases the loading of the transformer. In [26] the authors state that the best solution is to connect the DG closer to the loads being served. Additionally, the studies in [15], [38] conclude that the integration of DG can minimize the losses, reduce overall risks, maintain the lifetime of the grid equipment and improve the thermal loading of the transformers and feeders. The worst-case scenario, which increases the risk of overloading, happens when the DG production is at the maximum and the system load is at the minimum [35].

In [30] Bertini et al. propose a systematic methodology that calculates the HC, while taking into account the thermal overloading of the components.

From the feeder ampacity perspective, Shayani et al. [24] proposed the following equation to estimate the maximum DG capacity for a feeder without exceeding its thermal limits, Eq. 2.3:

$$P_{DG} = 2 * P_{load} + (1 - S_{load}) \tag{2.3}$$

where the P_{DG} is the installed active power of DG in pu, P_{load} is the active power of the load in pu and S_{load} is the apparent power of the load. According to Eq. 2.3, the installed PV should be enough to supply the active power of the load, export the same amount of active power to the grid and compensate for any line loss if the load is below the rated value.

Power quality and Protection

Additional power quality criteria, such as harmonics, imbalances, voltage dips or flicker can also limit the voltage related hosting capacity of distribution grids [15]. Moreover, high DG penetration could mask a fault in the system by providing short-circuit current and impact the protection coordination, set-points and ratings of interrupting devices, fault detection systems, etc [39]. Since the study is focusing only on overvoltage and overloading issues, these aspects of high DG penetration impact are excluded from the scope of this thesis. The reader can refer to the following articles for additional literature on power quality and protection problems: power quality - [11], [14], [40]–[54], protection - [38], [55]–[58]

2.1.2 HC calculation techniques

Various methods have been used in different studies to determine and improve the HC of the distribution grid. These methods mainly differ by the grid structure, loading profile, location of DG, control strategies and calculation methods.

Depending on the availability of grid data, studies were completed based on either generic grid structures [31], [59] or real distribution grid structures [22], [60], [61]. Variable load profile is considered by Menniti et al. [62] while presenting their HC determination approach. The authors used mathematical models to study the relationship between the HC and loading capacity. In [63], Rossi et al. presented a novel solution for evaluation of the HC considering the risk of network bottlenecks. They examined DG allocation impact on the HC by implementing stochastic DG allocation in their approach. The authors concluded that the HC has to be identified by a probability density function and not by a single value. Ballanti et al. [16] used a single PV connection point at the furthest bus for the HC assessment. On the contrary to [16], Quintero-Molina et al. [17] considered three different DG connection points: head of the feeder, middle of the feeder and end of the feeder. However, only one DG is connected per assessment scenario and there is no combination of several DGs connected at different locations. In [64], the authors assess the techno-economical feasibility of different active and reactive power control systems in Germany. They concluded that the reactive power control is effective in increasing the HC. In [65]–[67], the main results of an Italian project to enhance the HC of MV grids via advanced control are demonstrated. Regarding their assessment methodology the studies can be categorized into those using deterministic approaches (i.e., simulation of specific scenarios) [31], [60], [61] and those using probabilistic approaches (e.g., using Monte-Carlo simulations) [22], [59].

2.1.3 HC enhancement techniques

Currently, with the increasing PV installations all over the world, the enhancement of the HC of the grid is one of the important goals for the DSOs [22], [30], [67]–[69]. Technical solutions enhancing the grid HC are categorized into three categories in [70]: DSO solutions, prosumer solutions and interactive solutions. Below various enhancement techniques are presented.

Reactive power control

Voltage rise problems are a dominant limitation for high DG penetration. Reactive power control is believed to be one of the most effective methods for tackling the overvoltage problems. Different reactive power control strategies can be used such as capacitor banks, static VAR compensators (SVC), static synchronous compensators (STATCOM), static synchronous series compensators (SSSC) and inverter based DGs.

In [71], [72] stochastic mathematical models aiming to maximize the grid HC are presented. The authors underline that the DG penetration can be increased and the system losses can be reduced by utilizing reactive power control and storage systems. They concluded that the proposed models are suitable for smart grids, where the integration of large-scale DG is preferable. In [73], Meuser et.al investigated the HC enhancement impact of reactive power control and improved OLTC tap control. The authors highlighted that unbalances in reactive power flows may occur with reactive power control in rural areas. Therefore, it is advised to place the DG near the substation transformer for balancing reactive power needs. Different reactive power control methods and their effect on HC enhancement is examined in [74]. In the study, the authors assessed several control techniques, such as fixed power factor control, $P(cos(\phi))$ and $Q(V)$. In [75], Seuss et al. examined the effect of local Volt/VAR control technique on the feeder HC. The study concluded, that the reactive power capabilities of the inverters enhance the HC. In [76], Ding et al. presented a stochastic analysis of PV penetration. They concluded that the control of the power factor of the inverter has a positive impact on HC enhancement.

Active power control

The active power control in cases of high DG penetration is mostly implemented as active power curtailment. The active power is curtailed to match the load requirements and to keep the grid within the operational limits. Active power curtailment is mostly implemented in centralized DG stations, where the DSOs can control the output power of the DG. In [77], Etherden et al. discuss the impact of active power curtailment on the grid HC enhancement. In their work, they assess the HC based on the overvoltage and thermal overloading limiting indices. Additionally, the study emphasizes the role of advanced communication in the achievement of optimal power curtailment.

In [78], [79], several case studies for LV and MV networks are presented. They discuss the impact of active power curtailment and dynamic line rating in grid HC enhancement. The authors categorize the active power curtailment into hard and soft curtailments. During hard curtailment all the DG output is curtailed once a limiting index is violated. On contrary, the soft curtailment technique curtails the DG partially. In [80], the fixed power curtailment and Volt/Watt techniques are examined. The study shows that the fixed curtailment is more efficient than the Volt/Watt control under the worst-case scenarios. However, the authors highlight that the uncertainties in load profile and DG penetration make it difficult to choose the most optimum curtailment technique.

Energy storage

Another technique to enhance the HC of the grid and overcome the overvoltage resulting from high penetration of DG is the utilization of an energy storage. Battery energy storage enables mutual decoupling of the demand and generation. Accurate sizing and allocation of the BES can delay the need of network reinforcement. The impact of customer-owned and DSO-owned BES on the grid HC enhancement are investigated in [81]–[91].

In [86], a systematic approach for BES utilization decision making in the context of HC enhancement is presented. Correct sizing and allocation of the BES can delay the needed standard reinforcements. In this regard, Etherden et al. [85] presented a BES sizing methodology based on analytical simulation studies. The authors concluded that BES can increase the grid HC. However, economic feasibility studies should be conducted. In his study [87], Poulios investigated the optimal sizing and allocation of BES to increase the HC of a low voltage grid in Zurich, while taking into account the economic aspects. The author concluded that further reduction of BES prices is needed to get an economically competitive solution. Jayasekara et al. [88] investigated the optimal BES sizing in MV and LV distribution grids in Western Australia. A cost-based multi-objective optimization tool was introduced. The investigations are done for three objectives: voltage regulation, network loss reduction and peak load reduction. The study concluded that the system configuration, generation profile and loading profile impact the benefits obtained by the BES. In [89]–[91] the efficient control and utilization of BES and its impact on the HC enhancement are discussed.

Network reconfiguration

Network reconfiguration is an efficient technique for grid HC enhancement.

In [92], Capitanescu et al. investigated the impact of network reconfiguration on the grid HC enhancement in active distribution networks (ADN). The network reconfiguration has been categorized into static and dynamic categories. In the static reconfiguration, all the reconfiguration is done during the grid planning stage. In the dynamic one, the reconfigurations are performed via remotely controlled tie-switches. The study concluded that the static reconfiguration has the potential to significantly increase the HC of the grid, but the dynamic one can enhance the HC only if sufficient number of remotely controlled tie-switches are available. The drawbacks of the dynamic reconfiguration are the frequent utilization of the tie-switches, which leads to higher wear and tear costs and the increased risk of tie-switch failure. In real-life networks with large number of tie-switches the network reconfiguration is a highly complicated optimization problem.

In [93], Takenobu et al., in order to decrease the time needed for grid reconfiguration analysis to enhance the HC, presented a time-efficient methodology, where the optimization problem is divided into small sub-problems which represent the main reconfiguration problem. The proposed methodology has been tested on a real Japanese distribution network consisting of 235 switches. It was successful in finding the global optimum solution in 49 h. In [94], Fu et al. investigated multi-period reconfiguration to find the minimal number of switching events to enhance the HC.

However, in most of the studies the impact of grid reconfiguration on the HC enhancement is considered only for radial configurations [95]–[98].

OLTC control and harmonic mitigation

Control of OLTC tap position and the harmonic mitigation are also viable techniques for grid HC enhancement [52], [99]. However they are out of the scope of this thesis. The reader can refer to the following articles for additional information on OLTC control and harmonic mitigation for HC enhancement: OLTC control - [100]–[105], harmonic mitigation - [106]–[110].

2.2 Conclusion

In this section the concept of hosting capacity has been presented, main limiting indices and the state of the art of hosting capacity enhancement techniques have been discussed.

The overvoltage and the thermal overloading of the lines and transformers are identified as the main limiting indices for evaluating the hosting capacity of the grid. Reactive power control and active power curtailment are proven to be one of the main and effective techniques to enhance the hosting capacity of the grid. If the reactive power control is mostly a locally controlled strategy via the droops, the active power curtailment mostly depends on a centralized control, where the curtailment signal is sent by the distribution system operator. The drawback of such strategies is the dependency on the communication. The bidirectional connection has also the problems of the cybersecurity, thus one-way communication has been proposed by [111]. Even though the one-way communication is prone to cyber-attacks, the failure of the communication and delays in the transmission can pose severe problems for the stability of the system. Thus, there is a need to have an alternative solution to curtail the active power output of the PV plants without relying on the communication, which can be a fail-safe back-up solution.

To overcome the communication problems and to enhance the PV hosting capacity of the grid, extended active and reactive current droops are proposed, where $I_d(V), I_q(V)$ droops with variable gains are used.

With the emerging promising battery technologies and the decrease of the battery prices, the interest in battery usage in power systems is increasing. New opportunities open up to use the capabilities of the battery energy storage for the increase of PV hosting capacity of the grid by using the batteries not only for peak shaving and overvoltage protection but also for other ancillary services, such as reactive power support and overloading protection.

In order to protect the transformer from overloading via communicationless active power curtailment, the extended droops are combined with a battery energy storage to force the inverters to curtail their active power output in order to decrease the loading of the transformer.

Chapter 3

Modeling and control

This chapter focuses on the power system and PV plant modeling and control. The choice of the modeling and simulation environments is presented. The selected grid model is presented in details and the assumptions made for further investigation are justified. The modeling and control of the PV plants is described in details.

3.1 Modeling of the grid

As mentioned in the previous chapters, the research goals of the thesis are to determine the influence of the grid reconfiguration and grid-code modification on the HC of the grid, as well as the development of novel control strategies to protect the grid from possible overvoltages and overloading caused by integration of PV.

In order to achieve these goals, the power system and the PV plants need to be modeled, so that the developed solutions can be tested by means of numerical simulations. However, only one model will not be sufficient to achieve all the goals, as the the problems to be solved differ in their nature and require assessment and analysis of parameters with different characteristics. Thus, different types of models need to be used. For example, the HC calculation is a static analysis problem, where the steady-state performance is of interest. On the opposite, the overvoltage control via droops and the transformer overloading protection require analysis of not only the steady-state performance of the control but also of the transient performance during the changes in the system, such as the load changes or the solar irradiance change.

A Luxembourgish medium voltage grid representative model is used as the basis for the grid model used in the study. The grid model is a derivative from a previous grid model developed in MATPOWER package within the RE-DESG FNR project for investigation of reliable operation of the grid protection

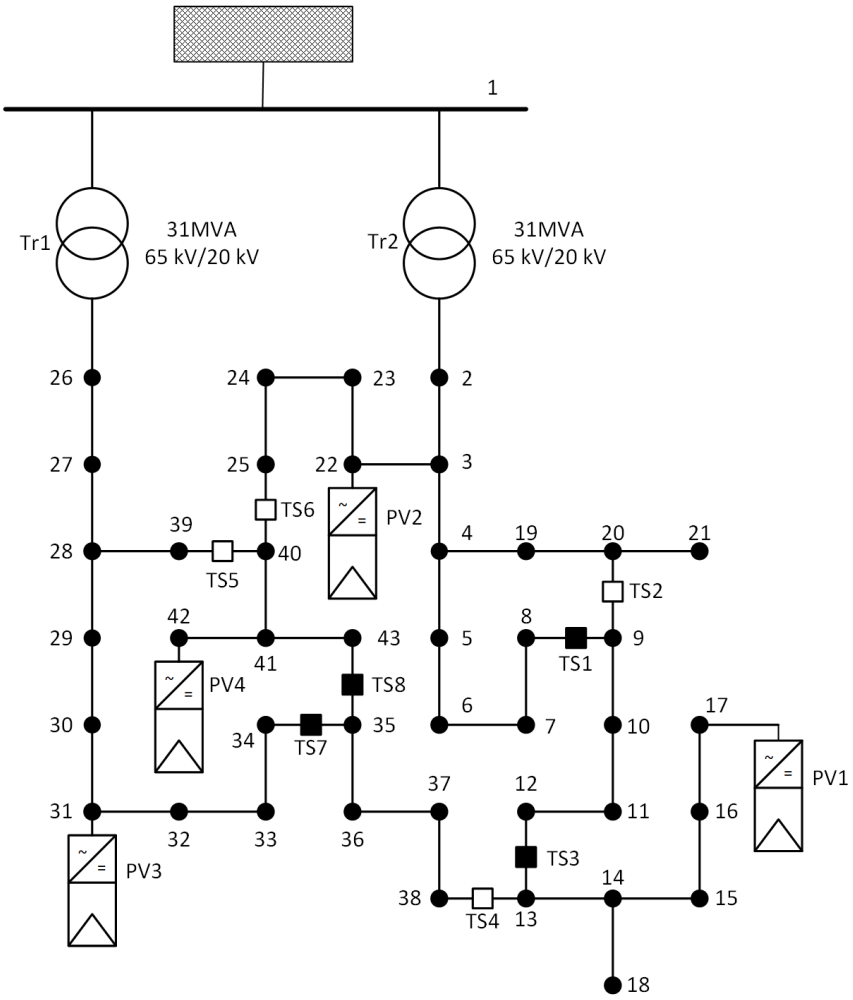

FIGURE 3.1: Base test grid structure.

[57]. The base version of the grid model is presented in the Figure 3.1. It consists of a 65kV high voltage slack bus, two 31MVA 65kV/20kV transformers, 43 medium voltage buses and 44 20kV lines, parameters of which are taken from CIGRE MV benchmark test model [112] and eight tie-switches, which allow to change the configuration of the grid and have meshed configurations. In order to model a distributed PV generation in the grid a combination of different connection locations is selected, four PV plants are connected to the grid at the buses 17, 22, 31, 42. Different modifications of the presented grid model are used in the next chapters of this thesis to test and verify the proposed solutions.

3.1.1 Static modeling

For the grid reconfiguration analysis and HC calculation, the static model of the grid is made in the Pandapower software package, which is based on

Python. It is a joint development of the research group Energy Management and Power System Operation, University of Kassel and the Department for Distribution System Operation at the Fraunhofer Institute for Energy Economics and Energy System Technology (IEE), Kassel [113].

The pandapower is an easy to use network calculation program package aimed at automation of analysis and optimization in power systems. It is built on the data analysis library pandas and the power system analysis toolbox PYPOWER. Pandapower is mainly used for static analysis of three-phase power systems.

The main advantages for which pandapower has been chosen are the faster power flow solver compared to MATPOWER and PYPOWER, and the possibility of using the Python library NetworkX for graph searches and graph analysis [113], [114].

The power flow solver of pandapower is based on the Newton-Raphson method. The solver is an improved, more robust, faster and more user friendly modification of the PYPOWER solver. Some parts of the pandapower solver are accelerated using the JIT compiler numba. This makes the pandapower Newton-Raphson significantly faster than the PYPOWER solver from which it was originally derived [113].

Additionally, pandapower provides the possibility to translate pandapower networks into NetworkX graphs. Once a network is translated into an abstract graph, all graph searches implemented in the NetworkX library can be used to analyze the network structure. Moreover, pandapower also provides some predefined search algorithms to tackle common graph search problems in electric networks, such as finding unsupplied buses or identifying buses on main or secondary network feeders [115], [116].

3.1.2 Dynamic modeling

For the implementation and assessment of the developed droop control and overloading control strategies, the dynamic model of the grid and the PV plant are made using the MATLAB Simulink software.

3.2 Modeling and control of the PV plant

This section discusses the structure, the modeling and the control of the PV plant in MATLAB Simulink.

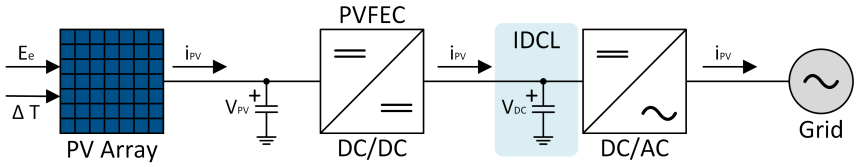

FIGURE 3.2: Typical PV plant consisting of two converters and intermediate DC link.

3.2.1 PV plant

One of the most widespread grid connected PV systems is the two-stage grid-tied PV power interface. This power interface is chosen because of its advantages in terms of the modular design and possibility of decoupled control [117], [118]. The simplified PV plant model consists of the PV array, PV front-end converter (PVFEC) for DC-DC conversion, the intermediate DC link (IDCL), and the grid connected converter for DC-AC conversion and power feed-in to the grid, as shown in Figure 3.2.

The power output of the PV plant is partially characterized by the availability of the resources and environmental conditions, namely the solar irradiance and the temperature of the cell. The dynamic interference of the DC-DC and DC-AC converters is decoupled by the high capacitance value of the IDCL. Thus, the DC-DC converter control utilizes a maximum power point tracking (MPPT) algorithm and is responsible for the maximum power extraction from the PV panels and injection into the grid, whereas, the DC-AC converter control regulates the IDCL voltage and provides grid-tied functionality, such as reactive power support and power quality improvement. In general, the operation of the PV plant includes two DC voltage regulation loops. The first control loop regulates the PV output voltage to the optimal operating point in order to extract the maximum available power through the MPPT control of the DC-DC converter and send it to the IDCL. The second control loop regulates the voltage of the IDCL, thus regulating the amount of active power to be injected into the grid. The IDCL voltage fluctuates depending on the power balance between the PV generation and the grid injection by the grid-tied converter.

3.2.2 Photovoltaic modules

The PV array consists of 5 series connected SunPower SPR-305E-WHT-D modules per string. The number of parallel strings depends on the total installed active power of the PV plant. The details of the selected module are

presented in Table 3.1.

TABLE 3.1: SunPower SPR-305E-WHT-D module data

Maximum Power (W)	305.226
Cells per module	96
Open circuit voltage, Voc (V)	64.2
Short-circuit current, Isc (A)	5.96
MPP voltage (V)	54.7
MPP current (A)	5.58
Temperature coefficient of Voc (%/deg.C)	-0.27269
Temperature coefficient of Isc (%/deg.C)	0.061745

The characteristic I-V curves of one PV module for irradiance and cell temperature variation are presented in Figures 3.3 and 3.4.

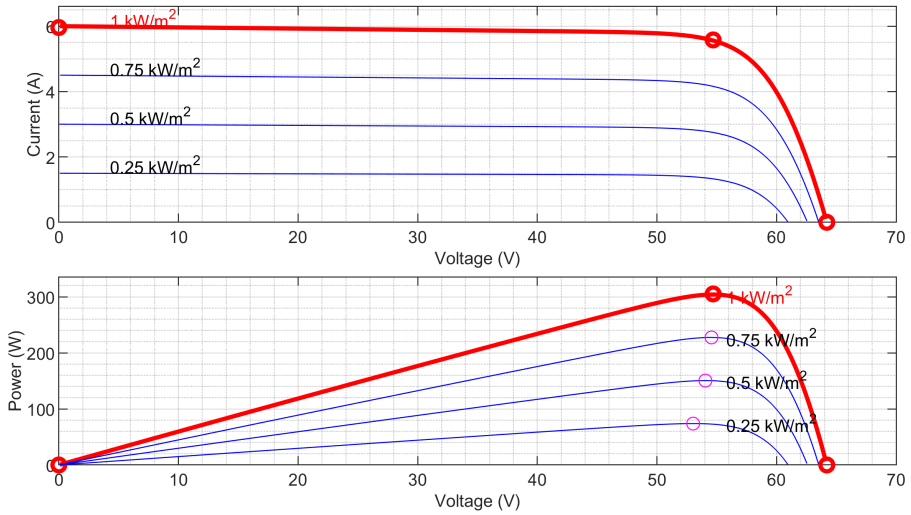

FIGURE 3.3: I-V curve of the SunPower SPR-305E-WHT-D at a constant cell temperature of 25 ℃.

3.2.3 DC-DC Converter and MPPT

A non-isolated DC-DC boost converter is used as the PVFEC because it is one of the most common converters used due to the voltage step-up requirement and its simplicity. According to [117], [118] the boost topology is superior to the buck in terms of price and better dynamics. The circuit schematics of the DC-DC boost converter is depicted in Figure 3.5.

An essential component of a PV plant is the MPPT controller, which is responsible for extracting the maximum possible solar energy [117]. In this study the MPPT is performed using an "Incremental Conductance + Integral

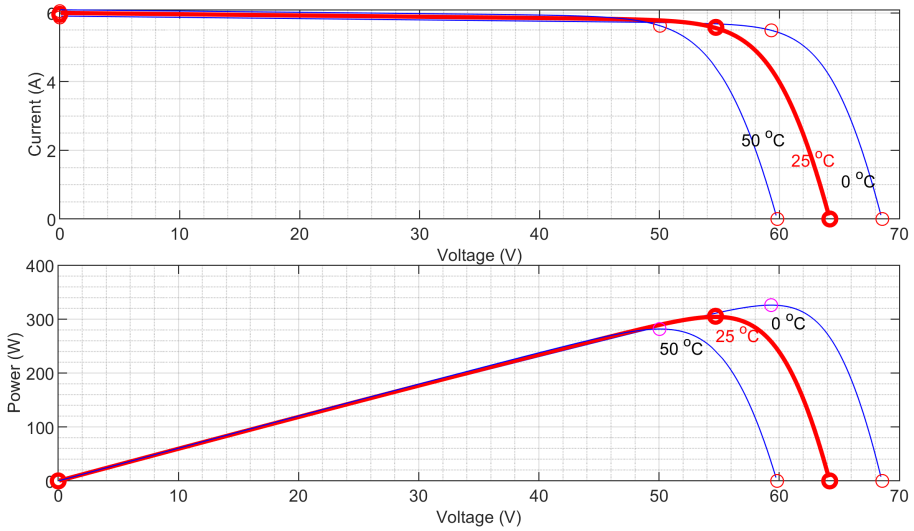

FIGURE 3.4: I-V curve of the SunPower SPR-305E-WHT-D module at a constant sun irradiance of $1KW/m^2$.

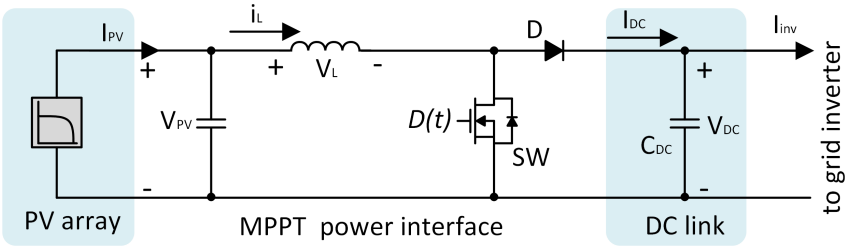

FIGURE 3.5: Schematics of the DC-DC converter including the PV array and boost converter topology.

Regulator" technique. The details of the MPPT controller and the algorithm will not be discussed in this thesis, since they are out of the scope.

3.2.4 DC-AC Grid-Tied Converter and Control

The DC-AC converter used in the study is a three-level three-phase voltage source inverter (VSI). The high capacitance intermediate DC link capacitors are acting as a buffer for the reactive power flow between the inverter and the grid. Regulation of the DC link capacitor voltage controls the amount of active power injected to the grid.

The control diagram of the PV inverter is presented in Figure 3.6. The control consists of an inner current control loop and an outer control loop. The inner current control loop regulates the dq currents I_d and I_q to follow their reference signals I_{dref} and I_{qref}. The reference signals are obtained from the outer loop. During normal operating conditions, the active current reference I_{dref} is obtained from the DC link capacitor voltage regulation loop.

However, during the overvoltages the I_{dref} is obtained from the active current curtailment loop. The reactive current reference I_{qref} is obtained from the reactive current droop control. These outer loop controls will be discussed in more details in the next chapters of the thesis.

The control diagram also shows the phase locked loop (PLL) and measurements block. This block is responsible for the determination of the synchronizing phase angle and abc to dq reference frame transformations that are important for the 3-phase inverter system controls. This requires transforming the inverter terminal voltage from abc, $V_{S(abc)}$, to dq frame, $V_{S(dq)}$, with ensuring $\theta = \omega t$ in steady state. The three phase voltages are first transformed to the stationary $\alpha\beta 0$ reference frame by using the non-normalized Clarke transformation. The voltage vector and transformation matrix are expressed as 3.1 and 3.2, correspondingly.

$$V_{S(\alpha\beta 0)} = \begin{bmatrix} v_{S(\alpha)} \\ v_{S(\beta)} \\ v_{S(0)} \end{bmatrix}^T = \begin{bmatrix} T_{\alpha\beta 0} \end{bmatrix} \begin{bmatrix} v_{S(a)} \\ v_{S(b)} \\ v_{S(c)} \end{bmatrix} \tag{3.1}$$

$$\begin{bmatrix} T_{\alpha\beta\gamma} \end{bmatrix} = \frac{2}{3} \begin{bmatrix} 1 & -\frac{1}{2} & -\frac{1}{2} \\ 0 & \frac{\sqrt{3}}{2} & -\frac{\sqrt{3}}{2} \\ \frac{1}{2} & \frac{1}{2} & \frac{1}{2} \end{bmatrix} \tag{3.2}$$

Neglecting the zero sequence component, the voltage on the $\alpha\beta$ reference frame is derived as:

$$V_{S(\alpha\beta)} = \begin{bmatrix} v_{S(\alpha)} \\ v_{S(\beta)} \end{bmatrix} = V_S \begin{bmatrix} cos(\omega t + \phi) \\ sin(\omega t + \phi) \end{bmatrix} \tag{3.3}$$

where ϕ represents a reference phase angle and V_S is the voltage magnitude. The voltage vector is then derived in dq frames as:

$$V_{S(dq)} = \begin{bmatrix} v_{S(d)} \\ v_{S(q)} \end{bmatrix} = \begin{bmatrix} cos(\theta_s) & sin(\theta_s) \\ -sin(\theta_s) & cos(\theta_s) \end{bmatrix} V_{S(\alpha\beta)} \tag{3.4}$$

where θ_s is the rotational transformation angle determined by the PLL.

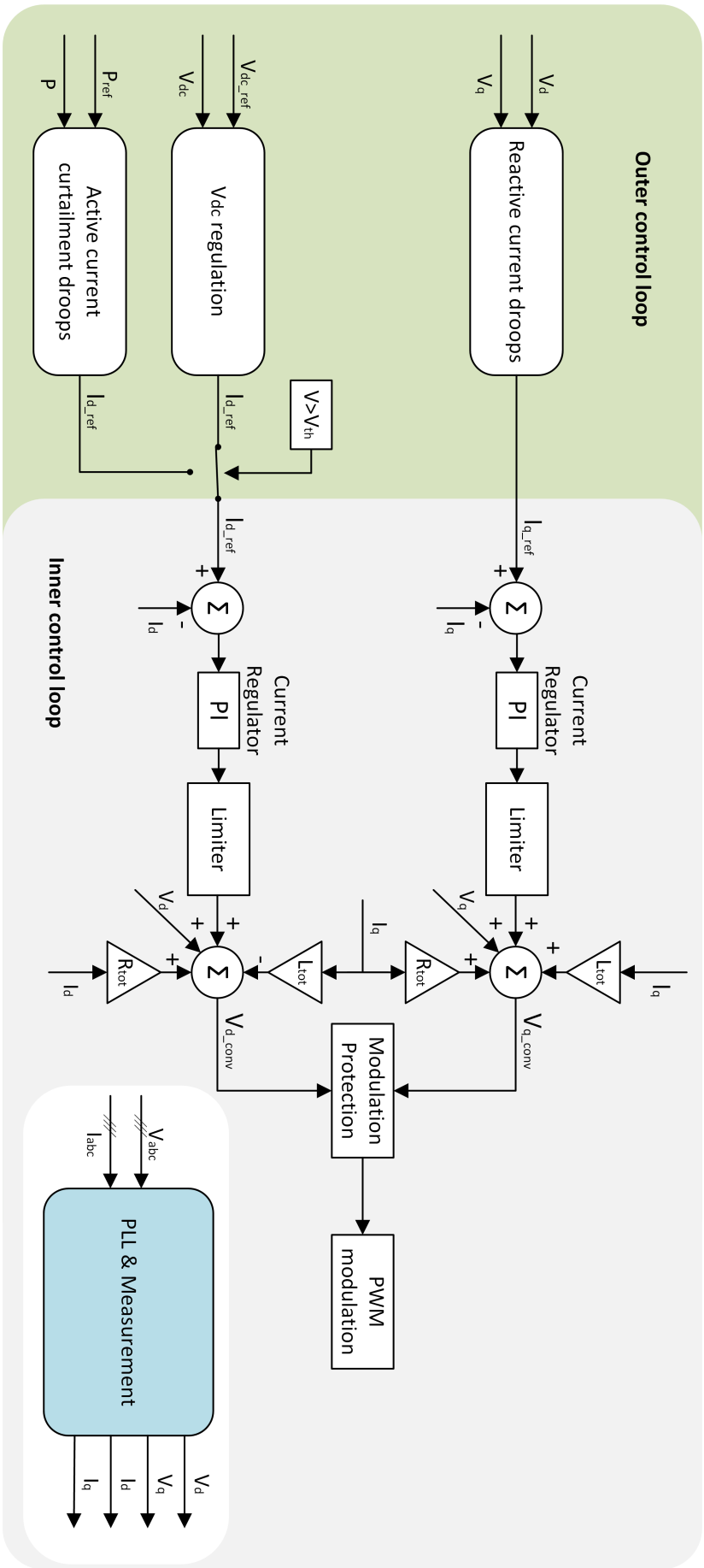

FIGURE 3.6: Control diagram of the DC-AC converter.

Chapter 4

Grid Reconfiguration Analysis

In this chapter, the influence of grid reconfiguration and grid code change on the PV hosting capacity (HC) improvement of a medium voltage (MV) grid with meshing possibilities is assessed. The grid reconfiguration analysis is performed for all the possible switch configurations. First, the grid is transformed into a graph, and then graph analysis tools are used to assess the configuration. To assess the cross-influence of PVs and the influence of their location, four PV plants are connected at different parts of the grid. Also, to assess the impact of grid code modification on the hosting capacity, several PV inverter control case scenarios are considered. The chapter concludes with a grid reconfiguration summary showing the connection between the configuration number, the tie-switch configuration and the distribution of the PV hosting capacity. This summary provides the grid operators a reconfiguration degree of freedom to safely reconfigure the system in cases of system contingencies, while keeping the PV hosting capacity of the grid within a certain range.

4.1 Introduction

As concluded from Chapter 2, the grid reconfiguration and grid code modification are possible solutions to improve the HC of the grid. Both, the grid reconfiguration and the grid code modification are considered as low cost or no cost solutions and should be the first measure to be considered by the grid operators in order to increase the HC of the grid.

To show the potential of a proper grid reconfiguration, an algorithm has been developed to analyze the HC of all the possible radial and meshed configurations. The algorithm permits to consider several DGs connected at different buses during the HC calculation, on contrary to [16], [17].

The detailed description of the reconfiguration analysis and HC calculation algorithms, the implementation of the algorithms on a test-network and the results of static analysis of the potential of grid reconfiguration and grid code improvement to increase the HC of the grid are presented in the following sections.

4.2 Subset Sorting and Hosting Capacity Calculation

This section presents analysis of the developed grid reconfiguration and the HC calculation algorithms.

Since the HC is a static characteristic of a grid, the static model of the system is chosen for the reconfiguration analysis and the HC determination. To assess the influence of the grid reconfiguration and grid-code modification on the HC of the grid an algorithm is developed using the built-in pandapower tools and several Python libraries.

The algorithm analyzes all the possible grid configurations, sorts them into meshed and radial groups and calculates the HC. The overview of the grid reconfiguration analysis algorithm is presented in Figure 4.1.

First, the safe operating conditions of the grid are defined. The limiting indices for overcurrent and overvoltage are set based on the requirements of the grid operator.

After the limiting indices are defined, the first grid configuration is selected. The selected configuration is transformed into a graph by using a built-in pandapower function. This allows the use of python NetworkX graph analysis library to sort the grid configurations into meshed and radial groups. First, the grid configuration is checked for the presence of isolated buses by using pandapower topological search tools. If the configuration has an isolated bus, then that configuration is discarded, since in the normal operating conditions all the buses should be energized. If all the buses of the network are properly energized, the configuration is tested on the presence of cycles by using the NetworkX graph analysis tools. If the configuration has a cycle in it then it is labeled as a meshed network, otherwise it is labeled as a radial network. After the configuration has been labeled, the HC of that configuration is calculated and the next configuration is selected. This process is repeated until all the switch configurations in the network are analyzed.

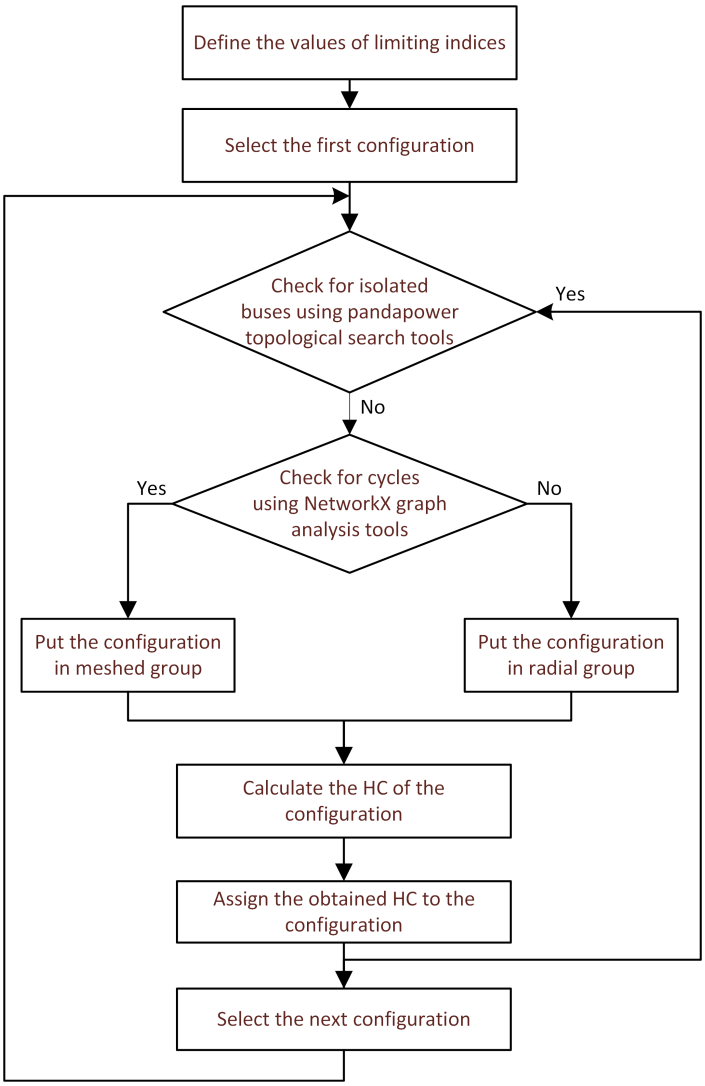

FIGURE 4.1: Subset sorting overview

The crucial part of the reconfiguration analysis algorithm is the HC calculation, which is presented in more details in Figure 4.2.

In order to determine the HC of the configuration, first the connection points for the PV plants are defined. Next, the initial values of the HC, active and reactive power outputs of the PV plants are set to zero. A flag is set for each PV plant, that will be set to TRUE if there is a violation of limiting indices at the PCC. Initially all the flags are set to FALSE. Next, the increment steps for the active and reactive power output of the PV plants are defined.

After the initialization steps are completed, the outputs of all the PV plants are sequentially increased step by step until all the flags are set to TRUE. In the first step, the active power output of the first PV plant is increased by the defined step. After each increment of the active power a power flow analysis is run to check for violations of the limiting indices. If a violation is detected and an overvoltage exists and the PV inverter reactive power

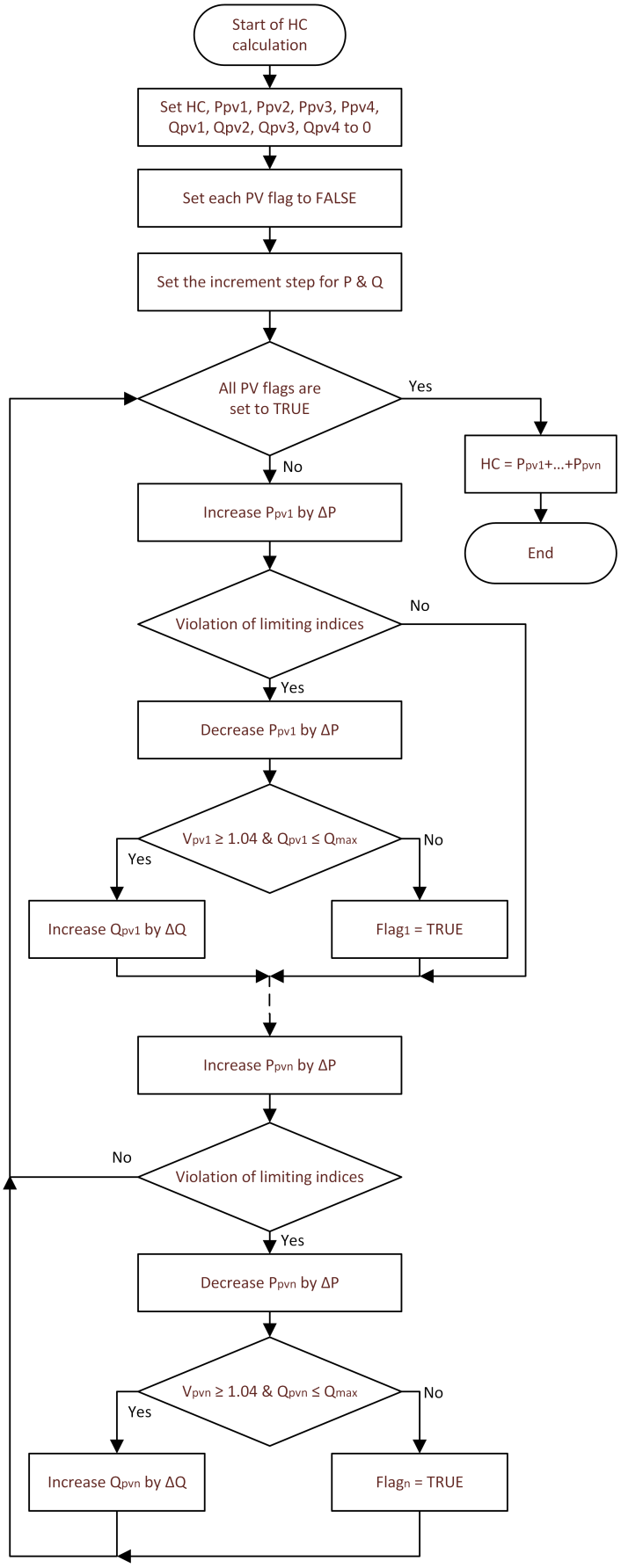

FIGURE 4.2: HC calculation algorithm

reserve is not reached, the active power output is reset to the previous value and the reactive power output is increased. Otherwise, in case of overloading or in absence of reactive power reserve, the active power output is reset to the previous value and the flag is set to TRUE. In the next steps, the same procedure is performed for other PV plants until all of them reach the power output value at which all the flags are set to TRUE. Once all the flags are set to TRUE, the total output active power of all the PV plants is assigned to the configuration as the HC limit.

After the HC is calculated for all the configurations, the impact of the reconfiguration is assessed and the distribution of the HC is analyzed to provide the grid operators with a degree of freedom in reconfiguration while keeping the integration level of PVs within certain values.

The power flow analysis is done by the pandapower tool using the iterative Newton-Rhapson solver algorithm with maximum number of iterations of 100. The used Newton-Rhapson algorithm is a PYPOWER implementation with Numba accelerations.

4.3 Representative System Case Study

In this section the application of the grid reconfiguration analysis algorithm on a representative Luxembourg MV network model is presented.

4.3.1 Test Network

The selected test network is a 43-bus 20 kV model representation of the typical Luxembourgish MV grid structure, developed in the REDESG FNR project, with reference line parameters defined by CIGRE for MV benchmark test model. The models developed in the REDESG FNR project have also been used for investigation of reliable operation of protection equipment [57]. The grid is presented in Figure 4.3. It is a MV network with meshing possibilities. The network consists of:

- HV supply grid with a short circuit capacity of 300 MVA
- Two 31 MVA 65/20 kV transformers with U_k=12%
- 43 buses
- 44 lines with an average X/R ratio of 1.4

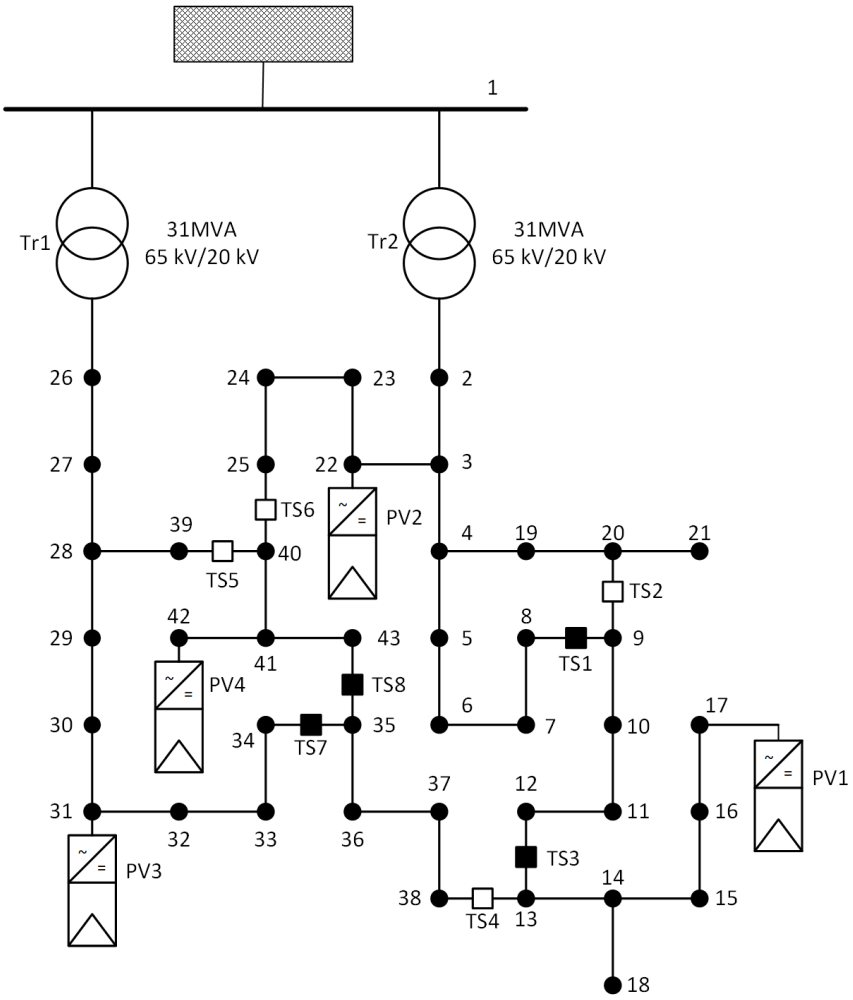

FIGURE 4.3: Test grid structure

- Eight tie-switches: TS1 through TS8
- Four PV plants allocated at buses 17, 22, 31 and 42
- No loads

4.3.2 Assumptions

Several assumptions are made for simplifications in this study:

- The grid under study is a balanced three-phase system operating in steady state with a constant frequency of 50 Hz
- Limitations from frequency control do not affect the study
- The protection equipment is properly configured for each grid configuration

4.3.3 Limiting indices

The limiting indices are selected according to the current grid code limitations for normal grid operation [9], [115]. The limiting indices are chosen as following:

- 1.04 p.u. voltage for overvoltage,
- 100% of rated current for transformer overloading,
- 100% of rated current for line overloading.

4.3.4 Case scenarios

Several cases are taken into account in order to evaluate the influence of the grid code changes on the improvement of the HC of the grid. These cases are:

Base case

In the base case, the inverters work in unity power factor mode and inject only active power. This corresponds to the operation point **a** on Figure 4.4;

Current grid code case

In this case, the inverters' operation range is limited within the power factor range of $cos\phi = \pm 0.9$, in line with the current VDE AR-4110:2018 grid codes [9]. Thus, the maximum reactive power is $Q_{max} = 0.484 \cdot P_{inst}$. This corresponds to the operation point **b** on Figure 4.4;

Improved grid code case

In this case, when the reactive power capability of the inverter at $cos\phi = \pm 0.9$ is reached and the voltage limitations are violated, the inverters are forced to decrease their active power output by up to 20% and keep the same reactive power value as before the curtailment (point **c'** on Figure 4.4). In contrary, in the current grid code case the curtailment of the active power would lead to a decrease in reactive power reserve of the inverter (point **b'** on Figure 4.4).

Keeping the same reactive power reserve level leads to increased reactive power support compared to the current grid code case and wider power factor range. Since $P_1 = 0.8 \cdot P_{inst}$ and $Q_{max1} = 0.484 \cdot P_{inst} = 0.605 \cdot P_1$, the extended

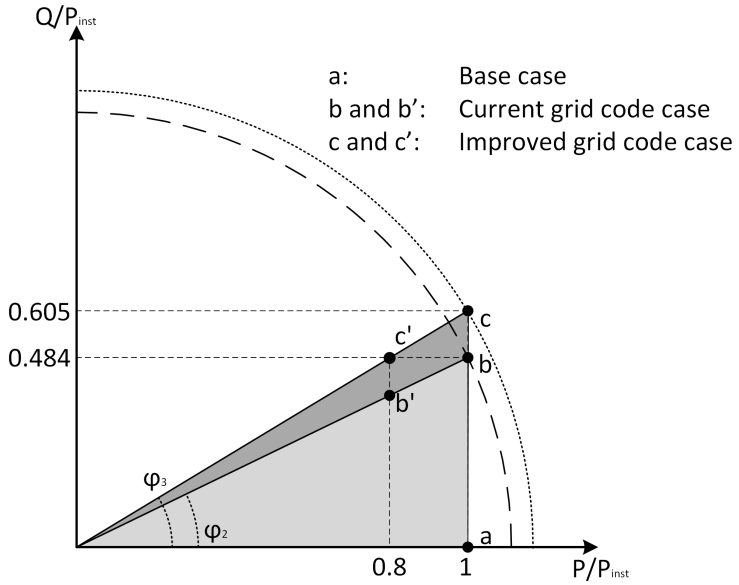

FIGURE 4.4: Case studies

power factor value is $cos\phi = arctan(Q_{max1}/P_1) = arctan(0.605) = 0.855$. Thus, the improved grid codes should allow the grid-connected inverters to work in a wider power factor range when in the active power curtailment mode.

On the other hand, in order to avoid active power curtailment and at the same time provide extra reactive power reserve, the plant operators can oversize their inverters to be able to operate with maximum active power output at extended power factor range of, $cos\phi = \pm 0.855$. Thus, when a curtailment signal is received the operating point of the inverter will move from operating point **b** to **c** and then to **c'** if curtailment is still needed, instead of immediately jumping from operating point **b** to **c'** (Figure 4.4).

In all the cases, no load situation is considered, since it is the worst possible load condition for PV integration [119].

4.4 Results

Grid subset analysis is performed the first, based on the algorithm described in Section 4.2 and Figure 4.1. The results are presented in Table 4.1. We can see that more than half of all the possible configurations are not valid configurations, as they have isolated buses. The subset analysis algorithm automatically ignores the invalid configurations, thus cutting down the running time by more than 50%.

TABLE 4.1: Grid subset analysis summary

Configuration	Number
Meshed	81
Radial	31
Isolated	144
Total	256

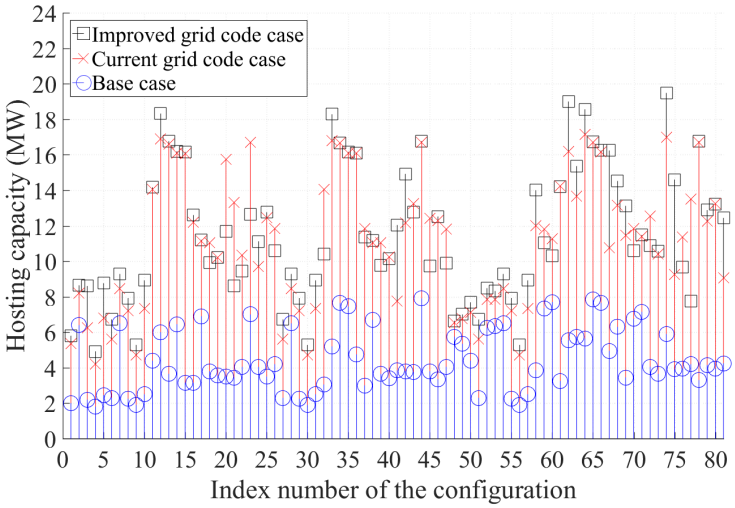

FIGURE 4.5: HC for each configuration of the meshed subset

To assess the potential HC improvement by means of grid reconfiguration and grid code improvement, HC calculations are performed for all three cases, as described in Section 4.2 and presented in Figure 4.2. In all the cases, the increment step value for the active power is taken as 50 kW and 10 kVAr for the reactive power.

The results for grid reconfiguration and grid code improvement analysis are presented in Figure 4.5 for the meshed configurations and in Figure 4.6 for the radial configurations. The performed subset analysis for the radial and meshed groups are summarized in Table 4.2 and Table 4.3. From these tables it can be observed that the binary representation of the configuration number corresponds to the switch configuration. Thus, by knowing the configuration number the grid operator can easily tell which switches are closed and which are open.

As presented in the sorted HC distribution plots (Figure 4.7 and Figure 4.8), by just using proper grid configuration the HC can be increased up to 4 times. The grid code improvements suggested in the third case can increase the HC by an additional 13% compared to the second case for the meshed subset (Figure 4.7) and by 15% for the radial subset (Figure 4.8). This is

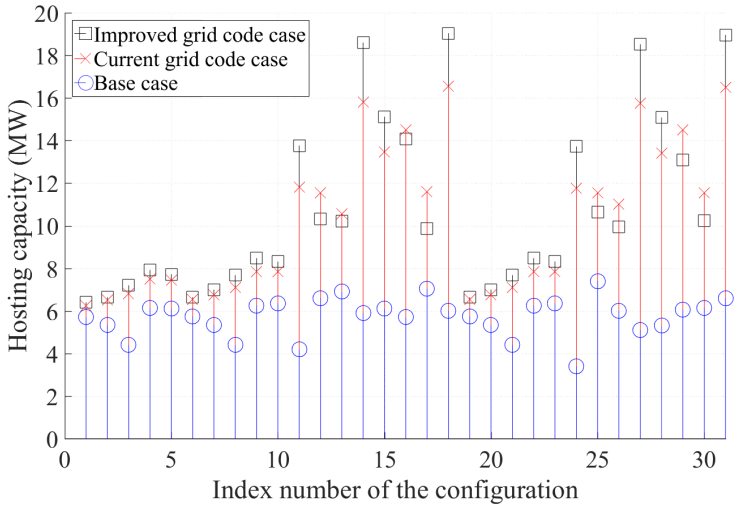

FIGURE 4.6: HC for each configuration of the radial subset

TABLE 4.2: Sorted radial group switch configurations and HC for the third case

Index#	Conf.#	TS1	TS2	TS3	TS4	TS5	TS6	TS7	TS8	HC(kW)
1	51	0	0	1	1	0	0	1	1	6400
2	53	0	0	1	1	0	1	0	1	6640
6	83	0	1	0	1	0	0	1	1	6640
19	147	1	0	0	1	0	0	1	1	6640
7	85	0	1	0	1	0	1	0	1	7000
20	149	1	0	0	1	0	1	0	1	7000
3	54	0	0	1	1	0	1	1	0	7200
8	86	0	1	0	1	0	1	1	0	7680
21	150	1	0	0	1	0	1	1	0	7680
5	58	0	0	1	1	1	0	1	0	7720
4	57	0	0	1	1	1	0	0	1	7920
10	90	0	1	0	1	1	0	1	0	8320
23	154	1	0	0	1	1	0	1	0	8320
9	89	0	1	0	1	1	0	0	1	8480
22	153	1	0	0	1	1	0	0	1	8480
17	116	0	1	1	1	0	1	0	0	9880
26	166	1	0	1	0	0	1	1	0	9960
13	102	0	1	1	0	0	1	1	0	10200
30	180	1	0	1	1	0	1	0	0	10240
12	101	0	1	1	0	0	1	0	1	10320
25	165	1	0	1	0	0	1	0	1	10640
29	177	1	0	1	1	0	0	0	1	13080
24	163	1	0	1	0	0	0	1	1	13720
11	99	0	1	1	0	0	0	1	1	13760
16	113	0	1	1	1	0	0	0	1	14080
28	170	1	0	1	0	1	0	1	0	15080
15	106	0	1	1	0	1	0	1	0	15120
27	169	1	0	1	0	1	0	0	1	18520
14	105	0	1	1	0	1	0	0	1	18600
31	184	1	0	1	1	1	0	0	0	18960
18	120	0	1	1	1	1	0	0	0	19040

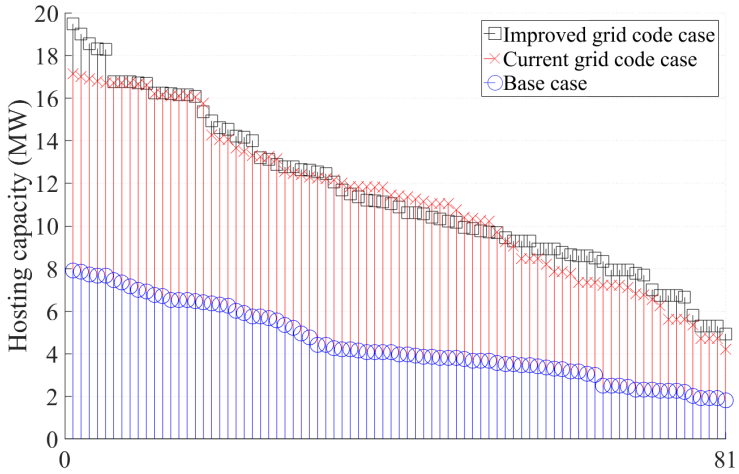

FIGURE 4.7: Sorted HC distribution for the meshed subset

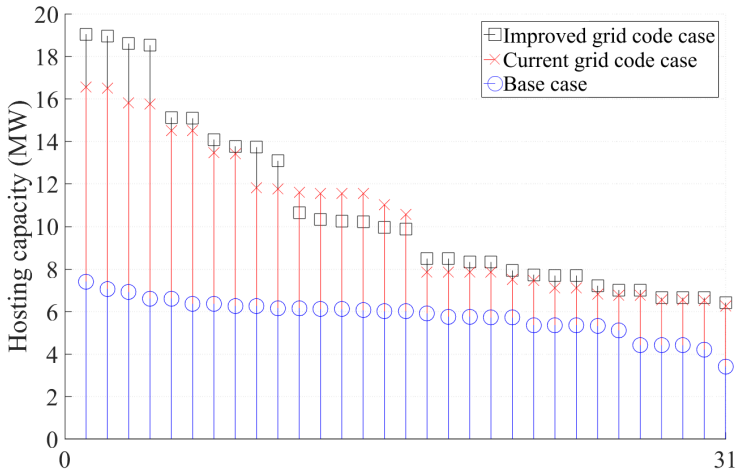

FIGURE 4.8: Sorted HC distribution for the radial subset

due to the higher reactive power reserve provided by the oversizing of the inverters and subsequent wider power factor range of 0.855 lead/lag compared to 0.9 lead/lag in the current grid code case.

The proposed changes in the grid codes utilize the grid closer to the maximum thermal limits. In the improved grid code case, with the increased reactive power reserve, the lines and the transformers work closer to their thermal limits, as it can be seen from the Figure 4.9 - Figure 4.14.

TABLE 4.3: Sorted meshed group switch configurations and HC for the third case

Index#	Conf.#	TS1	TS2	TS3	TS4	TS5	TS6	TS7	TS8	HC (kW)
4	62	0	0	1	1	1	1	1	0	4920
9	94	0	1	0	1	1	1	1	0	5280
30	158	1	0	0	1	1	1	1	0	5280
56	222	1	1	0	1	1	1	1	0	5280
1	55	0	0	1	1	0	1	1	1	5800
48	211	1	1	0	1	0	0	1	1	6640

Continued on next page

Table 4.3 – continued from previous page

Index#	Conf.#	TS1	TS2	TS3	TS4	TS5	TS6	TS7	TS8	HC (kW)
6	87	0	1	0	1	0	1	1	1	6720
27	151	1	0	0	1	0	1	1	1	6720
51	215	1	1	0	1	0	1	1	1	6720
49	213	1	1	0	1	0	1	0	1	7000
50	214	1	1	0	1	0	1	1	0	7680
77	251	1	1	1	1	1	0	1	1	7760
8	93	0	1	0	1	1	1	0	1	7920
29	157	1	0	0	1	1	1	0	1	7920
55	221	1	1	0	1	1	1	0	1	7920
53	218	1	1	0	1	1	0	1	0	8320
52	217	1	1	0	1	1	0	0	1	8480
3	61	0	0	1	1	1	1	0	1	8600
21	122	0	1	1	1	1	0	1	0	8600
2	59	0	0	1	1	1	0	1	1	8640
5	63	0	0	1	1	1	1	1	1	8760
10	95	0	1	0	1	1	1	1	1	8920
31	159	1	0	0	1	1	1	1	1	8920
57	223	1	1	0	1	1	1	1	1	8920
7	91	0	1	0	1	1	0	1	1	9280
28	155	1	0	0	1	1	0	1	1	9280
54	219	1	1	0	1	1	0	1	1	9280
22	123	0	1	1	1	1	0	1	1	9440
76	250	1	1	1	1	1	0	1	0	9680
45	189	1	0	1	1	1	1	0	1	9720
39	182	1	0	1	1	0	1	1	0	9760
47	191	1	0	1	1	1	1	1	1	9880
18	118	0	1	1	1	0	1	1	0	9920
40	183	1	0	1	1	0	1	1	1	10160
19	119	0	1	1	1	0	1	1	1	10200
60	230	1	1	1	0	0	1	1	0	10320
32	167	1	0	1	0	0	1	1	1	10400
73	247	1	1	1	1	0	1	1	1	10560
26	127	0	1	1	1	1	1	1	1	10600
70	244	1	1	1	1	0	1	0	0	10600
72	246	1	1	1	1	0	1	1	0	10880
59	229	1	1	1	0	0	1	0	1	11040
24	125	0	1	1	1	1	1	0	1	11120
38	181	1	0	1	1	0	1	0	1	11160
17	117	0	1	1	1	0	1	0	1	11200
37	179	1	0	1	1	0	0	1	1	11360
71	245	1	1	1	1	0	1	0	1	11480
20	121	0	1	1	1	1	0	0	1	11680
41	185	1	0	1	1	1	0	0	1	12040
81	255	1	1	1	1	1	1	1	1	12440
46	190	1	0	1	1	1	1	1	0	12520
16	115	0	1	1	1	0	0	1	1	12600
23	124	0	1	1	1	1	1	0	0	12640
25	126	0	1	1	1	1	1	1	0	12760
43	187	1	0	1	1	1	0	1	1	12760
79	253	1	1	1	1	1	1	0	1	12880
69	243	1	1	1	1	0	0	1	1	13120
80	254	1	1	1	1	1	1	1	0	13200
58	227	1	1	1	0	0	0	1	1	14000
11	103	0	1	1	0	0	1	1	1	14160
61	231	1	1	1	0	0	1	1	1	14200

Continued on next page

Table 4.3 – continued from previous page

Index#	Conf.#	TS1	TS2	TS3	TS4	TS5	TS6	TS7	TS8	HC (kW)
68	241	1	1	1	1	0	0	0	1	14520
75	249	1	1	1	1	1	0	0	1	14600
42	186	1	0	1	1	1	0	1	0	14920
63	234	1	1	1	0	1	0	1	0	15360
36	175	1	0	1	0	1	1	1	1	16080
15	111	0	1	1	0	1	1	1	1	16160
35	174	1	0	1	0	1	1	1	0	16160
14	110	0	1	1	0	1	1	1	0	16200
66	238	1	1	1	0	1	1	1	0	16240
67	239	1	1	1	0	1	1	1	1	16240
34	173	1	0	1	0	1	1	0	1	16680
65	237	1	1	1	0	1	1	0	1	16720
13	109	0	1	1	0	1	1	0	1	16760
44	188	1	0	1	1	1	1	0	0	16760
78	252	1	1	1	1	1	1	0	0	16760
33	171	1	0	1	0	1	0	1	1	18280
12	107	0	1	1	0	1	0	1	1	18320
64	235	1	1	1	0	1	0	1	1	18560
62	233	1	1	1	0	1	0	0	1	19000
74	248	1	1	1	1	1	0	0	0	19480

Figure 4.13 and Figure 4.14 show that in the improved grid code case, with the proposed reactive power reserve improvement via curtailment or oversizing of the inverters, the line loading is a major limitation for the grid integration of PVs. Also, we observe that for the base case, when the inverters work at unity power factor, the lines are less loaded in the meshed configurations than in the radial configurations. Although the HC changes are not significant between meshed and radial subsets for the base case (Figure 4.7 and Figure 4.8), the average loading of the lines decreases from 75.6% to 44.6%. Thus, the selection of meshed configurations is more preferable.

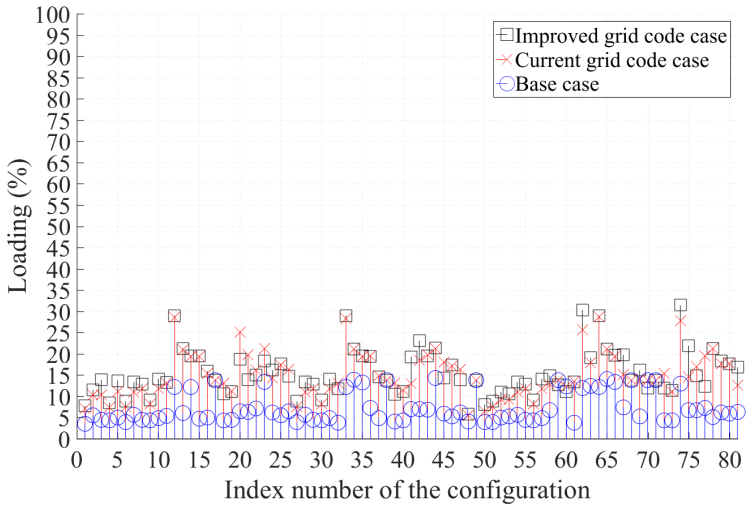

FIGURE 4.9: Transformer Tr1 loading for the meshed subset

FIGURE 4.10: Transformer Tr1 loading for the radial subset

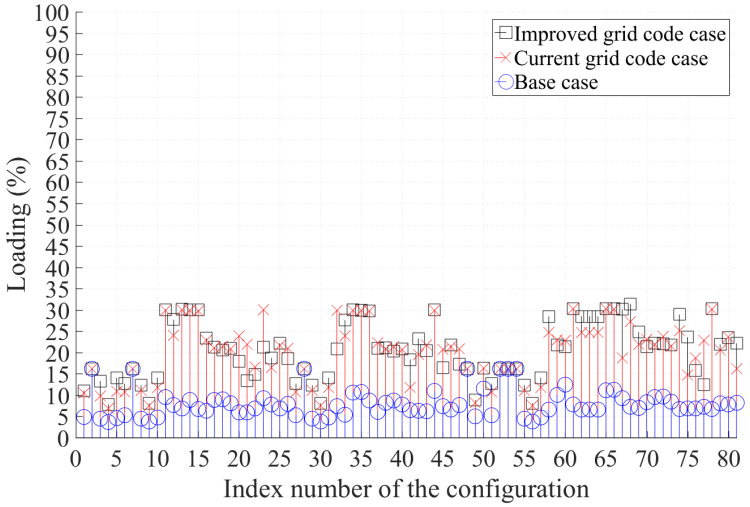

FIGURE 4.11: Transformer Tr2 loading for the meshed subset

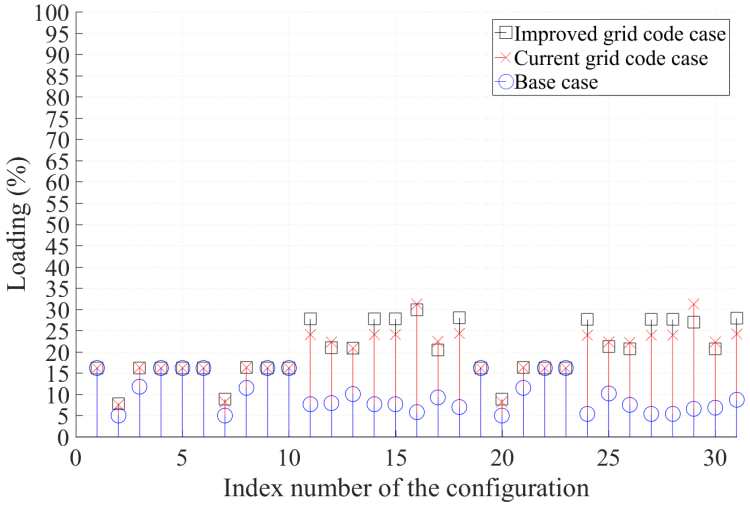

FIGURE 4.12: Transformer Tr2 loading for the radial subset

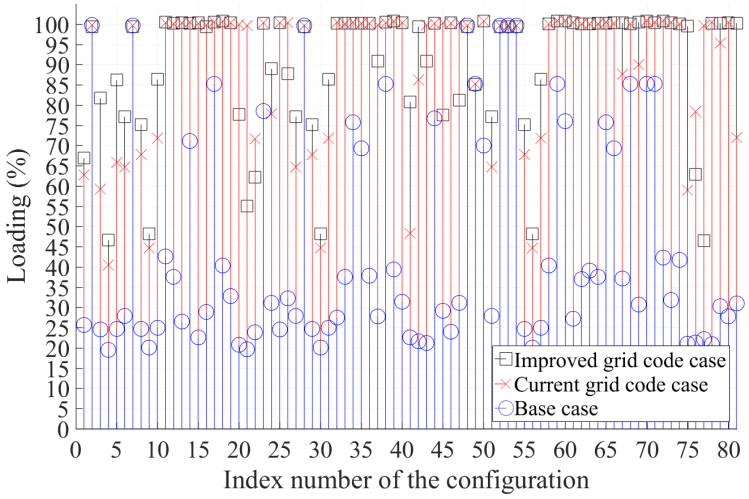

FIGURE 4.13: Line loading for the meshed subset

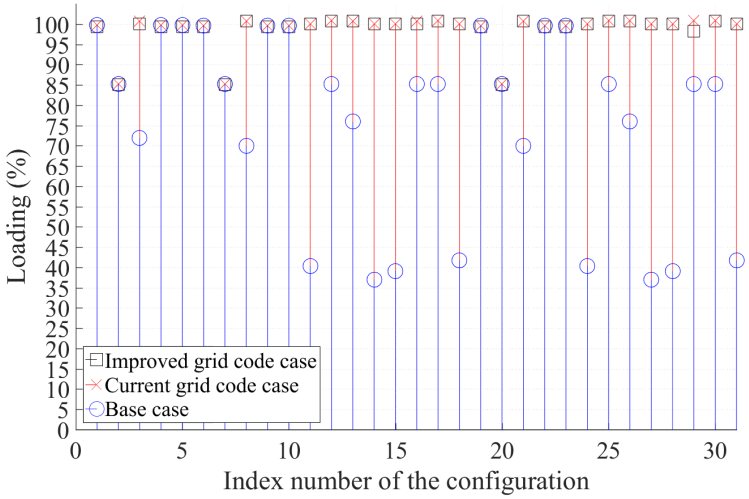

FIGURE 4.14: Line loading for the radial subset

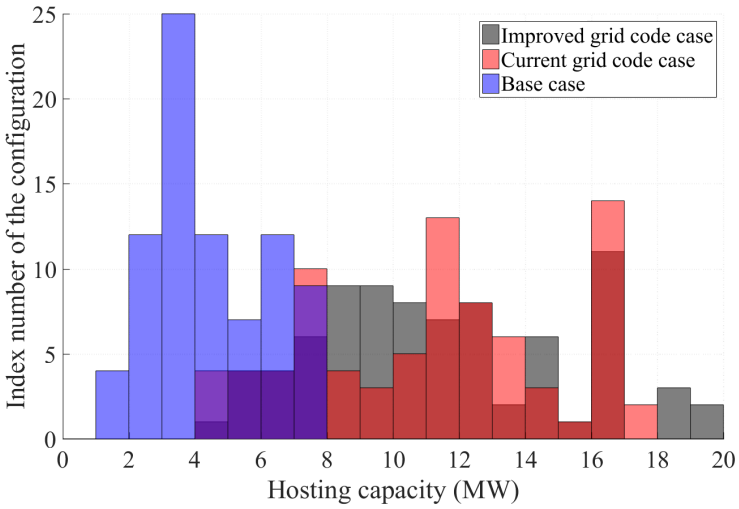

FIGURE 4.15: Reconfiguration degree of freedom for the meshed subset

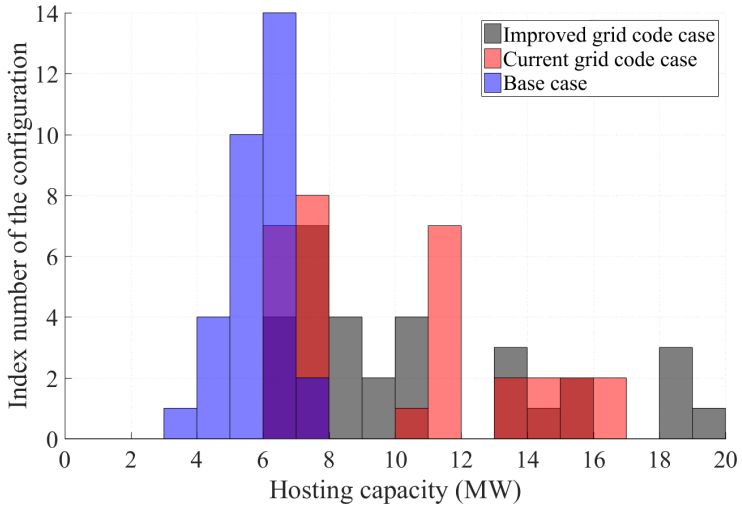

FIGURE 4.16: Reconfiguration degree of freedom for the radial subset

Figure 4.15 and Figure 4.16 present the number of possible configurations for a specified range of HC for each case, for meshed and radial subsets respectively. As observed, there are more configurations with higher HC in the meshed subsystem than in the radial subsystem. The average HC of the meshed subset is 7% higher than the one of the radial subset. Similarly, the maximum HC of the meshed subset is 2% higher than the one of the radial subset. These histograms provide the grid operators with a degree of freedom in reconfiguration during the system contingencies to keep the integration level within certain values.

4.5 Conclusion

In this chapter, an analysis of PV hosting capacity improvement in a medium voltage network via grid reconfiguration and grid code improvements is presented. Grid code improvements, by the means of power factor extension and PV inverter oversizing proved to considerably increase the hosting capacity of the system and utilize the grid closer to the designed limits. Meshed grid configurations are able to decrease the loading of the lines and provide higher number of configurations with high values of hosting capacity. Using the versatility of the Pandapower software, it has been shown that grid reconfiguration analysis should be the first consideration in PV hosting capacity improvement for the grid operators since it can substantially increase the hosting capacity and does not require any additional expensive grid reinforcement. Additionally, grid reconfiguration degree of freedom is introduced

as a means to safely reconfigure the system without substantial decrease in the hosting capacity. In addition, the grid reconfiguration analysis provides opportunity for an interdisciplinary research on pattern recognition in grid configuration subsets. For example, finding certain switches which should always be kept closed in order to accommodate a certain amount of PV.

Chapter 5

Extended Current Droop Control of PV Plants

This chapter presents the developed extended active and reactive current droops for controlling the output of the PV plants connected in a meshed medium voltage (MV) grid. Four PV plants are connected at different points of the grid to evaluate the load sharing capability, the cross-influence of PV plants and the influence of their connection location. The static and dynamic performance of the droops is analyzed. Abrupt load variation is performed to assess the dynamic performance of the proposed extended droop control. The superiority of the extended droops over the traditional droops during voltage fluctuations in the grid is demonstrated via simulations.

5.1 Droop control

As mentioned in the Chapter 2 the reactive power control and active power curtailment are one of the main solutions to overcome the overvoltage and overloading problems when enhancing the HC.

One of the most common control strategies used for controlling the overvoltages at the connection point is the droop control [120], [121].The droop control is also being used to ensure proper load sharing and parallel operation of the inverters in the grid [122], [123]. The advantages of droop control include the flexibility, high reliability, different power ratings and the absence of communication [124]–[126]. The droop control has its drawbacks amongst which are the poor harmonic sharing, coupling inductances, influence of system impedance and slow dynamic response [127]–[129]. To overcome the mentioned drawbacks several solutions have been proposed. Variable virtual droops have been proposed in [127], [130] to overcome the issues with coupling impedances. To enhance the dynamic response adaptive decentralised

droops are proposed in [131]. To overcome the problems associated with the line impedance Lin et al. [132] proposed a decoupled active and reactive power droops, Hanaoka et al. [133] presented reactive current addition to the droop control. In [134], Liu et al. enhanced droop control is demonstrated for meshed and radial DC microgrids. The control proposed by the authors takes into account the effects of communication delay and line impedance and eliminates the voltage deviation and enhances the load power sharing accuracy.

5.2 Extended current droops

The grid support capabilities of the inverters are limited by their power rating, the availability of the primary energy and more limiting, the grid codes. In the current VDE-AR 4110:2018 grid codes, the reactive power output is limited by the power factor and depends on the generated active power [9]. As a result, during sub-nominal active power production the full reactive power capability of the inverter is not being used (Figure 5.1a).

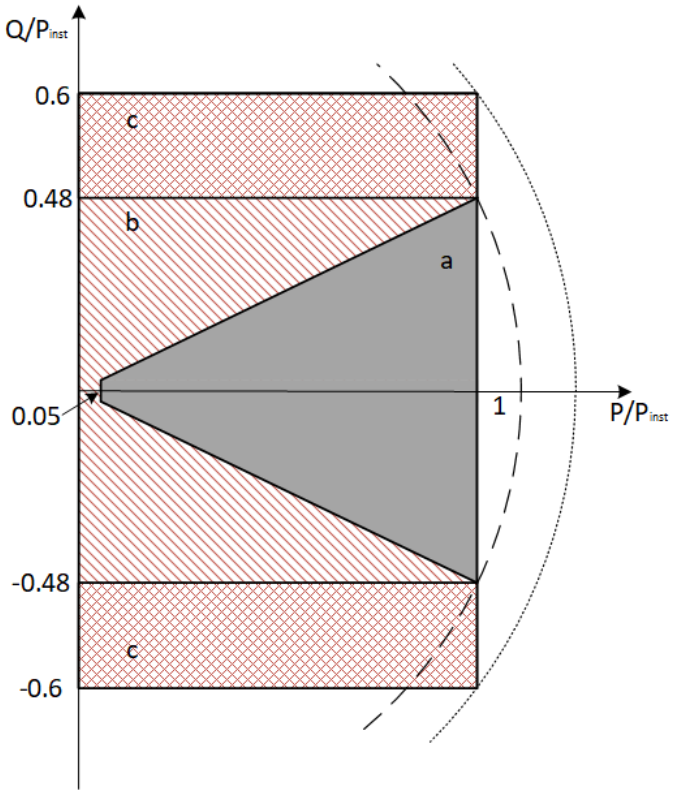

FIGURE 5.1: Reactive power capability requirement for PV inverters: a - VDE-AR 4110:2018, b - proposed for normal operation, c - proposed for contingencies

To overcome the current grid-code limitations and to boost the full usage of the reactive power support capability of the inverters during system contingencies, new requirements of reactive power capability are proposed (Figure 5.1b, c). In the proposed reactive power capability requirement, the reactive power output of the inverter is independent of the active power output, meaning that the inverters can provide reactive power support at their full reactive power capacity within the active power range of 0 to 100%. Thus, the maximum value of the reactive power will be limited only by the total installed power of the PV inverter (Figure 5.1b). Additionally, in the events of system contingency, the inverters will be able to provide extra reactive power capacity, if requested by the distribution system operator via centralized control or defined by the grid codes and local reactive power control scheme (Figure 5.1c): $-0.8 \leq cos\varphi \leq 0.8$, i.e $-0.6 * S \leq Q \leq 0.6 * S$.

In order to ensure proper load sharing and parallel operation of the inverters in the grid, droop control is commonly being used [129], [130], [134], [135]. Based on the proposed reactive power capability requirement, an improved, extended reactive and active current droops $I_q(V)/I_d(V)$ are developed (Figure 5.2). Compared to the regular droops, as presented in the VDE-AR 4110 grid code, the proposed reactive current droop increases the absolute maximum reactive current value when the voltage value is more than 1.04 p.u. (Eq. (5.1)).

$$\begin{cases} |I_{qref}| = -25 * 0.436 * I_{max} * (V_{PCC} - 1), & \text{if} \quad V_{PCC} \leq 1.04\ p.u. \\ |I_{qref}| = 0.6 * I_{max}, & \text{if} \quad V_{PCC} > 1.04\ p.u. \end{cases} . \quad (5.1)$$

In this manner, during full active power production, the power factor limitation of ± 0.9 is being changed to ± 0.8 when the voltage is higher than 1.04 p.u.. Thus, providing extra reactive power reserve and eliminating the extra losses caused by excess reactive power flow compared to regular full-time power factor ± 0.8 operation during normal operating conditions.

The developed extended current droops also comprise active power curtailment (APC) droop where the active power output of the PV plant is being linearly decreased from 100% to 0%, starting at 1.04 p.u. up to 1.1 p.u. voltage levels (Eq. (5.2)).

$$\begin{cases} |I_{dref}| = 0.8 * I_{max}, & \text{if} \quad V_{PCC} \leq 1.04\ p.u. \\ |I_{dref}| = \frac{0.8*(1.1-V_{PCC})}{1.1-1.04} * I_{max}, & \text{if} \quad 1.04\ p.u. < V_{PCC} < 1.1\ p.u. \\ |I_{dref}| = 0, & \text{if} \quad V_{PCC} \geq 1.1\ p.u. \end{cases} . \quad (5.2)$$

The combination of the proposed active and reactive current droops has been applied to the modeled test grid and the performance is compared with the no droop, regular reactive current droop and regular reactive current droop with APC droops cases. The details of the grid configuration and detailed analysis of the simulation results are presented in the next section.

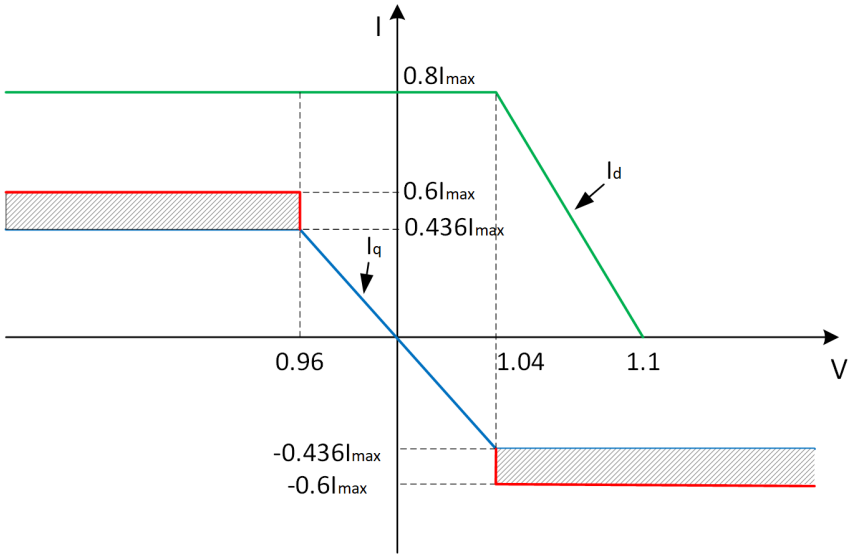

FIGURE 5.2: Extended reactive and active current droops

5.3 Test grid structure and simulation setup

To test the static and dynamic performance of the developed extended current droops, a modified version of the grid model used in the Chapter 4 is used as a test grid for this chapter and modeled in Matlab Simulink. Since the grid reconfiguration analysis has shown that the transformers have been underloaded compared to the lines and the average loading of the transformer Tr1 has been less compared to Tr2, a decision was made to remove Tr1 and to decrease the rated power of Tr2 from 31 MVA to 10 MVA. In this version of the grid model all the tie-switches are closed and the grid is highly meshed (Table. 5.1). To assess the cross-influence of PVs and the influence of PV location, four PV plants and five loads are connected at various points of the

TABLE 5.1: Tie-switch combination

Tie-switch Status	TS1 Closed	TS2 Closed	TS3 Closed	TS4 Closed
Tie-switch Status	TS5 Closed	TS6 Closed	TS7 Closed	TS8 Closed

TABLE 5.2: Load and PV data

	Connection bus	P [kW]	Q [kVAr]	Dispatching time
PVs				
PV 1	17	400	-300 to 300	No dispatching
PV 2	22	200	-150 to 150	No dispatching
PV 3	31	300	-225 to 225	No dispatching
PV 4	42	100	-75 to 75	No dispatching
Total		1000	-750 to 750	
Loads				
Load 1	17	250	0	Disconnect t=4s
Load 2	17	300	0	Disconnect t=2.5s
Load 3	26	272.1	55.2 inductive	Disconnect t=4s
Load 4	18	0	200 capacitive	Connect t=5.5s
Load 5	21	272.1	55.2 inductive	Disconnect t=2.5s
Total		1094.2	200, capacitive 110.4, inductive	

grid (Figure 5.3). The detailed load and PV parameters are presented in Table. 5.2.

To test the efficiency of the proposed extended current droops performance during grid disturbances and overvoltages, the grid is subjected to load changes at time points 2.5s, 4s and 5.5s. More specifically the loads 2 and 5 are disconnected at 2.5s to have a partial loading case, the loads 1 and 3 at 4s to have a no load case, and the load 4, which is a capacitive load, is connected at 5.5s to model a significant voltage rise in the grid.

In order to demonstrate their performance, the developed extended current droops are compared with other, more traditional PV control strategies, namely:

- No droop case: In this case the PV plants are operating at unity power factor and are injecting only active power.
- Reactive current droop case: In this case the PV plants are also taking part in the voltage regulation via droops within the power factor range of ± 0.9.

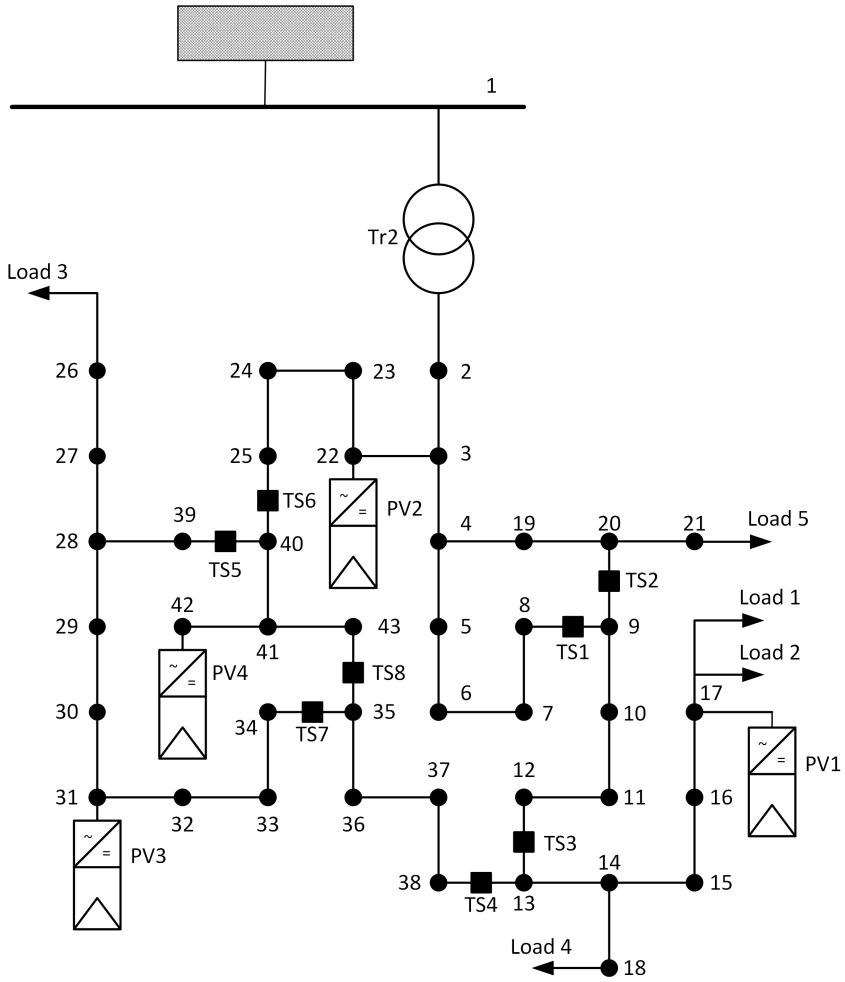

FIGURE 5.3: Test grid model with only one transformer at reduced nominal power

- Reactive current droop + APC case: In this case in addition to the previous case the active power is curtailed based on the proposed strategy.
- Extended reactive current droop + APC case: In this case the PV plants operate with the designed extended reactive current droops with active current curtailment.

5.4 Simulation results

In this section the simulation results are discussed. As mentioned in the previous section, the loads are being dispatched during the simulation at time points 2.5s, 4s and 5.5s, in order to have varying voltage levels in the grid and to test the static and dynamic performance of the proposed extended current droops. Thus, the simulation can be divided into four parts:

- full load, $0s \leq t \leq 2.5s$

- partial load, $2.5s \leq t \leq 4s$
- no load, $4s \leq t \leq 5.5s$
- capacitive load, $5.5s \leq t \leq 7s$

The main goal of the designed extended control is to maintain a lower voltage profile of the network and decrease the amount of curtailed active power during overvoltages. As it can be seen from Figure 5.4, the voltages at the PV connection points and the transformer secondary are lower with the proposed extended droop control compared with the other cases. This is mainly due to the fact that the proposed extended reactive current droop provides extra reactive power reserve at the times when the regular droop is not able to keep the voltage level below 1.04 p.u..

For the simplicity the performance of the extended droops only for PV1 inverter has been analyzed.

During the full load operation ($t = 0 - 2.5s$) all the control strategies perform well to keep the PCC voltage level below 1.04 p.u.. However, the droop control strategies maintain a lower voltage value because of reactive power support.

After load 2 and load 5 have been disconnected at $t = 2.5s$, the no droop control strategy is no more capable to keep the PCC voltage below 1.04 p.u.. On the contrary, the other three control strategies keep the voltage at PCC at 1.035 p.u. as they all use the same droop control following the ± 0.9 power factor limitation.

At $t = 4s$ load 1 and load 3 are being disconnected in order to have a no load case and to further increase the voltage level of the grid. In this case, we can see that the proposed extended current droop control is the only one to be able to keep the PCC voltage at 1.04 p.u. without curtailing the active power output (Figure 5.5), as a result of the extra reactive power capability added by the change of power factor limitation from ± 0.9 to ± 0.8.

In order to compare the curtailment performance of the proposed extended current droops with the regular droops, a capacitive load is connected at bus 18 at $t = 5.5s$ to increase the voltage levels of the grid. As we can see from Figure 5.4 and Figure 5.5, the extended current droops are able to keep the lowest voltage and to curtail only 7.9% of the active power output compared to 13.5% for the regular droop with APC, which is 41.5% less.

We have similar behavior for all other three PV plants connected to the grid (Figure 5.4 - 5.6). Moreover, the dynamic performance of the extended current droop control is compared with the other three control strategies. It is

able to keep the system stable and fast responding, as there are almost no oscillations and the voltage is settling within 60ms.

The reactive power reserve of the PV inverters has been increased by 37.6% with the use of the proposed extended droops. Thus, the inverters absorb more reactive power and consequently decrease the reactive power flow through the substation transformer, hence decreasing the loading of the transformer (Figure 5.6, Figure 5.8, Figure 5.9). The extended current droop strategy lowers the loading of the transformer by 23.8% and 3.3% compared to the no droop and regular droop with APC cases respectively.

Although the frequency stability is outside the scope of this thesis, the frequency response of the system is shown in Fig 5.10. We can see that the proposed extended current droop control strategy does not impair the frequency stability of the system. Moreover, in some cases the extended droop control can reduce the peaks of the frequency spikes during the sudden load changes.

5.5 Conclusion

The designed extended droop control with active power curtailment is a viable and non-expensive grid reinforcement strategy which can not only regulate the voltage at the point of common coupling, but also relax the transformer loading and improve overall voltage and frequency stability. Additionally, oversizing of the inverter by 12.5% compared to the VDE4110:2018 grid codes can increase the reactive power reserve of the inverters by 37.6% and result in up to 6.5% more PV injection into the grid compared to the regular droop case.

Thus, the grid code modification and the extended current droops can be a cost effective grid reinforcement solution without any change of the hardware infrastructure.

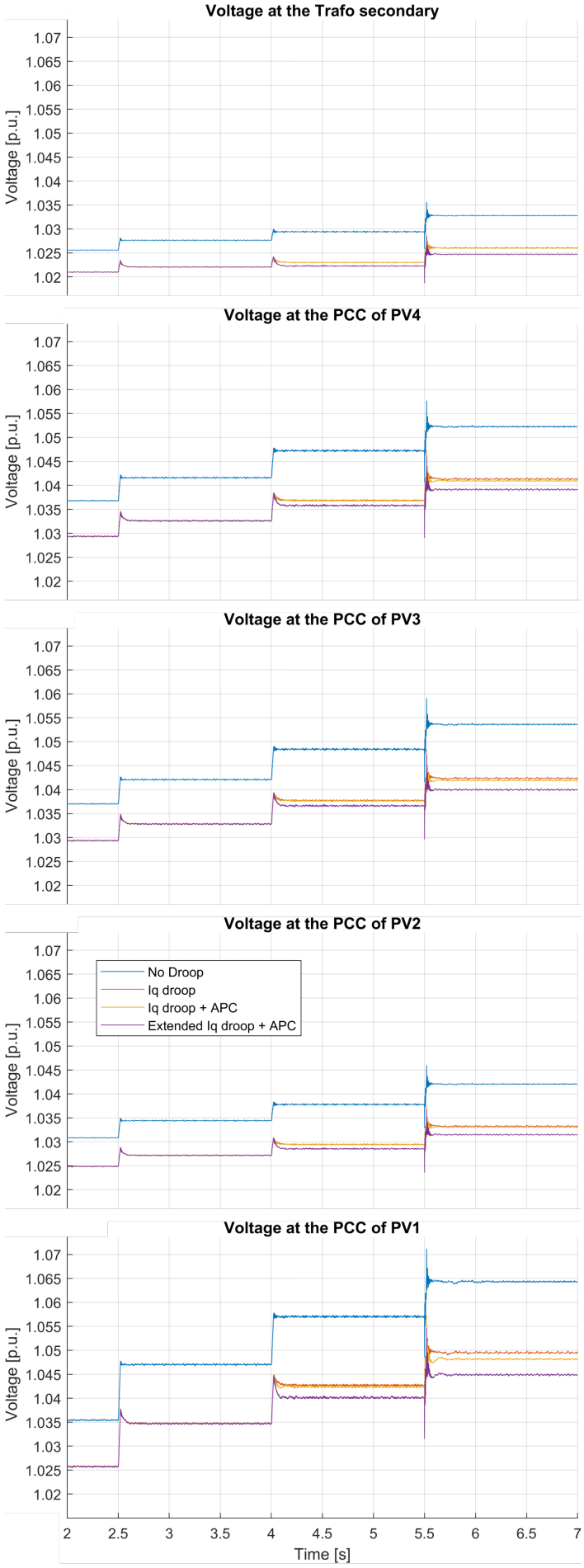

FIGURE 5.4: Voltages at the PV PCC and transformer secondary

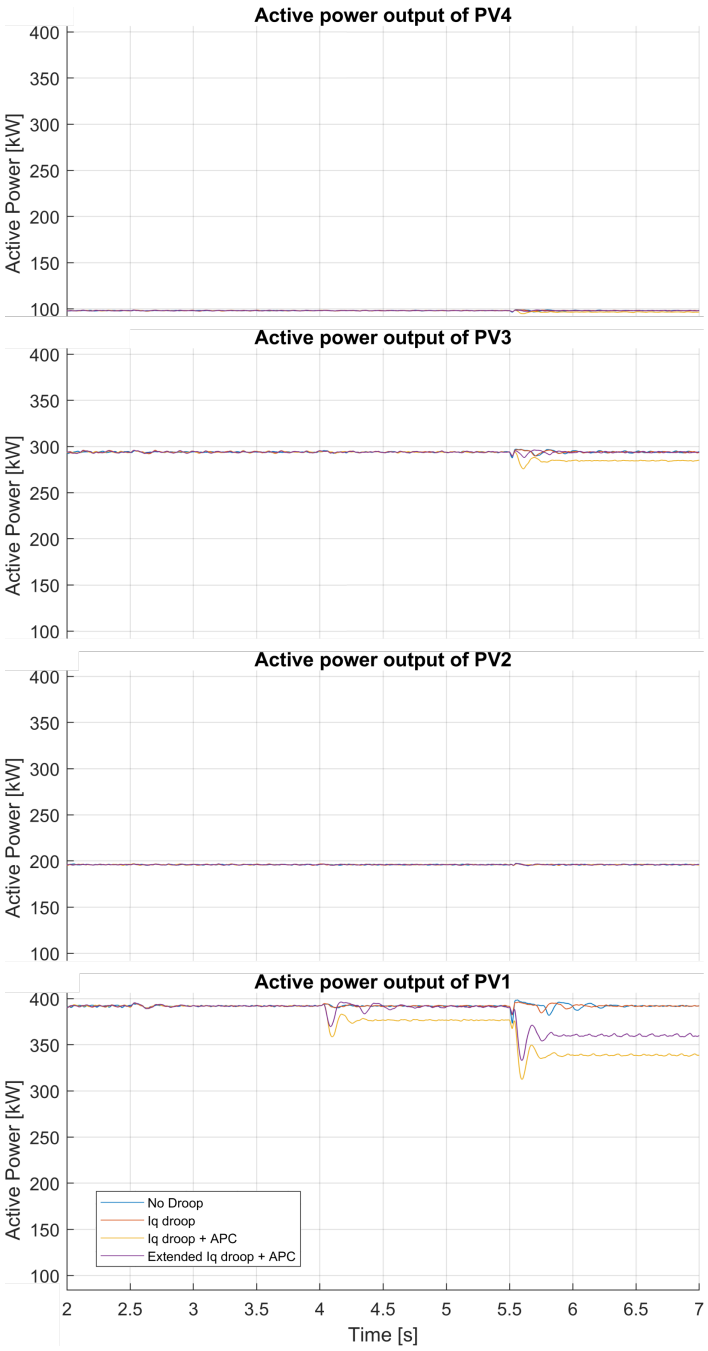

FIGURE 5.5: Active power outputs of PVs

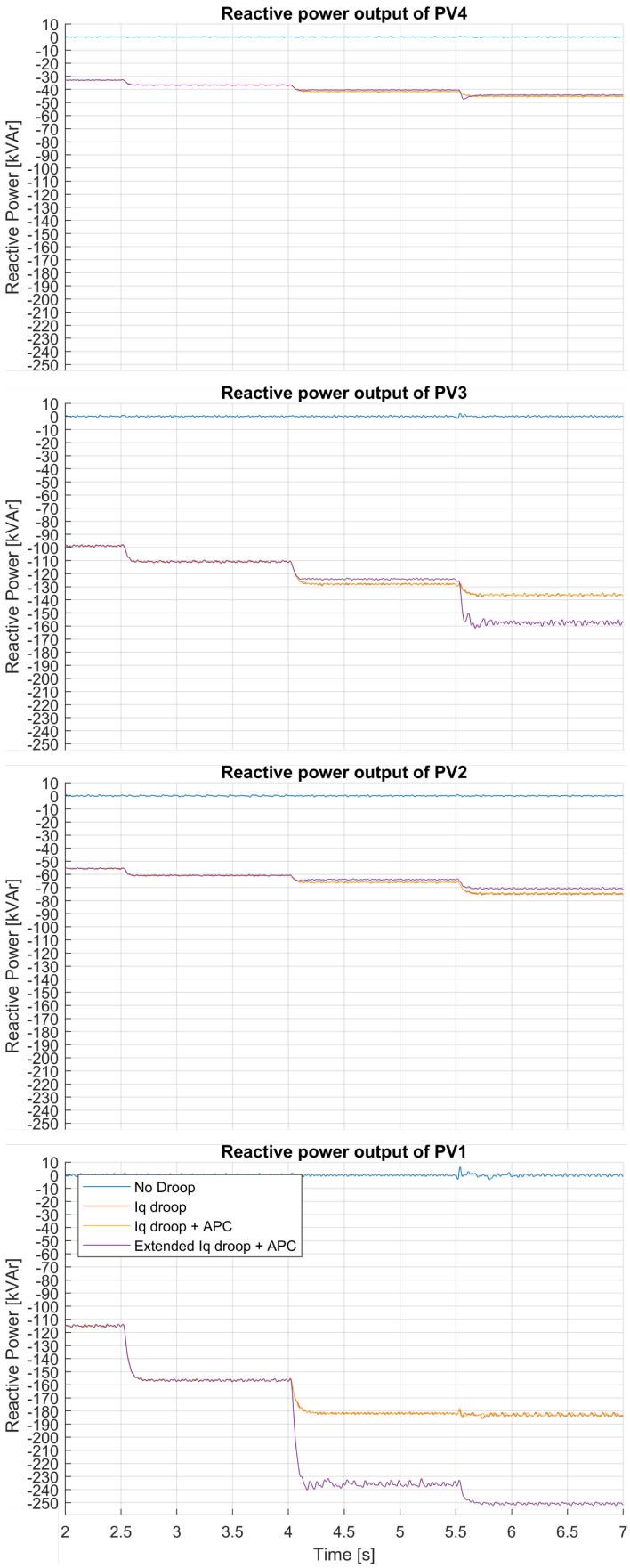

FIGURE 5.6: Reactive power outputs of PVs

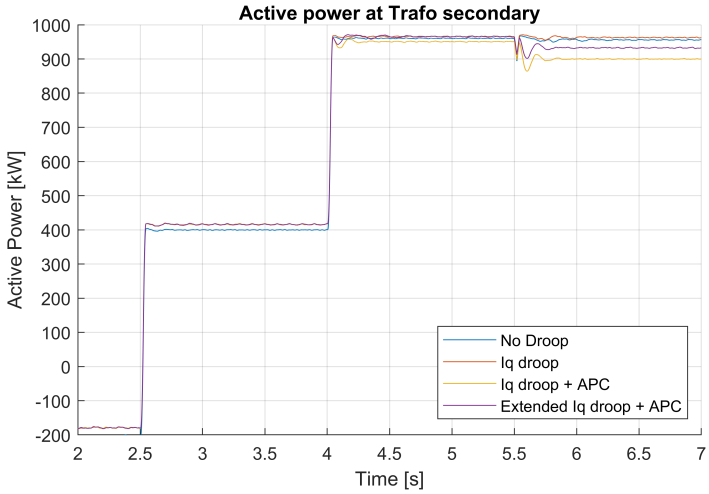

FIGURE 5.7: Active power at the transformer secondary

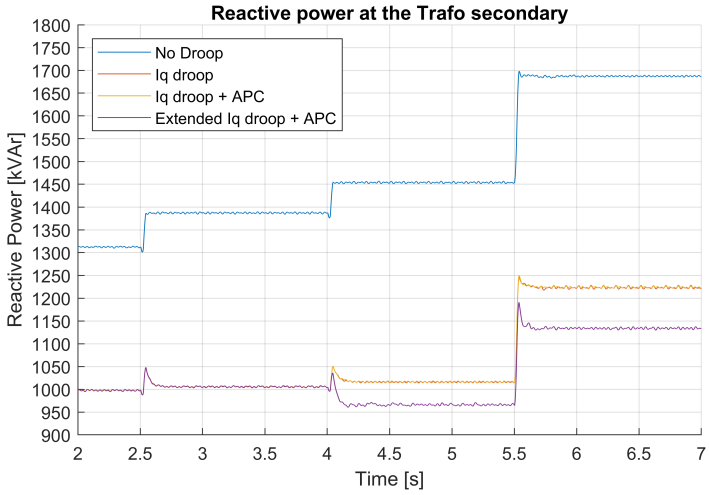

FIGURE 5.8: Reactive power at the transformer secondary

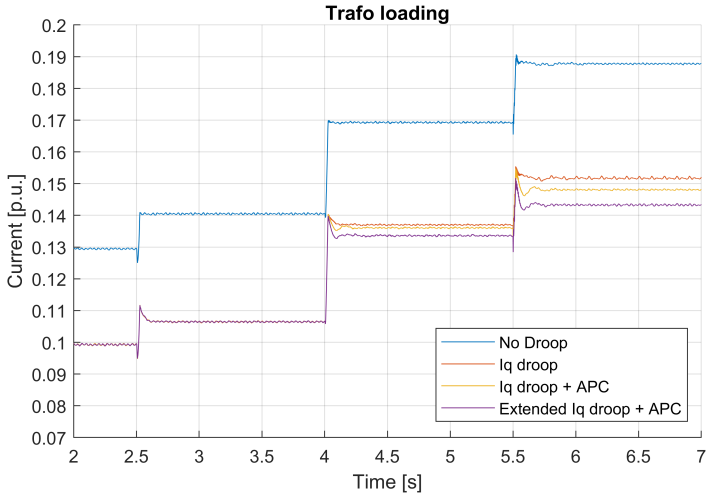

FIGURE 5.9: Transformer loading

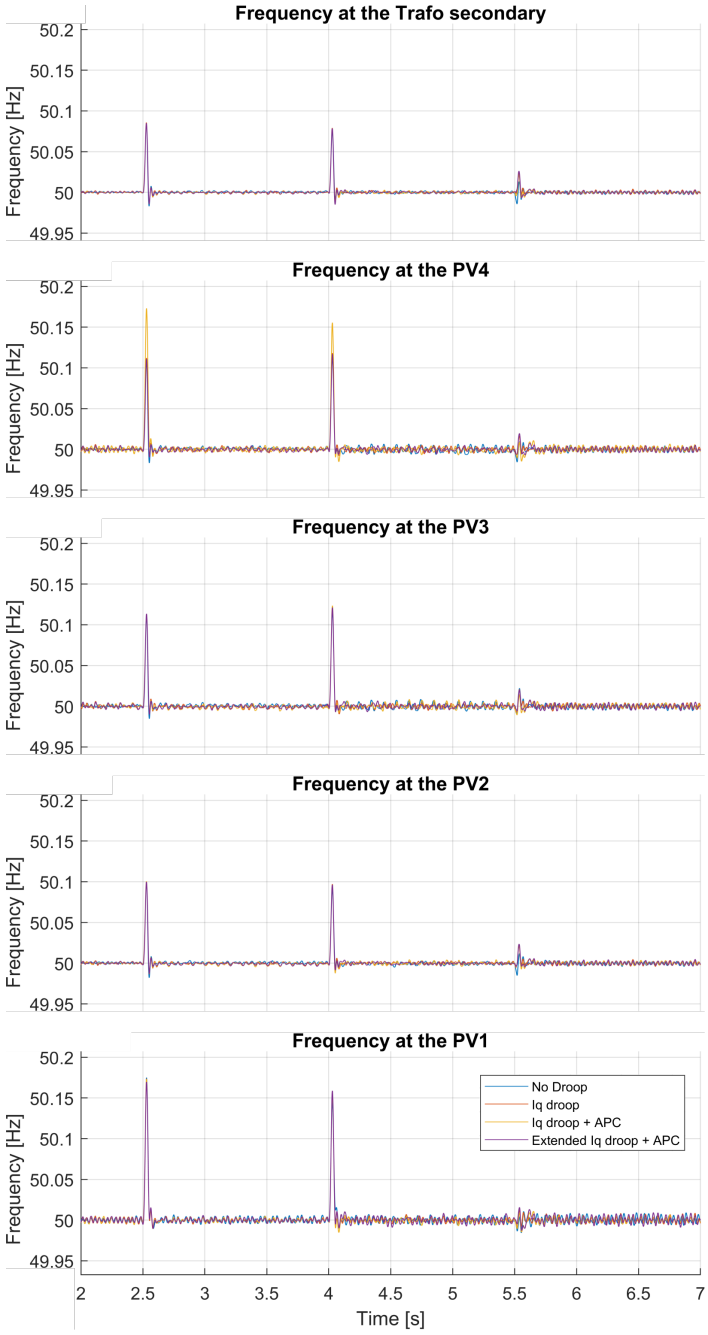

FIGURE 5.10: Frequency at the PV PCCs and transformer secondary

Chapter 6

Overloading Control of Substation Transformer

This chapter presents a comparison of two novel overloading prevention strategies of substation transformer. The strategies are designed to protect the transformer during high PV production and low load situations via reactive power control using a battery energy storage (BES) connected at the MV side of the substation transformer. The first strategy is based on reactive current droop control, whereas the second strategy relies on PI control of the reactive power. The proposed strategies do not depend on any communication means and are connection fail-safe. The proposed strategies are tested on a modified version of the meshed network used in the previous chapter. The hosting capacity (HC) improvement and their static and dynamic performance are assessed in comparison to the no curtailment case. Additionally, the influence of the substation transformer power rating on the system stability and PV output curtailment is analyzed.

6.1 Transformer overloading protection

As mentioned in the Chapter 2, the next limiting factor of the growth of installed PV capacity is the overloading of lines and transformers. The existing grids have been designed for a certain range of load and generation without considering the future increase in the number of PV installations and reverse power flows. The increased PV generation share in the grid can lead to critical situations, when the current flowing through the transformer may exceed the nominal value. Moreover, due to the intermittent nature of the solar irradiation, the output of the PVs can vary, which can lead to critical situations when PV production peaks can cause a short-term overloading of

transformer. For example, during low load and high PV production hours over the day.

One of the common solutions to the transformer overloading problem is the replacement of the transformer or the reinforcement of the substation by adding an additional transformer. From the economic point of view this solution might not be the most cost saving solution.

In this chapter two novel communication-less strategies for transformer active protection are proposed and compared against each other and no protection case. These strategies are based on deployment of a BES. The BES can not only store the excess active power and provide power when needed, but also provide ancillary grid support services like a flexible alternating current transmission system (FACTS) device. For example, BES can act as a static synchronous compensator (STATCOM) and provide reactive power support to the grid in addition to the already generated or stored active power if requested by the grid operator [136], [137]. Both designed strategies use a modified BES system connected at the transformer secondary side. The modified BES system is designed not only to shave the active power production peaks by charging up and providing active power when needed, but also it has reserved capacity for the provision of reactive power support to the grid. The main idea behind both strategies is to force the PV plants to curtail their active power output by artificially increasing the grid voltage. The difference between the two strategies is the implementation of BES control.

The detailed description of the strategies and the assessment of their performance are presented in the next sections.

6.1.1 Transformer protection droops

The main idea of the transformer protection droop (TPD) strategy is to indirectly force the PV inverters to curtail their active power output to protect the substation transformer from overloading without relying on communication. Since the PV inverters operate based on $I_q(V)/I_d(V)$ droops, the only solution to force them to curtail the active power, without a centralized curtailment signal, would be to artificially increase the voltage profile of the grid. To do so, the BES will inject reactive power into the grid based on droops (Eq. 6.1). The BES starts to inject reactive power when the loading of the transformer reaches 80%. The injection is done based on the droops and reaches the maximum value when the transformer loading is at 100%.

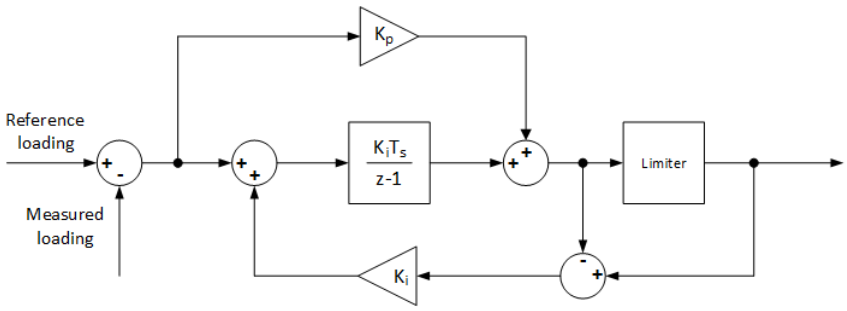

FIGURE 6.1: DLC control structure

$$\begin{cases} I_{qref\_BES} = -5 * (I_{Tr} - 0.8), & \text{if} \quad I_{Tr} > 0.8\ p.u. \\ I_{qref\_BES} = 0, & \text{if} \quad I_{Tr} \leq 0.8\ p.u. \end{cases} \tag{6.1}$$

6.1.2 Direct loading control

The direct loading control (DLC) strategy works in the same principle as the TPD. It also injects reactive power to the grid, in order to raise the voltage profile of the grid and force the $I_q(V)/I_d(V)$ droop controlled PV inverters to curtail their active power output. The only difference is the type of control used for controlling the reactive power output of the BES. On the contrary to the TPD strategy, the DLC strategy uses a PI controller with integrator anti windup to control the reactive power output of the BES, Figure 6.1. The developed DLC strategy, similar to the TPD strategy, is a local control strategy that does not rely on communication. It only relies on the local measurement of the current flowing through the transformer secondary winding. The DLC strategy is activated only when the transformer loading is more than 100%. After being activated the DLC controls the transformer loading at 100% and turns off when it is below 100%.

6.2 Test grid structure and simulation setup

A slightly modified version of the grid model used in the Chapter 5 is applied for assessing the performance of the TPD and DLC strategies and the influence of the total installed PV power and transformer power rating ratio on the voltage stability and overloading of the substation transformer. In comparison to the grid model used in the Chapter 5, the modified grid model has a BES system connected at the secondary side of the HV/MV substation transformer, at bus 2, it has a different load setup and the power rating of the

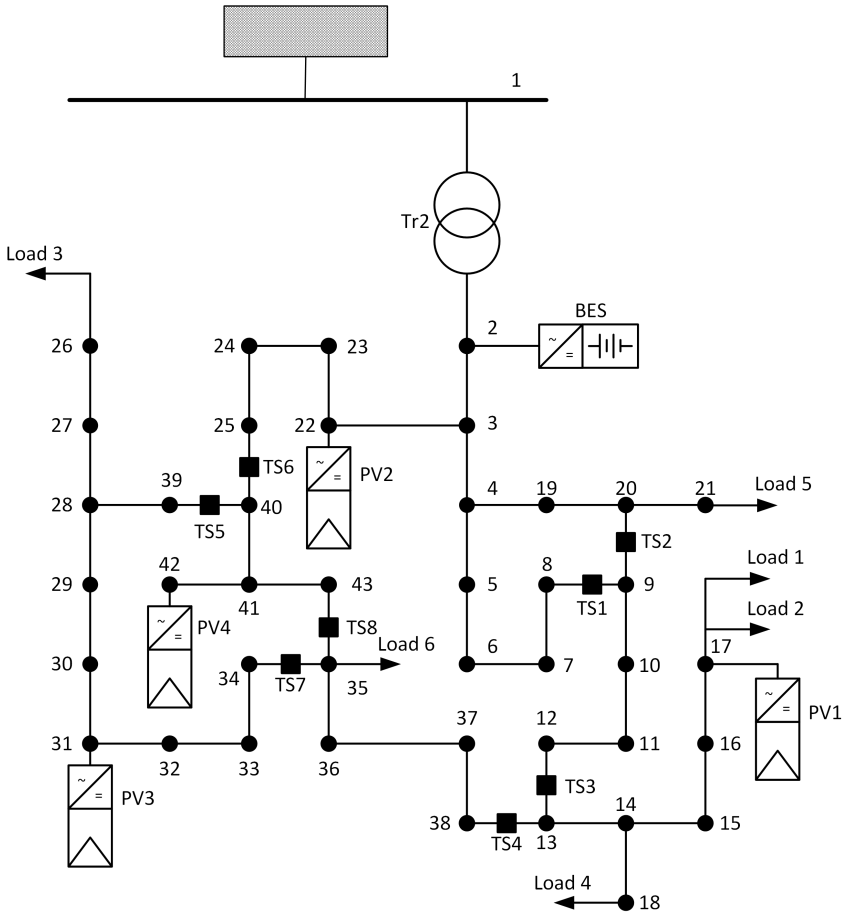

FIGURE 6.2: Test grid model

TABLE 6.1: Tie-switch configuration

Tie-switch Status	TS1 Closed	TS2 Closed	TS3 Closed	TS4 Closed
Tie-switch Status	TS5 Closed	TS6 Closed	TS7 Closed	TS8 Closed

HV/MV substation transformer is set to 1.25 MVA (Figure 6.2). The grid load and generation configuration data are presented in Table 6.2.

The simulations are divided into two parts: static and dynamic. In the static analysis, the influence of the ratio of the total installed PV power and the substation transformer power rating on the performance of the TPD and DLC strategies is assessed for different loading conditions. In the dynamic analysis, the focus is on the transient performance of the TPD and DLC strategies during the sudden load changes. The loading scenarios are presented in Table 6.3.

TABLE 6.2: Load and generator data

	Connection bus	P [kW]	Q [kVAr]	Dispatching time
Transformer				
Tr2	2		1250	No dispatching
Loads				
Load 1	17	250	0	Disconnect t=2.5s
Load 2	17	300	0	Disconnect t=1.5s
Load 3	26	272.1	55.2 inductive	Disconnect t=2.5s
Load 4	18	300	98 inductive	Disconnect t=3.5s
Load 5	21	272.1	55.2 inductive	Disconnect t=1.5s
Load 6	35	250	52 inductive	Disconnect t=2.5s
Total		1644.2	260.4	

TABLE 6.3: Loading scenarios

Scenario	P_{load} [kW]	Q_{load} [kVAr]	Time [s]
Full load	1644.2	260.4	0 to 1.5
Partial load 1	1072.1	205.2	1.5 to 2.5
Partial load 2	300	98	2.5 to 3.5
No load	0	0	3.5 to 4.5

6.3 Simulation results discussion

In this section the static and dynamic performance of the TPD and DLC strategies as well as the influence of the transformer rated power on the stability are analysed.

6.3.1 Static analysis

During the static analysis the total installed PV power is changed in relation to the substation HV/MV transformer power rating, from $0.9 * S_{Tr2}$ to $2 * S_{Tr2}$ with a step of 0.1. Also, the BES is sized to fill the reactive power gap between the substation transformer and the total installed PV plant reactive power reserve. The BES reactive power rating is determined the following way

$$\begin{cases} Q_{BES} = 0.6 * (S_{PV} - S_{Tr2}), & if S_{PV} > S_{Tr2}; \\ Q_{BES} = 0, & else. \end{cases} \tag{6.2}$$

Four loading scenarios are considered for static analysis: full load, partial load 1, partial load 2 and no load.

Full load case

This case corresponds to the time range from 0 seconds to 1.5 seconds, when all the loads are connected. In this case, the total active load is higher than the transformer rated power (Table 6.3). Thus, the transformer alone will not be able to feed all the load and will be overloaded.

As we can see from Figure 6.3, during the full loading case the transformer is not being overloaded. In this case, with the increase of the PV contribution the loading of the transformer is decreasing as the load is being partially fed by the PV plants and less power flows from the HV grid to the MV grid through the transformer, Figure 6.3. When the total installed PV power reaches 1.87 times the transformer rating, the active power flow through the transformer reverses and flows back to the grid. However, the loading of the transformer is an absolute value based on the magnitude of the total current flowing through the transformer and does not depend on the direction of the power flow, Figure 6.3.

Since there is no overloading of the transformer, the TPD and DLC strategies will not be employed. Thus, we will skip any further analysis of this case and proceed to the next case, which is the first partial loading case.

Partial load case 1

This case corresponds to the time range from 1.5 seconds to 2.5 seconds, when loads 2 and 5 are disconnected from the grid. In this scenario the total load is slightly lower than the rated power of the transformer (Table 6.3).In this case the transformer alone can feed the load.

As we can see from Figure 6.4, during the first partial loading case, again the transformer is not being overloaded. With the increase of total installed PV power the loading of the transformer decreases down to the point where the installed PV can feed all the loads and compensate the losses in the system. After this point, the loading of the transformer starts to increase because of the reverse power flows, Figure 6.4. In this case, the active power flow reverse happens when the total installed PV power reaches around 1.23 times the transformer rating.

As with the full load case, in this case also there is no overloading of the transformer and the TPD and DLC strategies will not activate. Thus, we will skip any further analysis of this case and proceed to the next case, which is the second partial loading case.

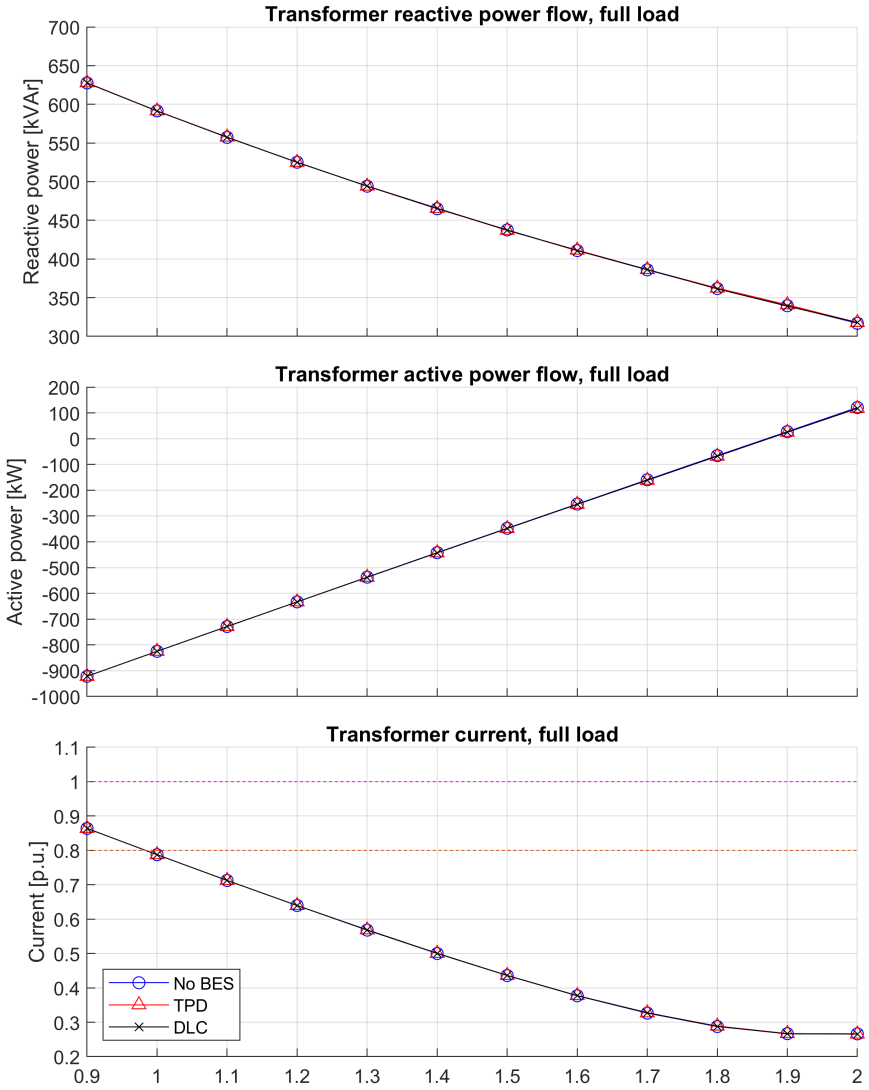

FIGURE 6.3: Transformer loading and power flow at full load

Partial load case 2

This case represents the time range from 2.5 seconds to 3.5 seconds, when in addition to the previous case the loads 1, 3 and 6 are disconnected. In this scenario, the total load is approximately the third of the transformer rating. The transformer alone can easily handle the load, but with the increase of PV contribution the reverse power flow can overload it.

As we can see from Figure 6.5, the active power flows from the MV grid to the HV grid and the transformer loading increases with the increase of PV contributions. The loading of the transformer crosses the 80% threshold when the total PV installations are equal to 1.4 times the transformer rated power. At this point, the TPD control is in action and the BES starts injecting reactive power into the grid based on the droop equation 6.1, Figure 6.6. On the contrary to the TPD control strategy, the DLC control strategy acts only

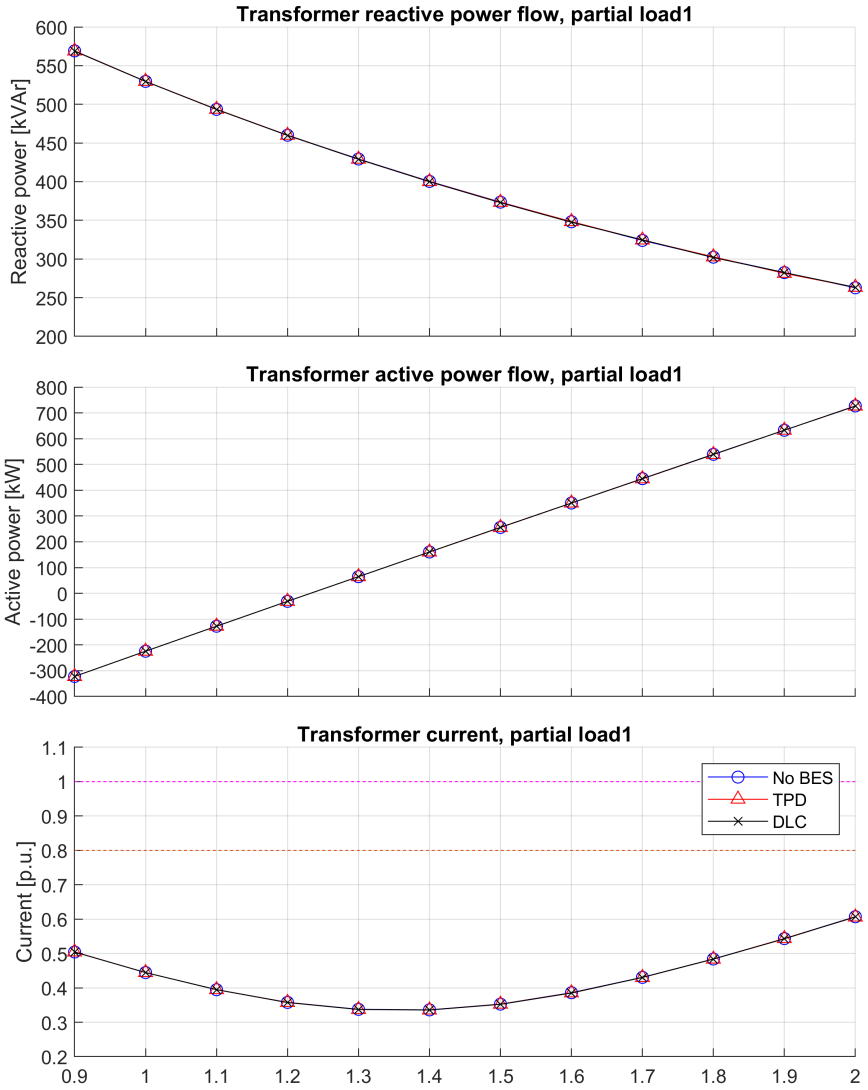

FIGURE 6.4: Transformer loading and power flow at partial load1

when the transformer loading reaches 100%. In the partial load2 case, this happens when the total installed PV power reaches 1.7 times the transformer rated power. From this moment on, the BES starts injecting reactive power into the grid, in order to control the loading of the transformer at 100%.

The PV inverters start to curtail their active power outputs when the voltage at the PCC is more than 1.04 pu, based on the extended droops presented in chapter 5. As we can see from Figure 6.7, the injection of reactive power by TPD and DLC increases the voltages at the PV connection buses above 1.04 pu, whereas without BES the voltages would be decreased. This in turn forces the PV inverters to curtail their active power output, Figure 6.8. Both the TPD and DLC control strategies force the inverters to curtail their active power outputs by 15 to 25% compared to no BES case, when the total installed PV power is 2 times more than the rated transformer power.

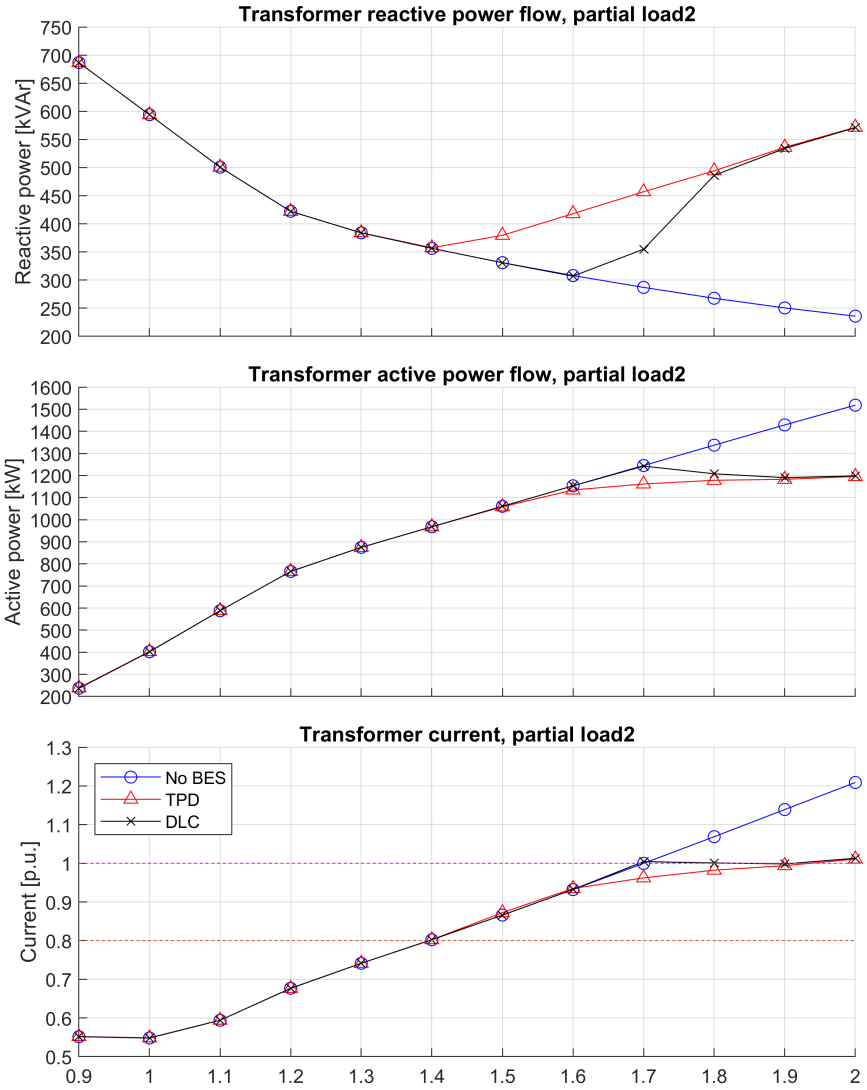

FIGURE 6.5: Transformer loading and power flow at partial load2

By increasing the voltage levels the TPD and DLC control strategies also force the PV inverters to increase their reactive power consumption as defined in the extended droops in Chapter 5, Figure 6.9. On the contrary, without BES deployment the reactive power consumption would increase much less, due to the decrease of voltages and increase of the total PV installation amount.

The curtailment of the active power outputs of the PV inverters and the extra reactive power provision by them change the power flows through the transformer and change it's loading. From Figure 6.5 we can notice, that in the case when the total installed PV is 2 times the transformer power, the active power flow through the transformer is being decreased by 303 kW and the reactive power flow is increased by 350 kVAr. However, since the initial

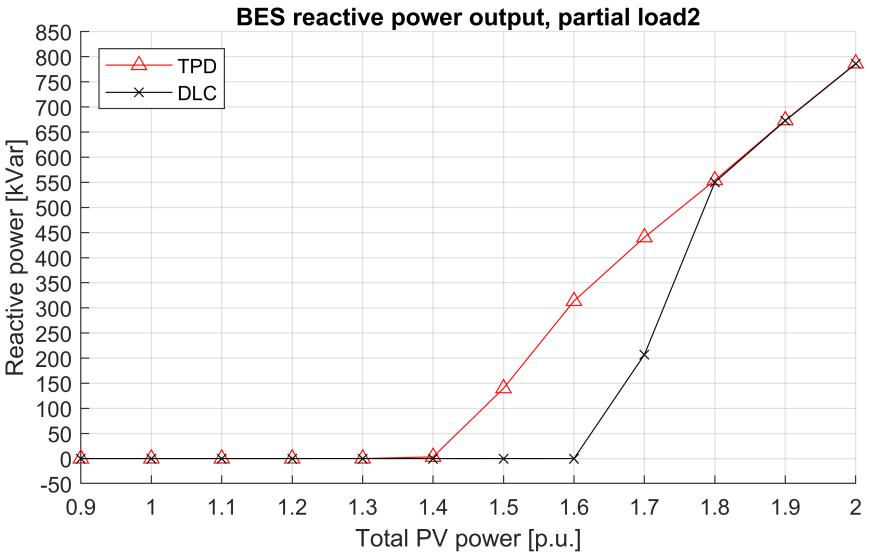

FIGURE 6.6: The reactive power output of BES at partial load2

active power flow through the transformer is significantly higher than the reactive power flow, a change of the active power flow through the transformer impacts the transformer loading more than the reactive power flow. Thus, for the case when the total installed PV is 2 times the transformer power, both the TPD and DLC control strategies are able to decrease the loading of the transformer by 20% compared to the configuration without BES, Figure 6.5.

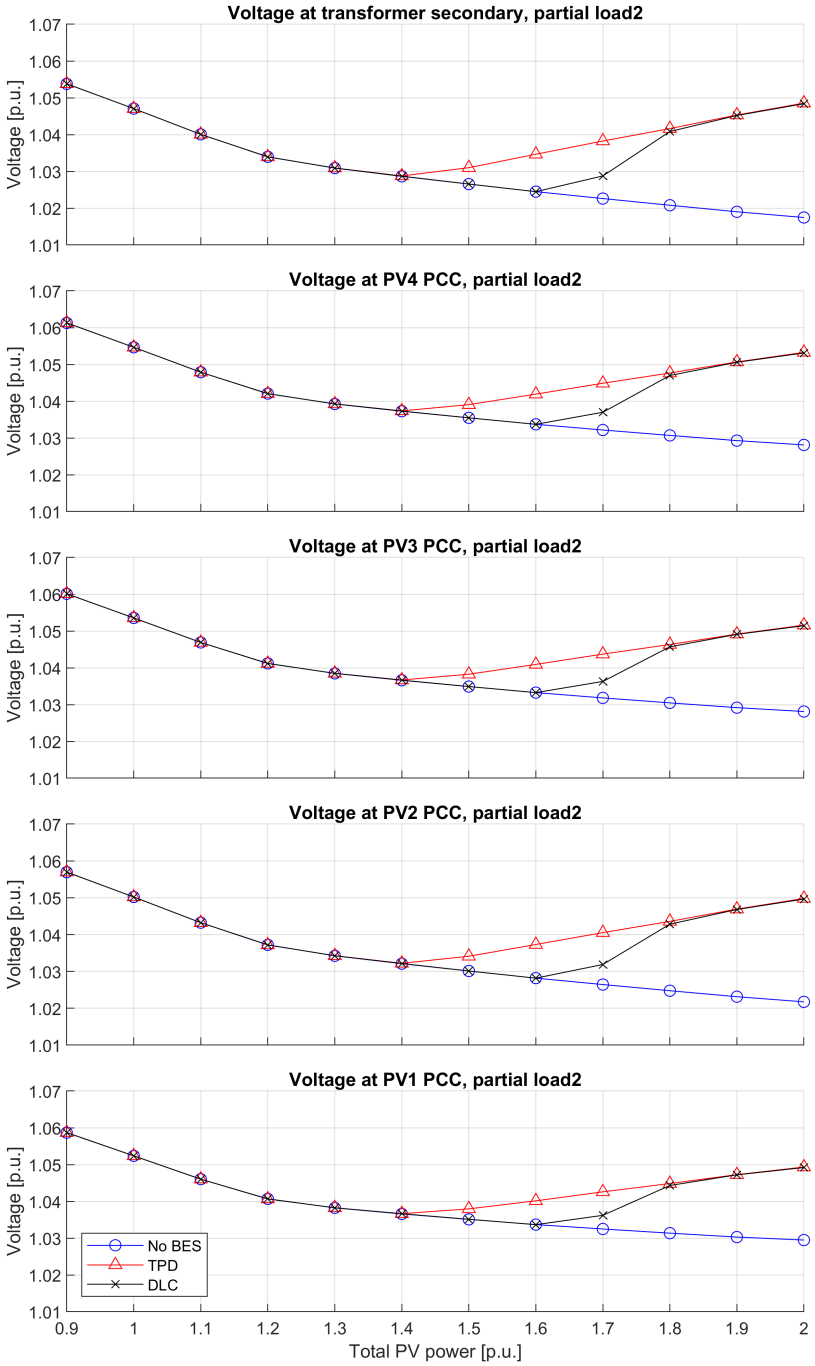

FIGURE 6.7: The voltages at the PV plants and transformer secondary at partial load2

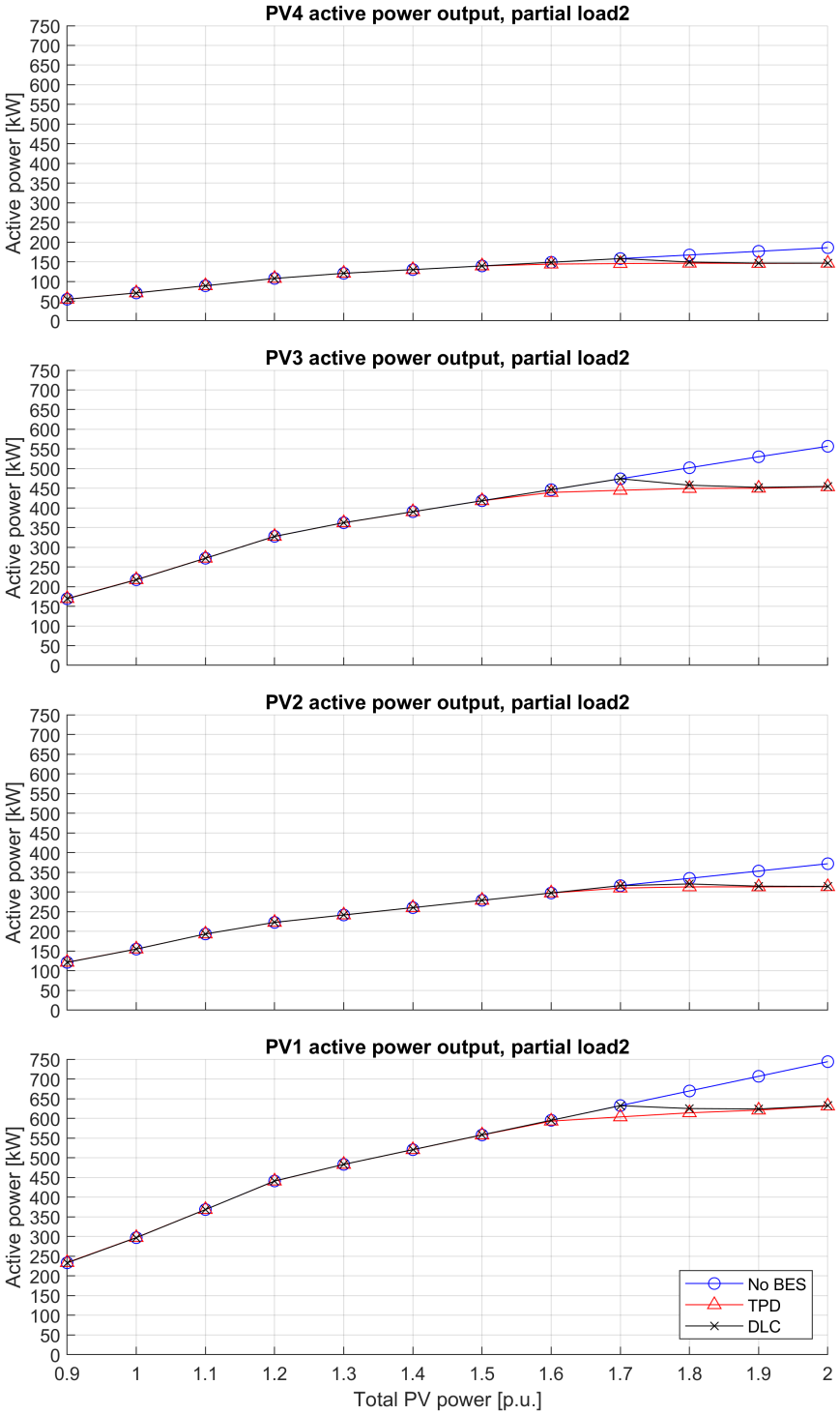

FIGURE 6.8: The active power outputs of PV plants at partial load2

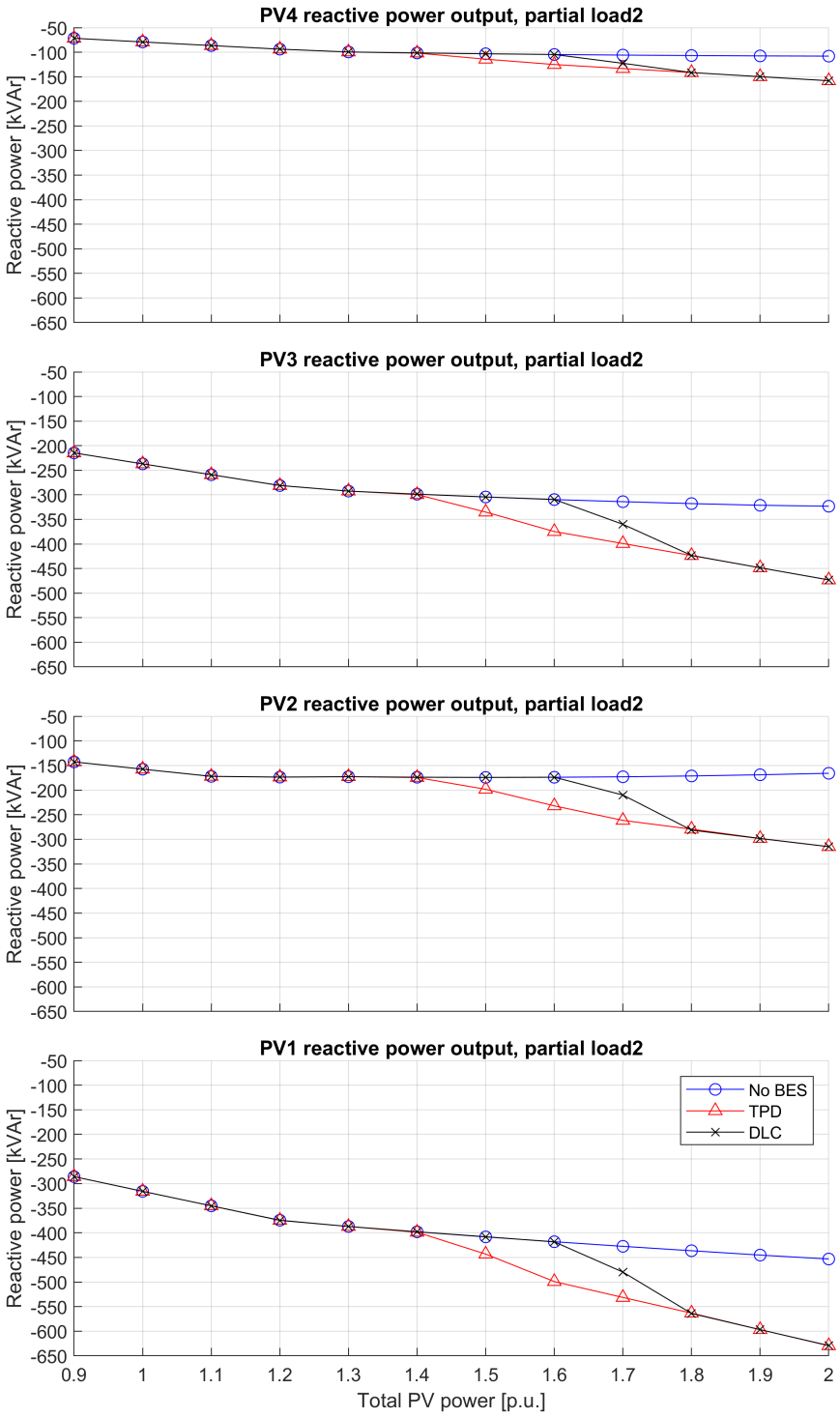

FIGURE 6.9: The reactive power outputs of PV plants at partial load2

No load case

This case corresponds to the time range from 3.5 seconds to 4.5 seconds, when all the loads are disconnected. Since there are no loads, the loading

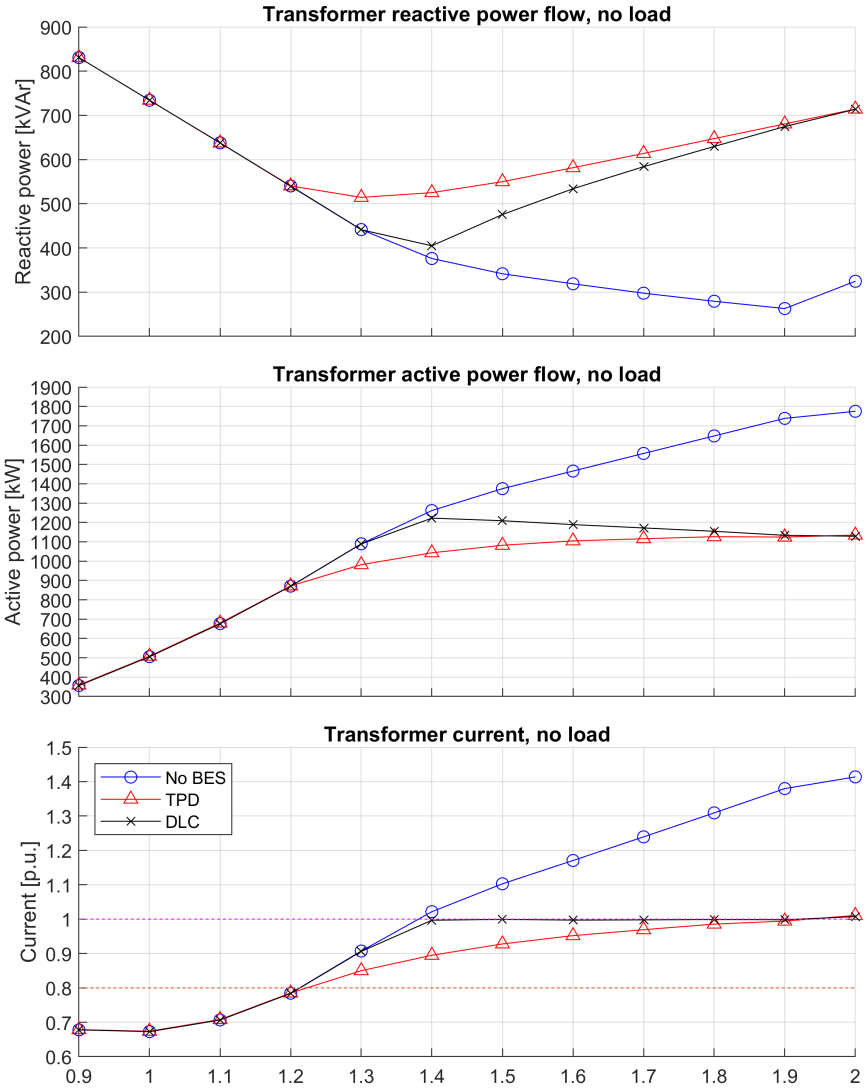

FIGURE 6.10: Transformer loading and power flow at no load

of the transformer is caused only by the reverse power flows because of PV injections.

As we can see from Figure 6.10, the transformer loading increases with the increase of PV installations.

As in the previous case, the TPD and DLC control strategies are in action when the loading of the transformer reaches the 80% and 100% loading thresholds respectively. In this case, the thresholds of 80% and 100% are being broken through when the total installed PV power is respectively 1.2 and 1.4 times the transformer rated power, Figure 6.10.

As we can see from Figure 6.11 and Figure 6.12, similar to the previous case, the injection of reactive power by TPD and DLC control strategies increases the voltages at the PV connection buses above 1.04 pu, whereas without BES the voltages would be decreased. This in turn forces the PV inverters to curtail their active power output, Figure 6.13. Both the TPD and

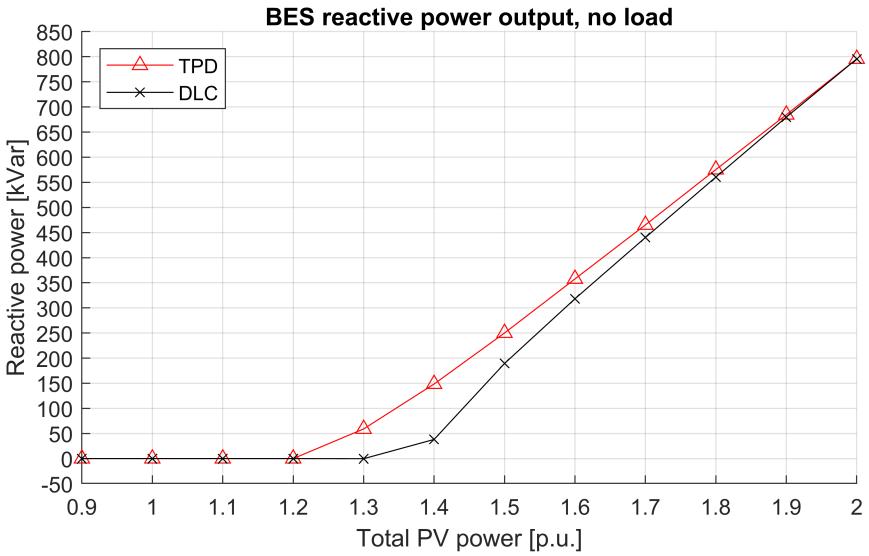

FIGURE 6.11: The reactive power output of BES at no load

DLC control strategies force the inverters to curtail their active power outputs by 28 to 42% compared to no BES case, when the total installed PV power is 2 times the rated transformer power.

The PV inverters are forced to increase their reactive power absorption as defined in the extended droops in Chapter 5, Figure 6.14. On the contrary, without BES deployment the reactive power consumption changes marginally, due to the decrease of the voltages and increase of the total installed PV power.

The decrease of the active power flow through the transformer is more important for the transformer loading than the reactive power flow, as the active power flowing through the transformer is higher than the reactive one, Figure 6.10. Thus, even if the absolute change in reactive and active power flows is the same, the total loading of the transformer has decreased.

As in the previous case, the TPD and DLC strategies change the power flows through the transformer and change its loading. From Figure 6.10 we can notice, that in the case when the total installed PV is 2 times the transformer power, the active power flow through the transformer is being decreased by 660 kW and the reactive power flow is increased by 380 kVAr. This leads to a decrease of the loading of the transformer by 41% compared to the configuration without BES, Figure 6.10.

Both the TPD and DLC strategies prove to be able to decrease the loading of the transformer by 41% compared to the grid configuration without BES and to keep the loading of the transformer within the acceptable limits in the steady-state operation, Figure 6.10.

Further investigation on dynamic performance and the robustness of the control strategies is carried out in the dynamic analysis section.

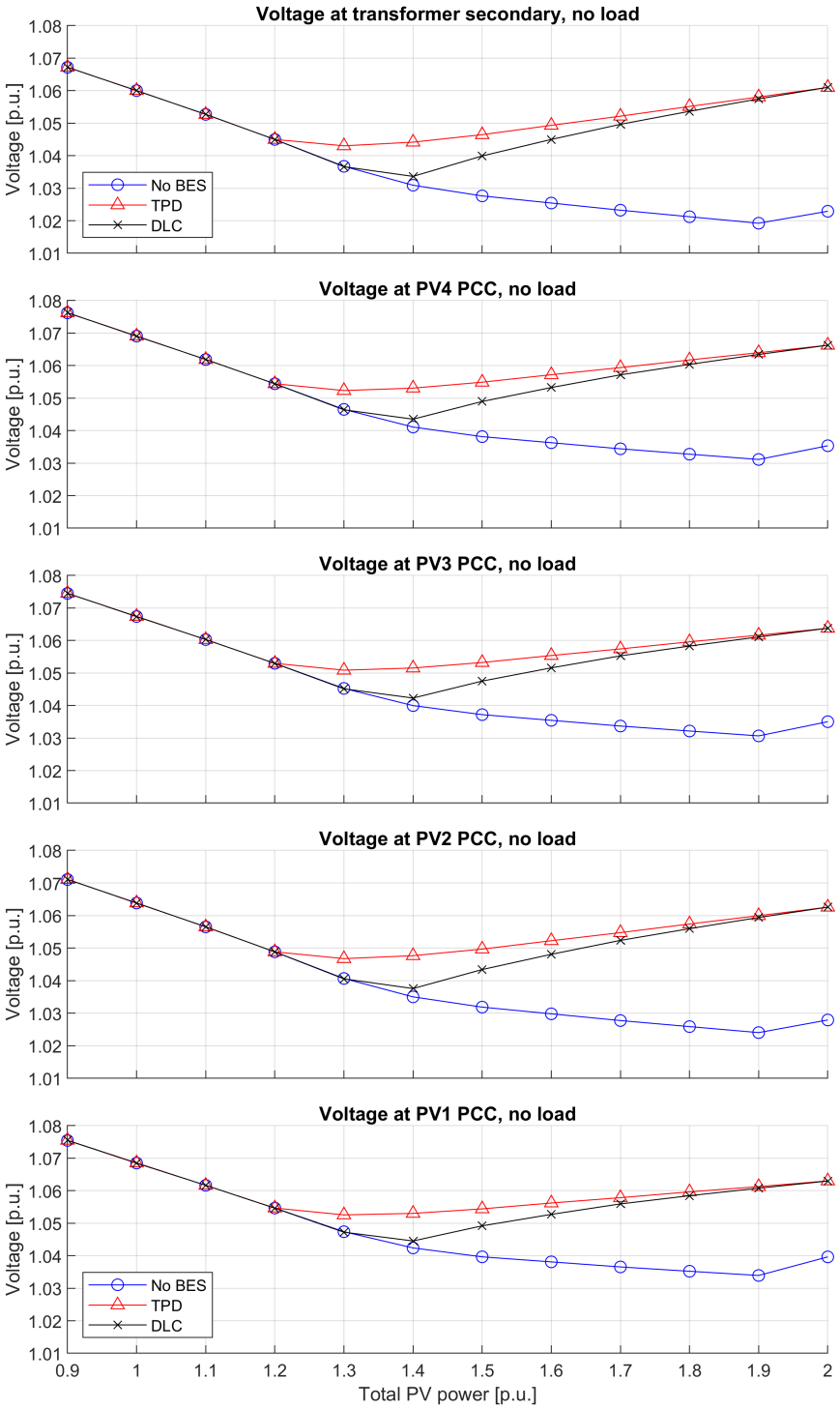

FIGURE 6.12: The voltages at PV PCCs at no load

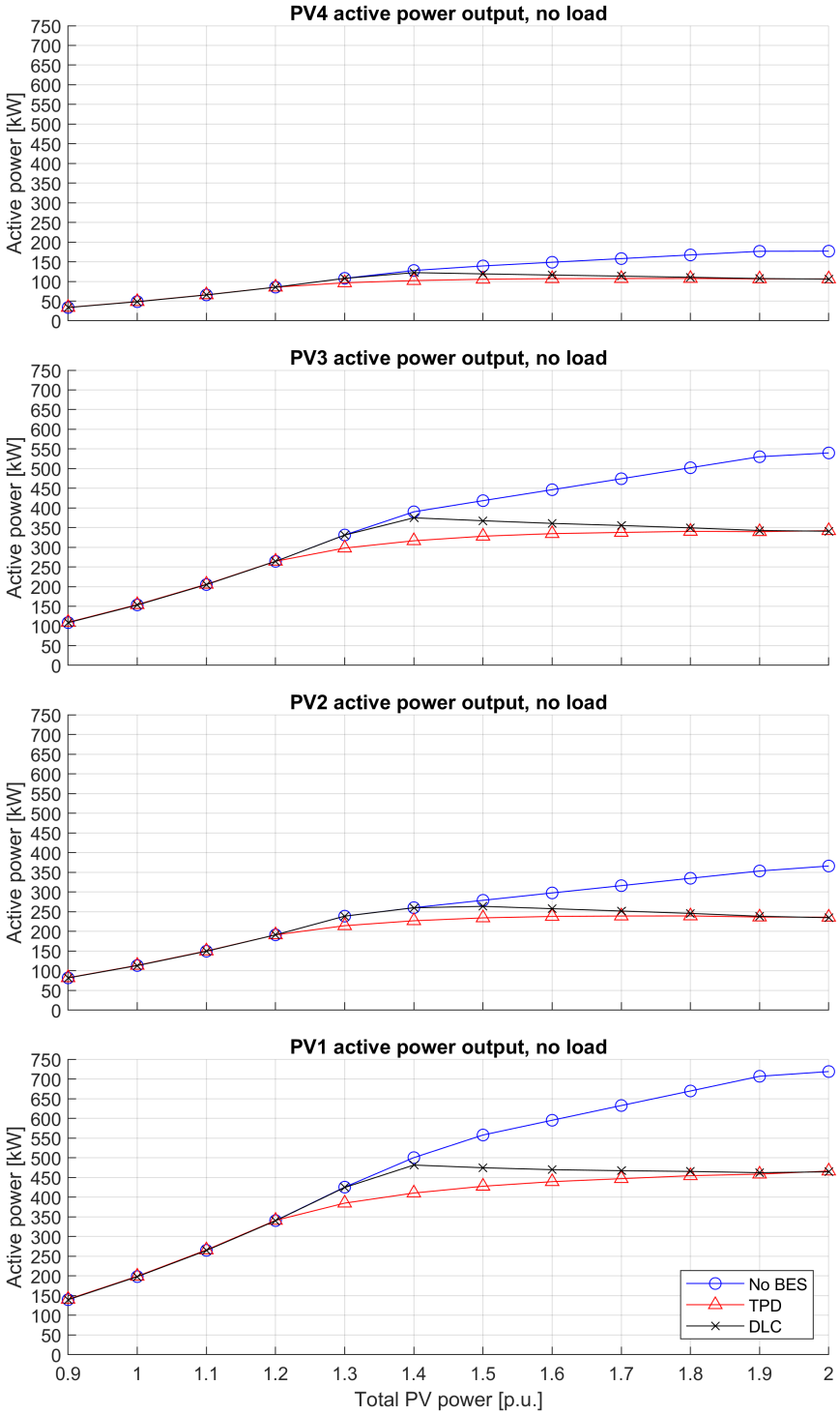

FIGURE 6.13: The active power outputs of PV plants at no load

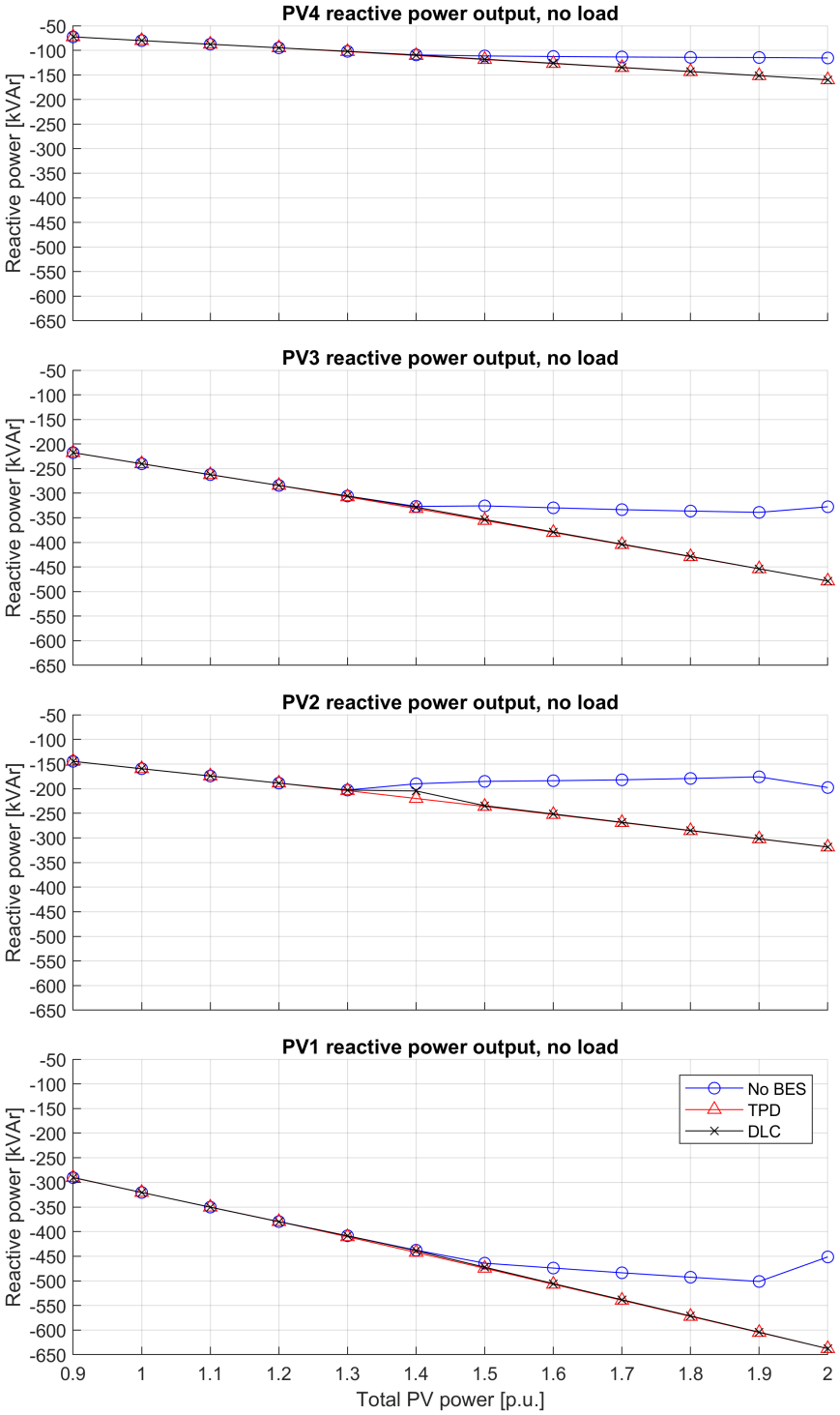

FIGURE 6.14: The reactive power outputs of PV plants at no load

6.3.2 Dynamic analysis

In this section, the dynamic performance of the TPD and DLC strategies is discussed. In order to test the dynamic performance of the TPD and DLC strategies, the grid is subject to abrupt load changes. Namely, at t = 1.5s load

2 and 5 are disconnected, at t = 2.5s loads 1, 3 and 6 are disconnected and finally at t = 3.5s the load 4 is disconnected, leading to the no load scenario which is considered to be the worst case scenario for PV integration.

To examine the dynamic response of the designed TPD and DLC control strategies, the detailed grid and PV plant models are used. The models are made and simulated in the Simulink environment.

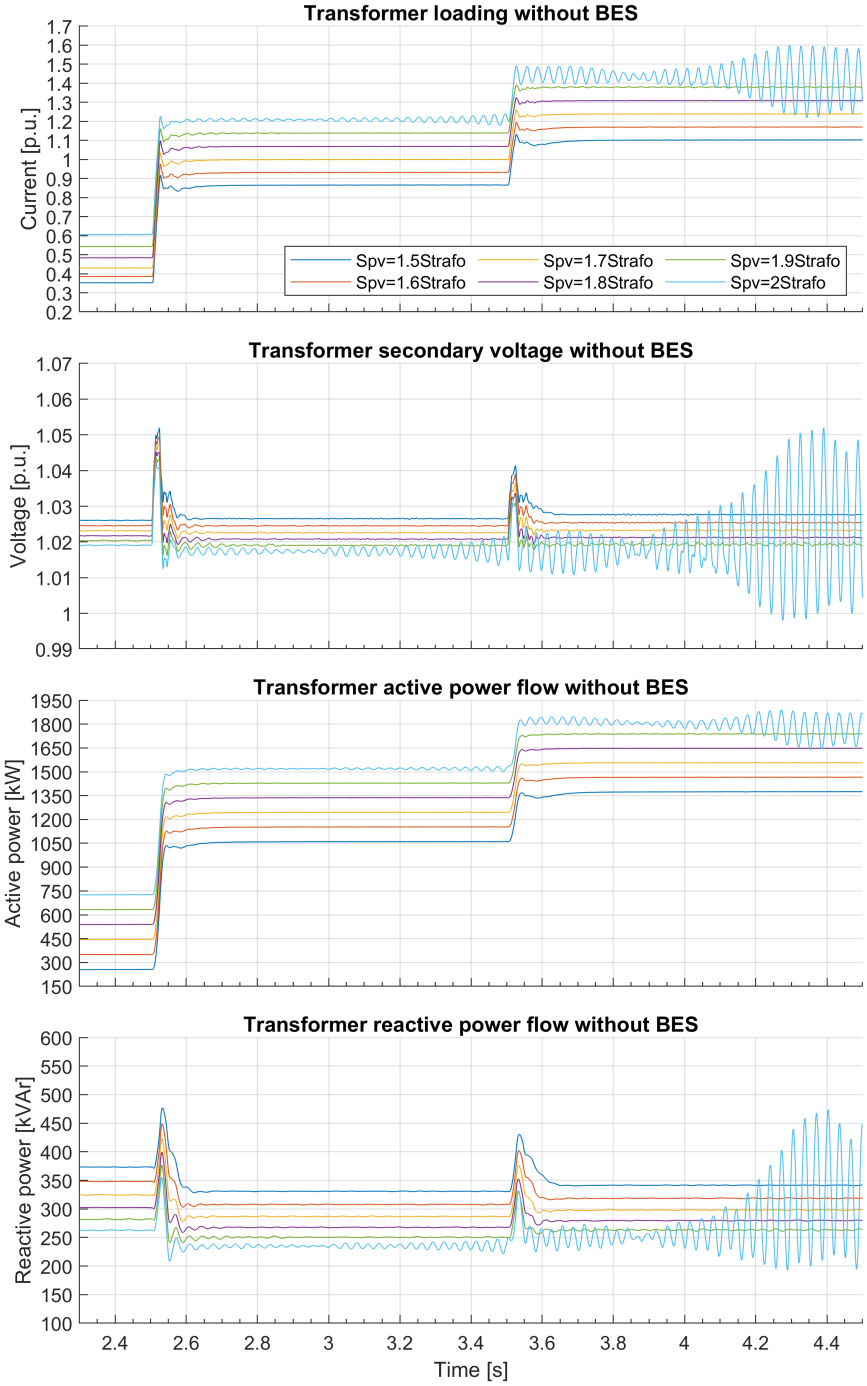

FIGURE 6.15: The dynamic response of the system to the load change without BES

From the static analysis, we can conclude that only the partial load2 and

no load cases where the total installed PV power is more than 1.5 times the transformer rating are of interest. Thus, the dynamic analysis is performed only for the cases with total installed PV power in the range from 1.5 to 2 times the transformer rating, in the time range of 2.4s to 4.5s. Also, the static analysis shows that the grid voltages have similar behaviour. Thus, the dynamic analysis will be focused on the transformer and BES responses.

First, the dynamic performance of the base scenario without a BES is assessed, Figure 6.15. Except when the total installed PV is twice the transformer rating, the system is stable. The voltage for all the cases is kept stable within normal operating range, with minor spikes during load commutation, which is within the acceptable limits. However, the transformer is being overloaded starting from $S_{PV} = 1.8 * S_{Tr2}$ at partial load2 case and for all the values of S_{PV} at no load case. When S_{PV} becomes twice the S_{Tr2}, the system becomes unstable violating the safe operational limits of the grid.

On the contrary to the system without BES, the TPD control strategy is designed to be able to keep the system stable when $S_{PV} = 2 * S_{Tr2}$, Figure 6.16. This is achieved by forcing the inverters to curtail their active power production and reducing the transformer loading. However, the TPD is not stable for all the range of the PV injections. Between $S_{PV} = (1.7to1.9) * S_{Tr2}$ the system is unstable after the last load is disconnected at t = 3.5s. Whereas between $S_{PV} = (1.5to1.6) * S_{Tr2}$, even though the system is oscillating, the oscillations are decreasing over time making the system stable. This behavior of TPD control is due to the characteristics of the droop control and the detailed technical model simulations for PV plant hardware, as the control exhibits the cross-influence of the controllers. Also, it can be noticed that with the increase of PV contribution the rate of the oscillations is decreasing, which highlights the non-linearity of the system.

To overcome the oscillatory behavior of the TPD control strategy, the DLC control strategy is presented. As in the TPD control strategy, the DLC control strategy also injects reactive power into the grid in order to increase the voltage levels and force the PV plants to curtail their active power output. However, since the DLC strategy is based on a PI controller, it can regulate the loading of the transformer precisely to the referenced value, Figure 6.17. The injection of extra reactive power to the grid by the DLC control strategy leads to an increase of voltage levels by around 0.038 pu in the worst case. As a result, the highest voltage in the grid is at the PV4 PCC at the value of 1.066 pu, which is within the acceptable operational voltage range of 0.9 - 1.1 pu, Figure 6.12. On the contrary to the TPD strategy, the DLC control

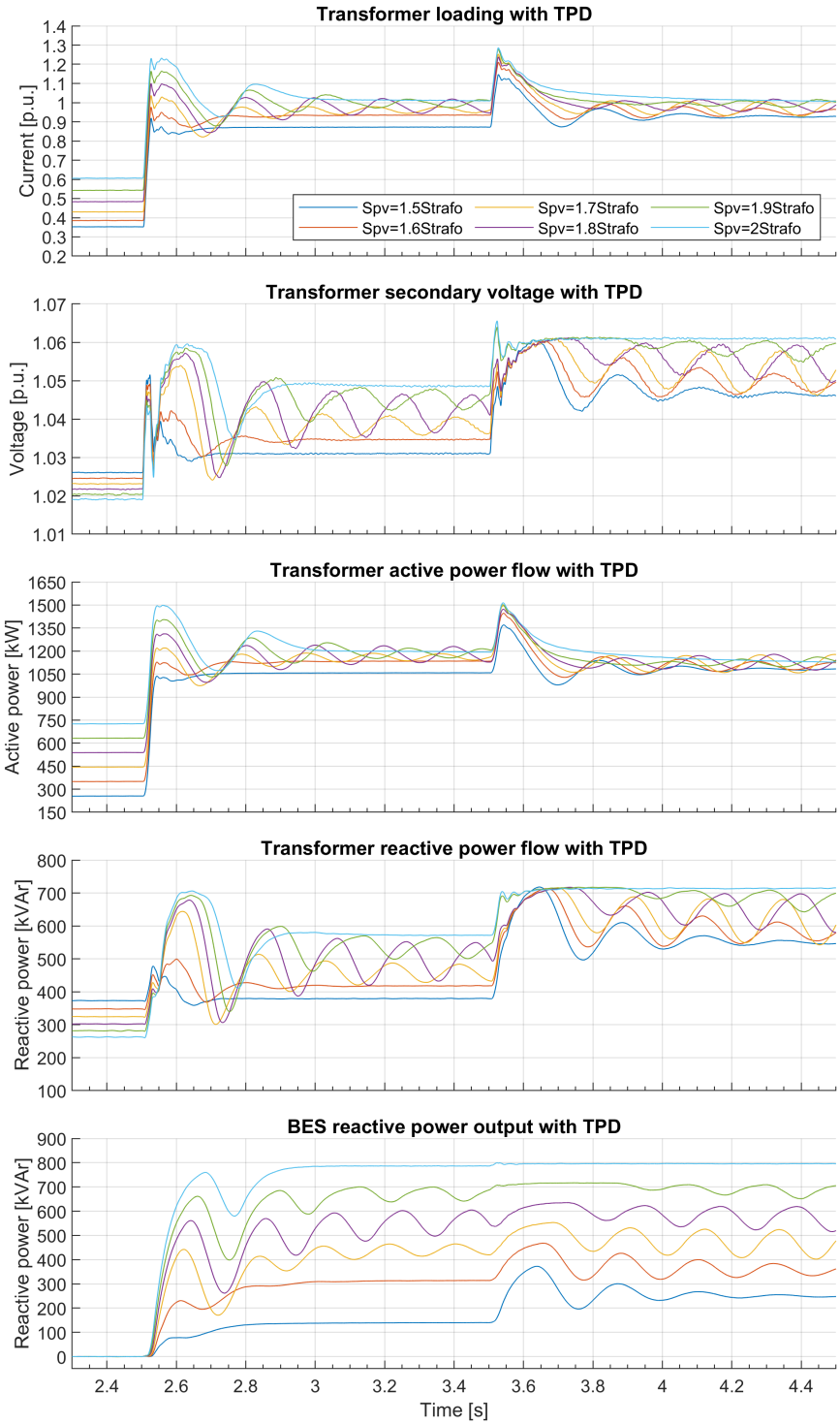

FIGURE 6.16: The dynamic response of the system to the load change with TPD

strategy is able to bring the system to steady-state over the all range of PV contribution change. In the worst case, the transformer loading settles within 700ms.

A more detailed comparison between the TPD and DLC control strategies is presented in Figure 6.18, where two PV injection cases are presented, $S_{PV} = 1.5 * S_{Tr2}$ and $S_{PV} = 1.8 * S_{Tr2}$. In both cases the DLC control strategy is superior to the TPD strategy, both in terms of settling time and overshoots.

The DLC strategy proved to be a robust control solution to prevent the overloading of the transformer and enhance the overall system stability.

6.4 Conclusions

Two communication-less transformer loading control strategies are designed and tested on the detailed model. The designed DLC and TPD control strategies rely only on the local substation transformer current measurements.

The static and dynamic performance of the designed DLC control strategy is superior to the TPD control strategy, which suffers from the characteristic of droop control and the cross-influence of the controls of system actors. It is a robust control strategy that not only ensures avoiding the transformer overloading and consequently increasing the HC of the grid, but also enhances the system stability during abrupt load changes in the grid.

The DLC control strategy is able to decrease the transformer loading by 41%, compared to the grid configuration without BES and to bring the system to the steady-state within 700ms in the worst case scenario.

Thus, the DLC control strategy is a viable communication-less solution forcing the inverters to curtail their active power outputs to prevent the transformer overloading. It can be used as a communication fail-safe backup active power curtailment strategy in the cases when the communication between the centralized controller and the PV plants is lost.

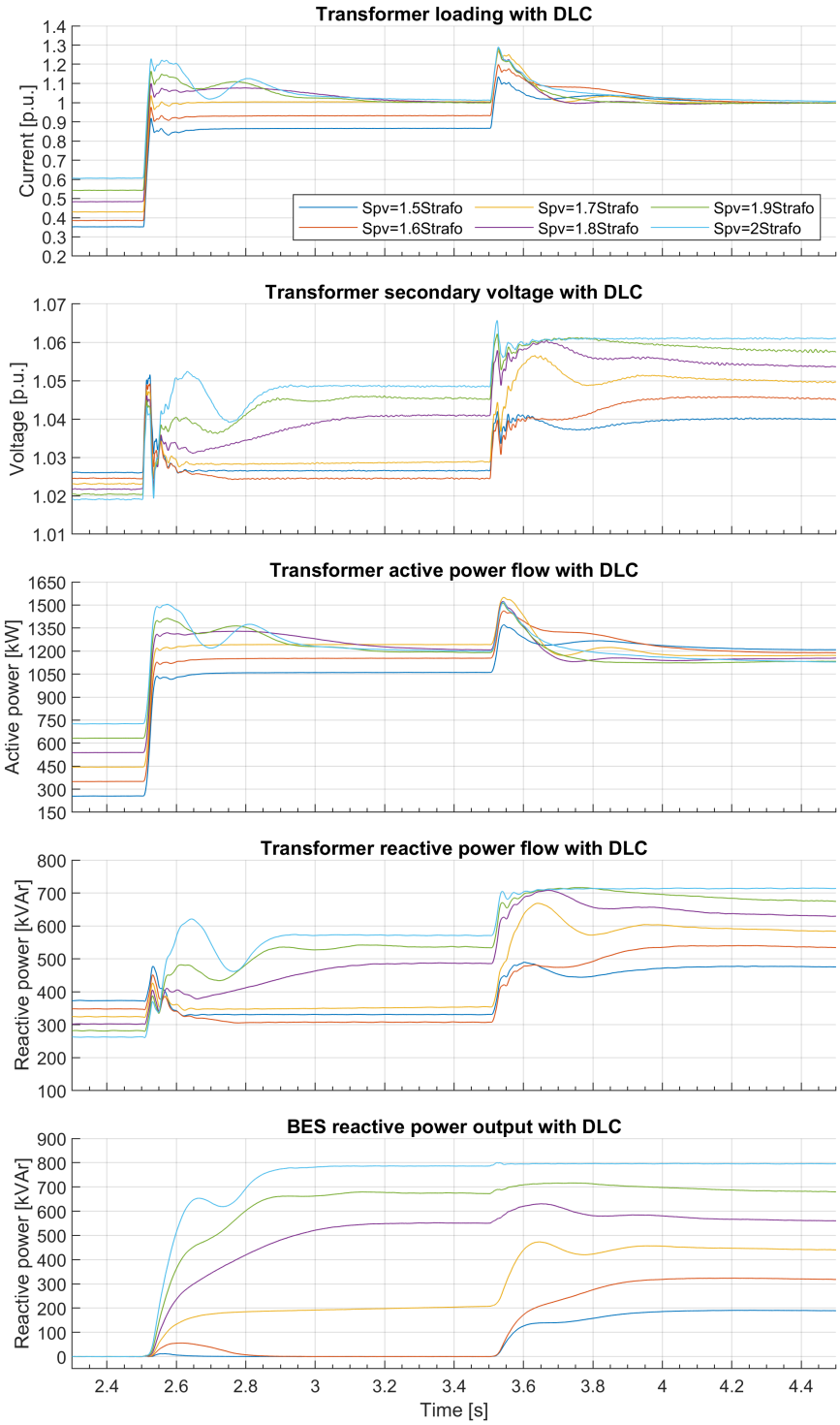

FIGURE 6.17: The dynamic response of the system to the load change with DLC

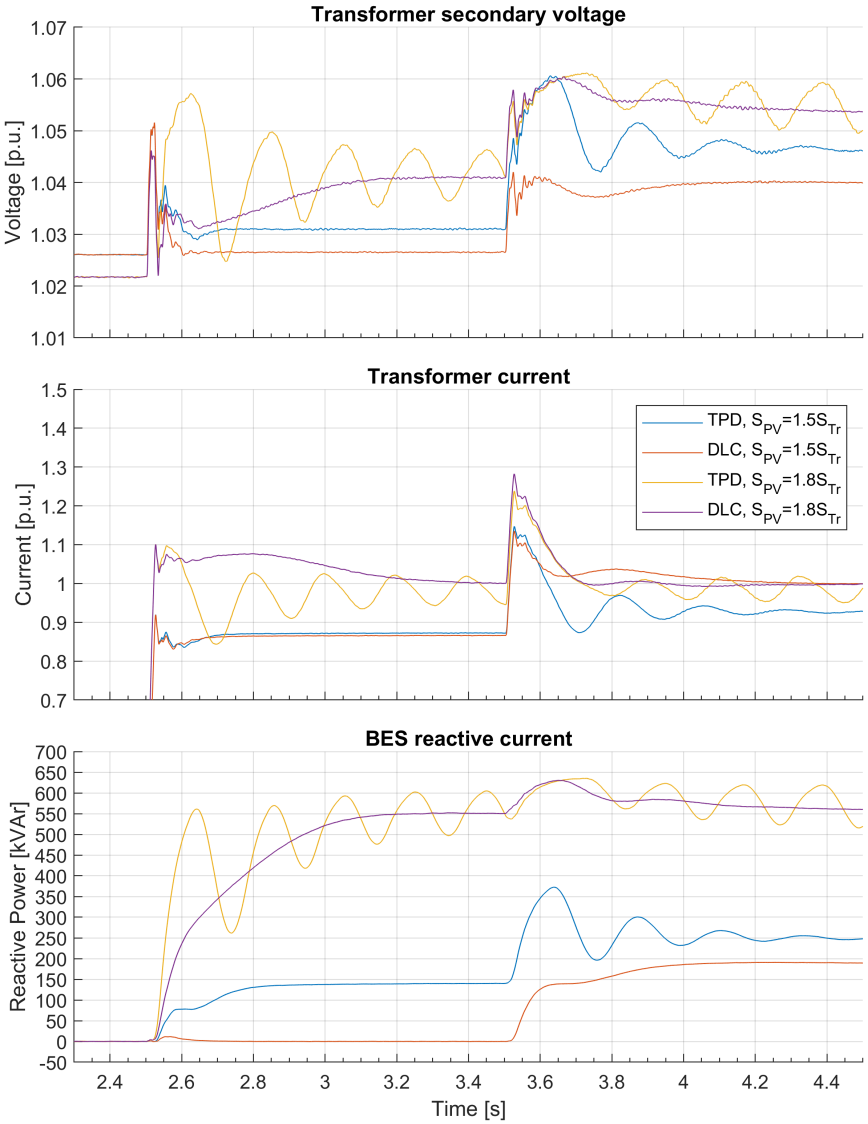

FIGURE 6.18: Comparison of TPD and DLC dynamic responses

Chapter 7

Conclusion

7.1 Summary

The present work has dealt with the technical assessment of chosen hosting capacity (HC) enhancement strategies. The focus was set on the investigation of grid reconfiguration, grid code modification, extended current droops and transformer loading control. The extended current droops and transformer loading control strategies rely only on local measurements. Thus, they are eliminating the dependency on communication as in the centralized voltage or power curtailment control strategies. The goal of this thesis was to present PV HC enhancement methodologies which can be applied by the grid operators either in the planning stage or during grid expansion and reinforcement when facing increasing PV penetration. The results highlight that proper grid reconfiguration, extended droops and transformer overloading prevention via battery energy storage (BES) can significantly increase the HC of the grid and should be the first consideration of grid operators when a need of grid reinforcement arises.

Chapter 2 presented the state of the art in HC enhancement. The main limiting factors of HC enhancement have been discussed. After which a detailed overview of possible HC enhancement techniques has been presented.

Chapter 3 discussed the selected test grid and PV plant models and the modeling tools. A representative grid model of Luxembourg's 20kV medium voltage (MV) grid was developed for investigating the performance of the developed HC enhancement strategies. Static and dynamic models have been developed using pandapower and MATLAB Simulink tools accordingly.

Chapter 4 investigated the potential of grid reconfiguration and grid code modification in HC enhancement. The reconfiguration analysis and the HC calculation algorithms allow the investigation of the impact of more than one PV plant at a time. The static grid model developed in pandapower is used

for reconfiguration analysis and HC calculation. The reconfiguration analysis is performed by using the NetworkX graph analysis library, where the grid configurations are categorized into meshed and radial groups. After the categorization, the HC for each meshed and radial configuration has been calculated using three grid code cases. Grid code improvements via power factor range extension and oversizing of the PV inverter increased the HC by 13% and 15% for the radial and meshed configurations respectively. It was shown, that proper grid configuration selection is important as it can substantially increase the HC. Moreover, proper grid reconfiguration helps to reduce the line loading. The average line loading in meshed configurations is 41% lower than the one for radial configurations.

Chapter 5 presented an extended strategy for active and reactive current droops. After discussing some of the recent developments in droop control, the extended droops were introduced. In the designed extended current droops, both the active and reactive currents depend on the voltage at the point of common coupling (PCC), $I_d(V), I_q(V)$. The designed strategy has been tested on the dynamic grid model and was assessed regarding the

- controller performance and voltage support capability
- robustness against load change
- HC enhancement

The designed extended droop control with active power curtailment (APC) proved to be a viable grid reinforcement strategy which can not only regulate the voltage at the PCC, but also relax the transformer loading and improve overall voltage and frequency stability. Additionally, oversizing of the inverter by 12.5% compared to the VDE4110:2018 grid codes can increase the reactive power reserve of the inverters by 37.6%. This increased reactive power reserve helped to lower the voltage profile of the feeder. Thus, resulting in curtailment of only 58.2% of the amount curtailed with regular droop control.

Chapter 6 presented a comparison of two novel communication-less transformer overloading protection strategies based on a BES: transformer protection droops (TPD) and direct loading control (DLC). The designed strategies do not rely on communication and were tested on a modified, detailed dynamic grid and PV plant models, where the total installed PV power varies between 0.9 to 2 times the transformer rating. The DLC control strategy overcomes the cross-influence of controllers and is superior to the TPD control strategy. It is a robust control strategy that not only ensured avoiding the

transformer overloading and consequently increasing the HC of the grid, but also enhanced the system stability during abrupt load changes in the grid. The DLC control strategy decreased the transformer loading by 41%, compared to the grid configuration without BES and brought the system to the steady-state within 700ms in the worst case scenario. It also ensured to keep the system voltages within safe operational limits. It can be used as a communication fail-safe backup active power curtailment strategy in the cases when the communication between the centralized controller and the PV plants is lost.

7.2 Outlook

The analysis of the grid reconfiguration show that certain switch patterns can be extracted that correspond to higher HC values. For large grids with high amount of tie switches it would be helpful to include data analysis and pattern recognition algorithms to automatically detect and create a database of switching sub-pattern configurations for certain ranges of HC.

Furthermore, the HC calculation is a time-intensive procedure. Thus, further investigation on more optimized HC calculation algorithms is needed.

As shown in the dynamic analysis section, the design of robust controllers for BES and PV with always changing grid parameters is a challenging task. Thus, further investigations are necessary to develop adaptive controllers that will ensure robust operation during grid parameter changes. Some examples of such controllers are the automatic gain controllers.

Bibliography

[1] *EEA greenhouse gases - data viewer — European Environment Agency*. [Online]. Available: https://www.eea.europa.eu/data-and-maps/data/data-viewers/greenhouse-gases-viewer.

[2] European Council, "2030 CLIMATE AND ENERGY POLICY FRAMEWORK," Tech. Rep., 2014.

[3] European Commision, "The 2030 Climate target plan," Tech. Rep., 2020.

[4] "LUXEMBOURG'S INTEGRATED NATIONAL ENERGY AND CLIMATE PLAN FOR 2021-2030," Tech. Rep.

[5] M. Obi and R. Bass, "Trends and challenges of grid-connected photovoltaic systems - A review," *Renewable and Sustainable Energy Reviews*, vol. 58, no. January, pp. 1082–1094, 2016, ISSN: 18790690. DOI: 10.1016/j.rser.2015.12.289. [Online]. Available: http://dx.doi.org/10.1016/j.rser.2015.12.289.

[6] M. A. Eltawil and Z. Zhao, "Grid-connected photovoltaic power systems: Technical and potential problems-A review," *Renewable and Sustainable Energy Reviews*, vol. 14, no. 1, pp. 112–129, 2010, ISSN: 13640321. DOI: 10.1016/j.rser.2009.07.015.

[7] *Call for Tenders Launched for Solar Power Plants*. [Online]. Available: https://chronicle.lu/category/energy/34280-call-for-tenders-launched-for-solar-power-plants.

[8] T. Stetz, "Autonomous Voltage Control Strategies in Distribution Grids with Photovoltaic Systems-Technical and Economic Assessment," Ph.D. dissertation, University of Kassel, Kassel, 2013.

[9] VDE, *VDE-AR-N 4110 Anwendungsregel:2018-11 Technische Regeln für den Anschluss von Kundenanlagen an das Mittelspannungsnetz und deren Betrieb (TAR Mittelspannung)*. 2018, vol. 2018-11.

[10] J. W. Simpson-Porco, F. Dörfler, and F. Bullo, "Voltage collapse in complex power grids," 2016. DOI: 10.1038/ncomms10790. [Online]. Available: www.nature.com/naturecommunications.

[11] A. Honrubia-Escribano, T. García-Sánchez, E. Gómez-Lázaro, E. Muljadi, and A. Molina-García, "Power quality surveys of photovoltaic power plants: Characterisation and analysis of grid-code requirements," in *IET Renewable Power Generation*, vol. 9, 2015. DOI: 10.1049/iet-rpg.2014.0215.

[12] Y. Yang, P. Enjeti, F. Blaabjerg, and H. Wang, "Wide-Scale Adoption of Photovoltaic Energy: Grid Code Modifications Are Explored in the Distribution Grid," *IEEE Industry Applications Magazine*, vol. 21, no. 5, pp. 21–31, 2015, ISSN: 1077-2618. DOI: 10.1109/MIAS.2014.2345837. [Online]. Available: http://www.scopus.com/inward/record.url?eid=2-s2.0-84939427384&partnerID=tZOtx3y1.

[13] E. Quitmann and E. Erdmann, "Power system needs – How grid codes should look ahead," no. March 2014, pp. 3–9, 2015. DOI: 10.1049/iet-rpg.2014.0107.

[14] M. Bollen and M. Hager, "Power quality: interactions between distributed energy resources, the grid, and other customers," *Electrical Power Quality and Utilisation. Magazine*, vol. 1, no. 1, 2005, ISSN: 1234-6799.

[15] M. Bollen and F. Hassan, *Integration of Distributed Generation in the Power System*. 2011. DOI: 10.1002/9781118029039.

[16] A. Ballanti and L. F. Ochoa, "On the integrated PV hosting capacity of MV and LV distribution networks," in *2015 IEEE PES Innovative Smart Grid Technologies Latin America, ISGT LATAM 2015*, 2016, pp. 366–370, ISBN: 9781467366052. DOI: 10.1109/ISGT-LA.2015.7381183.

[17] V. Quintero-Molina, M. Romero-L, and A. Pavas, "Assessment of the hosting capacity in distribution networks with different DG location," in *2017 IEEE Manchester PowerTech, Powertech 2017*, 2017, ISBN: 9781509042371. DOI: 10.1109/PTC.2017.7981243.

[18] P. Denholm, K. Clark, and M. O'Connell, "On the Path to SunShot: Emerging Issues and Challenges in Integrating Solar with the Distribution System," Tech. Rep., 2016.

[19] Y. J. Liu, Y. H. Tai, C. Y. Huang, H. J. Su, P. H. Lan, and M. K. Hsieh, "Assessment of the PV hosting capacity for the medium-voltage 11.4 kV distribution feeder," in *Proceedings of 4th IEEE International Conference on Applied System Innovation 2018, ICASI 2018*, IEEE, 2018,

pp. 381–384, ISBN: 9781538643426. DOI: 10.1109/ICASI.2018.8394262.

[20] M. S. S. Abad, J. Ma, D. Zhang, A. S. Ahmadyar, and H. Marzooghi, "Probabilistic Assessment of Hosting Capacity in Radial Distribution Systems," *IEEE Transactions on Sustainable Energy*, vol. 9, no. 4, pp. 1935–1947, Oct. 2018, ISSN: 19493029. DOI: 10.1109/TSTE.2018.2819201.

[21] N. Etherden, M. Bollen, S. Ackeby, and O. Lennerhag, "THE TRANSPARANT HOSTING-CAPACITY APPROACH-OVERVIEW, APPLICATIONS AND DEVELOPMENTS," in *23rd International Conference on Electricity Distribution*, 2015.

[22] T. Walla, J. Widén, J Johansson, and C Bergerland, "Determining and increasing the hosting capacity for photovoltaics in Swedish distribution grids," *27th European Photovoltaic Solar Energy Conference and Exhibition*, 2012.

[23] Conseil international des grands réseaux électriques. Comité d'études C6. and Impr. Conformes, *Capacity of distribution feeders for hosting DER*. CIGRE, 2014, ISBN: 9782858732821.

[24] R. A. Shayani and M. A. G. De Oliveira, "Photovoltaic generation penetration limits in radial distribution systems," *IEEE Transactions on Power Systems*, vol. 26, no. 3, 2011, ISSN: 08858950. DOI: 10.1109/TPWRS.2010.2077656.

[25] M. Emmanuel and R. Rayudu, *Evolution of dispatchable photovoltaic system integration with the electric power network for smart grid applications: A review*, 2017. DOI: 10.1016/j.rser.2016.09.010.

[26] Y. Yang and M. Bollen, *Power quality and reliability in distribution networks with increased levels of distributed generation*, 2008.

[27] P. Westacott and C. Candelise, "Assessing the impacts of photovoltaic penetration across an entire low-voltage distribution network containing 1.5 million customers," *IET Renewable Power Generation*, vol. 10, no. 4, pp. 460–466, Apr. 2016, ISSN: 1752-1424. DOI: 10.1049/IET-RPG.2015.0535. [Online]. Available: https://ietresearch.onlinelibrary.wiley.com/doi/full/10.1049/iet-rpg.2015.0535https://ietresearch.onlinelibrary.wiley.com/doi/abs/10.1049/iet-rpg.2015.0535https://ietresearch.onlinelibrary.wiley.com/doi/10.1049/iet-rpg.2015.0535.

[28] M. K. Gray and W. G. Morsi, "On the role of prosumers owning rooftop solar photovoltaic in reducing the impact on transformer's aging due to plug-in electric vehicles charging," *Electric Power Systems Research*, vol. 143, pp. 563–572, Feb. 2017, ISSN: 0378-7796. DOI: 10.1016/J.EPSR.2016.10.060.

[29] A. A. Raja, M. Mansoor, and F. Zahid, "Optimal sitting of distributed generation based on hosting capacity approach," *2018 International Conference on Engineering and Emerging Technologies, ICEET 2018*, vol. 2018-Janua, pp. 1–5, 2018. DOI: 10.1109/ICEET1.2018.8338630.

[30] D. Bertini, D. Falabretti, D. Moneta, M. Merlo, and A. Silvestri, "Hosting Capacity of Italian Distribution Networks," *CIRED 21st International Conference on Electricity Distribution*, no. 0930, 2011.

[31] T. Degner, F. I. Germany, S. M. a. Solar, *et al.*, "Increasing the photovoltaic-system hosting capacity of low voltage distribution networks," *21st Internationation Conference on Electricity Distribution (CIRED)*, no. 1243, 2011.

[32] G. Monfredini, M. Merlo, V. Olivieri, D. Moneta, P. Mora, and M. Gallanti, "MV NETWORK WITH DISPERSED GENERATION: VOLTAGE REGULATION BASED ON LOCAL CONTROLLERS," in *21st International COnference on Electricity Distribution*, 2011.

[33] F. Alalamat, "Increasing the hosting Capacity of Radial Distribution Grids in Jordan," Ph.D. dissertation, Upsala University, 2015. [Online]. Available: http://www.teknat.uu.se/student.

[34] L. Collins and J. K. Ward, "Real and reactive power control of distributed PV inverters for overvoltage prevention and increased renewable generation hosting capacity," *Renewable Energy*, vol. 81, 2015, ISSN: 18790682. DOI: 10.1016/j.renene.2015.03.012.

[35] R. Seguin, J. Woyak, D. Costyk, J. Hambrick, and B. Mather, "High-Penetration PV Integration Handbook for Distribution Engineers," *NREL - National Renewable Energy Laboratory*, 2016.

[36] M. Patsalides, G. Makrides, and A. Stavrou, "Assessing the photovoltaic (PV) hosting capacity of distribution grids," in *Mediterranean Conference on Power Generation, Transmission, Distribution and Energy Conversion (MedPower 2016)*, 2016, pp. 1–4. DOI: 10.1049/cp.2016.1051.

[37] S. M. Ismael, S. H. Abdel Aleem, A. Y. Abdelaziz, and A. F. Zobaa, "State-of-the-art of hosting capacity in modern power systems with distributed generation," *Renewable Energy*, vol. 130, pp. 1002–1020, 2019, ISSN: 18790682. DOI: 10.1016/j.renene.2018.07.008. [Online]. Available: https://doi.org/10.1016/j.renene.2018.07.008.

[38] W. Sun, "Maximising Renewable Hosting Capacity in Electricity Networks," Tech. Rep., 2015.

[39] R. A. Walling, R. Saint, R. C. Dugan, J. Burke, and L. A. Kojovic, "Summary of distributed resources impact on power delivery systems," *IEEE Transactions on Power Delivery*, vol. 23, no. 3, 2008, ISSN: 08858977. DOI: 10.1109/TPWRD.2007.909115.

[40] E. De Jaeger, A. Du Bois, and B. Martin, "Hosting capacity of LV distribution grids for small distributed generation units, referring to voltage level and unbalance," in *IET Conference Publications*, vol. 2013, 2013. DOI: 10.1049/cp.2013.1171.

[41] D. Schwanz, S. K. Ronnberg, and M. Bollen, "Hosting capacity for photovoltaic inverters considering voltage unbalance," in *2017 IEEE Manchester PowerTech, Powertech 2017*, 2017. DOI: 10.1109/PTC.2017.7981274.

[42] D. Schwanz, F. Moller, S. K. Ronnberg, J. Meyer, and M. H. Bollen, "Stochastic Assessment of Voltage Unbalance Due to Single-Phase-Connected Solar Power," *IEEE Transactions on Power Delivery*, vol. 32, no. 2, 2017, ISSN: 08858977. DOI: 10.1109/TPWRD.2016.2579680.

[43] M. Bollen, F. Sollerkvist, E. Larsson, and C. Lundmark, "Limits to the Hosting Capacity of the Grid for Equipament Emitting High-Frequency Distortion," *Proceedings of Nordic Distribution and Asset Management Conference*, 2006.

[44] H. Sharma, M. Rylander, and D. Dorr, "Grid impacts due to increased penetration of newer harmonic sources," *IEEE Transactions on Industry Applications*, vol. 52, no. 1, 2016, ISSN: 00939994. DOI: 10.1109/TIA.2015.2464175.

[45] S. K. Sharma, A. Chandra, M. Saad, S. Lefebvre, D. Asber, and L. Lenoir, "Voltage Flicker Mitigation Employing Smart Loads With High Penetration of Renewable Energy in Distribution Systems," *IEEE Transactions on Sustainable Energy*, vol. 8, no. 1, 2017, ISSN: 19493029. DOI: 10.1109/TSTE.2016.2603512.

[46] I. N. Santos, M. H. Bollen, and P. F. Ribeiro, "Methodology for estimation of harmonic hosting," in *Proceedings of International Conference on Harmonics and Quality of Power, ICHQP*, 2014. DOI: 10.1109/ICHQP.2014.6842849.

[47] M. H. Bollen, S. Bahramirad, and A. Khodaei, "Is there a place for power quality in the smart grid?" In *Proceedings of International Conference on Harmonics and Quality of Power, ICHQP*, 2014. DOI: 10.1109/ICHQP.2014.6842865.

[48] I. N. Santos, V. Ćuk, P. M. Almeida, M. H. Bollen, and P. F. Ribeiro, "Considerations on hosting capacity for harmonic distortions on transmission and distribution systems," *Electric Power Systems Research*, vol. 119, 2015, ISSN: 03787796. DOI: 10.1016/j.epsr.2014.09.020.

[49] X. Liang, "Emerging Power Quality Challenges Due to Integration of Renewable Energy Sources," *IEEE Transactions on Industry Applications*, vol. 53, no. 2, 2017, ISSN: 00939994. DOI: 10.1109/TIA.2016.2626253.

[50] A. Chidurala, T. K. Saha, and N. Mithulananthan, "Harmonic impact of high penetration photovoltaic system on unbalanced distribution networks - Learning from an urban photovoltaic network," *IET Renewable Power Generation*, vol. 10, no. 4, 2016, ISSN: 17521424. DOI: 10.1049/iet-rpg.2015.0188.

[51] P. K. Ray, S. R. Mohanty, and N. Kishor, "Classification of power quality disturbances due to environmental characteristics in distributed generation system," *IEEE Transactions on Sustainable Energy*, vol. 4, no. 2, 2013, ISSN: 19493029. DOI: 10.1109/TSTE.2012.2224678.

[52] S. Sakar, M. E. Balci, S. H. Aleem, and A. F. Zobaa, "Hosting capacity assessment and improvement for photovoltaic-based distributed generation in distorted distribution networks," in *EEEIC 2016 - International Conference on Environment and Electrical Engineering*, 2016. DOI: 10.1109/EEEIC.2016.7555515.

[53] L. D. Campello, P. M. Duarte, P. F. Ribeiro, and T. E. De Oliveira, "Hosting capacity of a university electrical grid considering the inclusion of wind-turbines for different background distortions," in *Proceedings of International Conference on Harmonics and Quality of Power, ICHQP*, vol. 2016-December, 2016. DOI: 10.1109/ICHQP.2016.7783335.

[54] T. E. De Oliveira, P. F. Ribeiro, and I. N. Santos, "Determining the harmonic hosting capacity of PV sources for a university campus," in *Proceedings of International Conference on Harmonics and Quality of Power, ICHQP*, vol. 2016-December, 2016. DOI: 10.1109/ICHQP.2016.7783371.

[55] H. Zhan, C. Wang, Y. Wang, *et al.*, "Relay protection coordination integrated optimal placement and sizing of distributed generation sources in distribution networks," *IEEE Transactions on Smart Grid*, vol. 7, no. 1, 2016, ISSN: 19493053. DOI: 10.1109/TSG.2015.2420667.

[56] H. Margossian, F. Capitanescu, and J. Sachau, "Feeder protection challenges with high penetration of inverter based distributed generation," *IEEE EuroCon 2013*, 2013. DOI: 10.1109/EUROCON.2013.6625157.

[57] H. Margossian, J. Sachau, and G. Deconinck, "Short circuit calculation in networks with a high share of inverter based distributed generation," *2014 IEEE 5th International Symposium on Power Electronics for Distributed Generation Systems (PEDG)*, pp. 1–5, 2014. DOI: 10.1109/PEDG.2014.6878629. [Online]. Available: http://ieeexplore.ieee.org/lpdocs/epic03/wrapper.htm?arnumber=6878629.

[58] J Deuse, S Grenard, M. H. J. Bollen, M Häger, and F Sollerkvist, "Effective impact of DER on distribution system protection," in *CIRED 19th International Conference on Electricity Distribution*, 2007.

[59] C. Bucher, G. Andersson, and L. Küng, "INCREASING THE PV HOSTING CAPACITY OF DISTRIBUTION POWER GRIDS – A COMPARISON OF SEVEN METHODS," *CEUR Workshop Proceedings*, vol. 1542, no. 9, 2015, ISSN: 16130073.

[60] B Bletterie, A Gorsek, B Uljanic, *et al.*, "Enhancement of the Network Hosting Capacity—Clearing Space for/with PV," *25th European Photovoltaic Solar Energy Conference*, no. September, 2010.

[61] E. Demirok, D. Sera, and R. Teodorescu, "Estimation of Maximum Allowable PV Power Connection to Low Voltage Residential Networks : A Case Study of Braedstrup," in *1st Solar Integration Workshop*, 2011.

[62] D. Menniti, M. Merlo, N. Scordino, and F. Zanellini, "Distribution network analysis: A comparison between hosting and loading capacities," in *SPEEDAM 2012 - 21st International Symposium on Power*

Electronics, Electrical Drives, Automation and Motion, 2012. DOI: 10.1109/SPEEDAM.2012.6264635.

[63] M. Rossi, G. Viganò, and D. Moneta, "Hosting capacity of distribution networks: Evaluation of the network congestion risk due to distributed generation," in *5th International Conference on Clean Electrical Power: Renewable Energy Resources Impact, ICCEP 2015*, 2015. DOI: 10.1109/ICCEP.2015.7177570.

[64] T. Stetz, F. Marten, and M. Braun, "Improved low voltage grid-integration of photovoltaic systems in Germany," *IEEE Transactions on Sustainable Energy*, vol. 4, no. 2, pp. 534–542, Apr. 2013, ISSN: 19493029. DOI: 10.1109/TSTE.2012.2198925. [Online]. Available: http://ieeexplore.ieee.org/document/6213176/.

[65] D. Stein, L. Consiglio, and J. Stromsather, "Enel's large scale demonstration project inside Grid4EU: The challenge of RES integration in the MV network," in *IET Conference Publications*, vol. 2013, 2013. DOI: 10.1049/cp.2013.1085.

[66] J. Varela, N. Hatziargyriou, L. J. Puglisi, M. Rossi, A. Abart, and B. Bletterie, "The IGREENGrid Project: Increasing Hosting Capacity in Distribution Grids," *IEEE Power and Energy Magazine*, vol. 15, no. 3, 2017, ISSN: 15407977. DOI: 10.1109/MPE.2017.2662338.

[67] M. Delfanti, M. Merlo, G. Monfredini, V. Olivieri, M. Pozzi, and A. Silvestri, "Hosting dispersed generation on Italian MV networks: Towards smart grids," in *ICHQP 2010 - 14th International Conference on Harmonics and Quality of Power*, 2010. DOI: 10.1109/ICHQP.2010.5625442.

[68] B. Currie, C. Abbey, G. Ault, *et al.*, "Flexibility is Key in New York: New Tools and Operational Solutions for Managing Distributed Energy Resources," *IEEE Power and Energy Magazine*, vol. 15, no. 3, 2017, ISSN: 15407977. DOI: 10.1109/MPE.2017.2660818.

[69] A. Arshad, M. Lindner, and M. Lehtonen, "An analysis of photovoltaic hosting capacity in Finnish low voltage distribution networks," *Energies*, vol. 10, no. 11, 2017, ISSN: 19961073. DOI: 10.3390/en10111702.

[70] M. Vandenbergh, V. Helmbrecht, D. Craciun, R. Hermes, and H. Loew, "Technical solutions supporting the large scale integration of photovoltaic systems in the future distribution grids," in *IET Conference Publications*, vol. 2013, 2013. DOI: 10.1049/cp.2013.0699.

[71] S. F. Santos, D. Z. Fitiwi, M. Shafie-Khah, A. W. Bizuayehu, C. M. Cabrita, and J. P. Catalão, "New Multistage and Stochastic Mathematical Model for Maximizing RES Hosting Capacity - Part I: Problem Formulation," *IEEE Transactions on Sustainable Energy*, vol. 8, no. 1, pp. 304–319, Jan. 2017. DOI: 10.1109/TSTE.2016.2598400.

[72] ——, "New Multi-Stage and Stochastic Mathematical Model for Maximizing RES Hosting Capacity - Part II: Numerical Results," *IEEE Transactions on Sustainable Energy*, vol. 8, no. 1, 2017, ISSN: 19493029. DOI: 10.1109/TSTE.2016.2584122.

[73] M. Meuser, H. Vennegeerts, and P. Schafer, "Impact of voltage control by distributed generation on hosting capacity and reactive power balance in distribution grids," in *CIRED 2012 Workshop: Integration of Renewables into the Distribution Grid*, 2012, pp. 87–87, ISBN: 978-1-84919-628-4. DOI: 10.1049/cp.2012.0747. [Online]. Available: http://digital-library.theiet.org/content/conferences/10.1049/cp.2012.0747.

[74] D Mende, T. Y. Fawzy, D Premm, and S Stevens, "Increasing the hosting capacity of distribution networks for distributed generation using reactive power control-potentials & limits," *The 2nd Integration Workshop on Integration of Solar Power into Power Systems*, pp. 153–159, 2012.

[75] J. Seuss, M. J. Reno, R. J. Broderick, and S. Grijalva, "Improving distribution network PV hosting capacity via smart inverter reactive power support," in *IEEE Power and Energy Society General Meeting*, vol. 2015-September, 2015. DOI: 10.1109/PESGM.2015.7286523.

[76] F. Ding, B. Mather, and P. Gotseff, "Technologies to increase PV hosting capacity in distribution feeders," in *IEEE Power and Energy Society General Meeting*, vol. 2016-November, 2016. DOI: 10.1109/PESGM.2016.7741575.

[77] N. Etherden and M. H. Bollen, "Increasing the hosting capacity of distribution networks by curtailment of renewable energy resources," in *2011 IEEE PES Trondheim PowerTech: The Power of Technology for a Sustainable Society, POWERTECH 2011*, 2011. DOI: 10.1109/PTC.2011.6019292.

[78] ——, "Overload and overvoltage in low-voltage and medium-voltage networks due to renewable energy - Some illustrative case studies," *Electric Power Systems Research*, vol. 114, 2014, ISSN: 03787796. DOI: 10.1016/j.epsr.2014.03.028.

[79] M. Bollen, N. Etherden, and J. Tjäder, "Increasing hosting capacity through dynamic line rating : risk aspects," 2015. [Online]. Available: http://urn.kb.se/resolve?urn=urn:nbn:se:ltu:diva-32138.

[80] J. Le Baut, P. Zehetbauer, S. Kadam, *et al.*, "Probabilistic evaluation of the hosting capacity in distribution networks," in *IEEE PES Innovative Smart Grid Technologies Conference Europe*, 2017. DOI: 10.1109/ISGTEurope.2016.7856213.

[81] International Electrotechnical Commission, "Electrical Energy Storage," Tech. Rep., 2011.

[82] International Electrotechnical Commision, "Grid integration of large-capacity Renewable Energy sources and use of large-capacity Electrical Energy Storage," Tech. Rep., 2012.

[83] A. K. Srivastava, A. A. Kumar, and N. N. Schulz, "Impact of distributed generations with energy storage devices on the electric grid," *IEEE Systems Journal*, vol. 6, no. 1, 2012, ISSN: 19328184. DOI: 10.1109/JSYST.2011.2163013.

[84] H. Sugihara, K. Yokoyama, O. Saeki, K. Tsuji, and T. Funaki, "Economic and efficient voltage management using customer-owned energy storage systems in a distribution network with high penetration of photovoltaic systems," *IEEE Transactions on Power Systems*, vol. 28, no. 1, 2013, ISSN: 08858950. DOI: 10.1109/TPWRS.2012.2196529.

[85] N. Etherden and M. H. Bollen, "Dimensioning of energy storage for increased integration of wind power," *IEEE Transactions on Sustainable Energy*, vol. 4, no. 3, 2013, ISSN: 19493029. DOI: 10.1109/TSTE.2012.2228244.

[86] N Etherden and M Bollen, "The use of battery storage for increasing the hosting capacity of the grid for renewable electricity production," *Conference on Innovation for Secure and . . .*, 2014.

[87] V. Poulios, E. Vrettos, F. Kienzle, E. Kaffe, H. Luternauer, and G. Andersson, "Optimal placement and sizing of battery storage to increase the PV hosting capacity of low voltage grids," in *International ETG*

Congress 2015; Die Energiewende - Blueprints for the New Energy Age, 2015.

[88] N. Jayasekara, M. A. Masoum, and P. J. Wolfs, "Optimal operation of distributed energy storage systems to improve distribution network load and generation hosting capability," *IEEE Transactions on Sustainable Energy*, vol. 7, no. 1, 2016, ISSN: 19493029. DOI: 10.1109/TSTE.2015.2487360.

[89] O. C. Rascon, B. Schachler, J. Buhler, M. Resch, and A. Sumper, "Increasing the hosting capacity of distribution grids by implementing residential PV storage systems and reactive power control," in *International Conference on the European Energy Market, EEM*, vol. 2016-July, 2016. DOI: 10.1109/EEM.2016.7521338.

[90] S. Hashemi and J. Østergaard, "Methods and strategies for overvoltage prevention in low voltage distribution systems with PV," *IET Renewable Power Generation*, vol. 11, no. 2, pp. 205–214, 2017, ISSN: 1752-1416. DOI: 10.1049/iet-rpg.2016.0277. [Online]. Available: http://digital-library.theiet.org/content/journals/10.1049/iet-rpg.2016.0277.

[91] S. Shao, F. Jahanbakhsh, J. R. Aguero, and L. Xu, "Integration of PEVs and PV-DG in power distribution systems using distributed energy storage - Dynamic analyses," in *2013 IEEE PES Innovative Smart Grid Technologies Conference, ISGT 2013*, 2013. DOI: 10.1109/ISGT.2013.6497881.

[92] F. Capitanescu, L. F. Ochoa, S. Member, H. Margossian, and N. D. Hatziargyriou, "Assessing the Potential of Network Reconfiguration to Improve Distributed Generation Hosting Capacity in Active Distribution Systems," vol. 30, no. 1, pp. 346–356, 2015.

[93] Y. Takenobu, S. Kawano, Y. Hayashi, N. Yasuda, and S. I. Minato, "Maximizing hosting capacity of distributed generation by network reconfiguration in distribution system," in *19th Power Systems Computation Conference, PSCC 2016*, 2016. DOI: 10.1109/PSCC.2016.7540965.

[94] Y. Y. Fu and H. D. Chiang, "Toward optimal multiperiod network reconfiguration for increasing the hosting capacity of distribution networks," *IEEE Transactions on Power Delivery*, vol. 33, no. 5, 2018, ISSN: 08858977. DOI: 10.1109/TPWRD.2018.2801332.

[95] C. Lueken, P. M. Carvalho, and J. Apt, "Distribution grid reconfiguration reduces power losses and helps integrate renewables," *Energy Policy*, vol. 48, 2012, ISSN: 03014215. DOI: 10.1016/j.enpol.2012.05.023.

[96] R. Čadenović and D. Jakus, "Maximization of distribution network hosting capacity through optimal grid reconfiguration and distributed generation capacity allocation/control," *Energies*, vol. 13, no. 20, 2020, ISSN: 19961073. DOI: 10.3390/en13205315.

[97] Z. X. Ma and F. Z. Wang, "Analysis on distribution power grid reconfiguration considers improving stability margin and economy based on FCM," *Journal of the Chinese Institute of Engineers, Transactions of the Chinese Institute of Engineers,Series A*, vol. 42, no. 2, 2019, ISSN: 21587299. DOI: 10.1080/02533839.2018.1553632.

[98] A. Nikoobakht, J. Aghaei, T. Niknam, H. Farahmand, and M. Korpås, "Electric vehicle mobility and optimal grid reconfiguration as flexibility tools in wind integrated power systems," *International Journal of Electrical Power and Energy Systems*, vol. 110, 2019, ISSN: 01420615. DOI: 10.1016/j.ijepes.2019.03.005.

[99] C. Schwaegerl, M. H. Bollen, K. Karoui, and A. Yagmur, "Voltage control in distribution systems as a limitation of the hosting capacity for distributed energy resources," in *IEE Conference Publication*, vol. 4, 2005. DOI: 10.1049/cp:20051229.

[100] A. Berizzi, C. Bovo, V. Ilea, *et al.*, "Advanced functions for DSOs control center," in *2013 IEEE Grenoble Conference PowerTech, POWERTECH 2013*, 2013. DOI: 10.1109/PTC.2013.6652343.

[101] A. Navarro-Espinosa and L. F. Ochoa, "Increasing the PV hosting capacity of LV networks: OLTC-fitted transformers vs. reinforcements," in *2015 IEEE Power and Energy Society Innovative Smart Grid Technologies Conference, ISGT 2015*, 2015. DOI: 10.1109/ISGT.2015.7131856.

[102] K. Rauma, F. Cadoux, N. Hadj-Saïd, A. Dufournet, C. Baudot, and G. Roupioz, "Assessment of the MV/LV on-load tap changer technology as a way to increase LV hosting capacity for photovoltaic power generators," in *IET Conference Publications*, vol. 2016, 2016. DOI: 10.1049/cp.2016.0644.

[103] C. Long, L. F. Ochoa, and S. Member, "Voltage Control of PV-Rich LV Networks : OLTC-Fitted Transformer and Capacitor Banks," pp. 2014–2015, 2015.

[104] M. Meuser, H. Vennegeerts, and H.-J. Haubrich, "IMPROVED GRID INTEGRATION OF DISTRIBUTED GENERATION IN EXISTING NETWORK STRUCTURES," in *21 st International Conference on Electricity Distribution*, 2011.

[105] D. A. Sarmiento, P. P. Vergara, L. C. Da Silva, and M. C. De Almeida, "Increasing the PV hosting capacity with OLTC technology and PV VAr absorption in a MV/LV rural Brazilian distribution system," in *Proceedings of International Conference on Harmonics and Quality of Power, ICHQP*, vol. 2016-Decem, 2016, pp. 395–399, ISBN: 9781509037926. DOI: 10.1109/ICHQP.2016.7783454.

[106] T. E. De Oliveira, P. M. Carvalho, P. F. Ribeiro, and B. D. Bonatto, "PV hosting capacity dependence on harmonic voltage distortion in low-voltage grids: Model validation with experimental data," *Energies*, vol. 11, no. 2, 2018, ISSN: 19961073. DOI: 10.3390/en11020465.

[107] S. Sakar, M. E. Balci, S. H. Abdel Aleem, and A. F. Zobaa, *Integration of large- scale PV plants in non-sinusoidal environments: Considerations on hosting capacity and harmonic distortion limits*, 2018. DOI: 10.1016/j.rser.2017.09.028.

[108] ——, "Increasing PV hosting capacity in distorted distribution systems using passive harmonic filtering," *Electric Power Systems Research*, vol. 148, 2017, ISSN: 03787796. DOI: 10.1016/j.epsr.2017.03.020.

[109] S. Cundeva, M. Bollen, and D. Schwanz, "Hosting capacity of the grid for wind generators set by voltage magnitude and distortion levels," in *IET Conference Publications*, vol. 2016, 2016. DOI: 10.1049/cp.2016.1062.

[110] Wei Sun, G. Harrison, and S. Djokic, "Incorporating harmonic limits into assessment of the hosting capacity of active networks," *CIRED 2012 Workshop: Integration of Renewables into the Distribution Grid*, pp. 325–325, 2012. DOI: 10.1049/CP.2012.086910.1049/CP.2012.0869. [Online]. Available: https://digital-library.theiet.org/content/conferences/10.1049/cp.2012.0869.

[111] F. Olivier, P. Aristidou, D. Ernst, and T. Van Cutsem, "Active Management of Low-Voltage Networks for Mitigating Overvoltages Due to Photovoltaic Units," *IEEE Transactions on Smart Grid*, vol. 7, no. 2, pp. 926–936, Mar. 2016, ISSN: 19493053. DOI: 10.1109/TSG.2015.2410171.

[112] Conseil international des grands reseaux electriques. Comite d'etudes C6. and Impr. Conformes), *Benchmark systems for network integration of renewable and distributed energy resources*. CIGRE, 2014, ISBN: 9782858732708.

[113] L. Thurner, A. Scheidler, F. Schafer, *et al.*, "pandapower - an Open Source Python Tool for Convenient Modeling, Analysis and Optimization of Electric Power Systems," *IEEE Transactions on Power Systems*, vol. 33, no. 6, pp. 6510–6521, 2018, ISSN: 08858950. DOI: 10.1109/TPWRS.2018.2829021.

[114] A Scheidler, L Thurner, M Kraiczy, and ..., "Automated grid planning for distribution grids with increasing PV penetration," *... Power into Power Systems ...*, 2016. [Online]. Available: https://www.uni-kassel.de/eecs/fileadmin/datas/fb16/Fachgebiete/energiemanagement/Mitarbeitende/Scheidler__Thurner__Kraiczy__Braun_-_Automated_Grid_Planning_for_Distribution_Grids_with_Increasing_PV_Penetration.pdf.

[115] L. Thurner, *Structural Optimizations in Strategic Medium Voltage Power System Planning Energy Management and Power System Operation*, M. Braun, Ed. Kassel: Kassel university press GmbH, 2018, vol. 4, p. 222, ISBN: 9783737605380. DOI: http://dx.medra.org/10.19211/KUP9783737605397. [Online]. Available: http://nbn-resolving.de/urn:nbn:de:0002-405399.

[116] *About pandapower - pandapower*. [Online]. Available: http://www.pandapower.org/about/.

[117] W. Xiao, N. Ozog, and W. G. Dunford, "Topology study of photovoltaic interface for maximum power point tracking," *IEEE Transactions on Industrial Electronics*, vol. 54, no. 3, pp. 1696–1704, Jun. 2007. DOI: 10.1109/TIE.2007.894732.

[118] W. Xiao, F. F. Edwin, G. Spagnuolo, and J. Jatskevich, "Efficient approaches for modeling and simulating photovoltaic power systems," *IEEE Journal of Photovoltaics*, vol. 3, no. 1, pp. 500–508, 2013. DOI: 10.1109/JPHOTOV.2012.2226435.

[119] S. Hashemi and J. Østergaard, "Efficient Control of Energy Storage for Increasing the PV Hosting Capacity of LV Grids," *IEEE Transactions on Smart Grid*, vol. 9, no. 3, pp. 2295–2303, 2018, ISSN: 19493053. DOI: 10.1109/TSG.2016.2609892.

[120] E. Planas, A. Gil-De-Muro, J. Andreu, I. Kortabarria, and I. Martínez De Alegría, *General aspects, hierarchical controls and droop methods in microgrids: A review*, 2013. DOI: 10.1016/j.rser.2012.09.032.

[121] J. M. Guerrero, J. C. Vásquez, and R. Teodorescu, "Hierarchical Control of Droop-Controlled DC and AC Microgrids – A General Approach Towards Standardization," no. November, 2009. DOI: 10.1109/IECON.2009.5414926.

[122] S. Khongkhachat and S. Khomfoi, "Droop control strategy of AC microgrid in islanding mode," *2015 18th International Conference on Electrical Machines and Systems, ICEMS 2015*, pp. 2093–2098, 2016. DOI: 10.1109/ICEMS.2015.7385385.

[123] Z. Shuai, S. Mo, J. Wang, Z. J. Shen, W. Tian, and Y. Feng, "Droop control method for load share and voltage regulation in high-voltage microgrids," *Journal of Modern Power Systems and Clean Energy*, vol. 4, no. 1, pp. 76–86, 2016, ISSN: 21965420. DOI: 10.1007/s40565-015-0176-1.

[124] M. C. Chandorkar, D. M. Divan, and B. Banerjee, "Control of distributed UPS systems," in *PESC Record - IEEE Annual Power Electronics Specialists Conference*, vol. 1, 1994. DOI: 10.1109/pesc.1994.349730.

[125] M. C. Chandorkar and D. M. Divan, "Decentralized operation of distributed UPS systems," in *Proceedings of the IEEE International Conference on Power Electronics, Drives & Energy Systems for Industrial Growth, PEDES*, vol. 1, 1996. DOI: 10.1109/pedes.1996.539675.

[126] J. M. Guerrero, N. Berbel, L. G. De Vicuña, J. Matas, J. Miret, and M. Castilla, "Droop control method for the parallel operation of online uninterruptible power systems using resistive output impedance," in *Conference Proceedings - IEEE Applied Power Electronics Conference and Exposition - APEC*, vol. 2006, 2006. DOI: 10.1109/apec.2006.1620772.

[127] J. M. Guerrero, L. García de Vicuña, J. Matas, M. Castilla, and J. Miret, "Output impedance design of parallel-connected UPS inverters with wireless load-sharing control," *IEEE Transactions on Industrial Electronics*, vol. 52, no. 4, 2005, ISSN: 02780046. DOI: 10.1109/TIE.2005.851634.

[128] S. J. Chiang and J. M. Chang, "Parallel control of the UPS inverters with frequency-dependent droop scheme," in *PESC Record - IEEE Annual Power Electronics Specialists Conference*, vol. 2, 2001. DOI: 10.1109/pesc.2001.954243.

[129] J. W. Kim, H. S. Choi, and B. H. Cho, "A novel droop method for converter parallel operation," *IEEE Transactions on Power Electronics*, vol. 17, no. 1, 2002, ISSN: 08858993. DOI: 10.1109/63.988666.

[130] K. De Brabandere, B. Bolsens, J. Van den Keybus, A. Woyte, J. Driesen, and R. Belmans, "A voltage and frequency droop control method for parallel inverters," *IEEE Transactions on Power Electronics*, vol. 22, no. 4, 2007, ISSN: 08858993. DOI: 10.1109/TPEL.2007.900456.

[131] Y. W. Li and C. N. Kao, "An accurate power control strategy for power-electronics-interfaced distributed generation units operating in a low-voltage multibus microgrid," *IEEE Transactions on Power Electronics*, vol. 24, no. 12, 2009, ISSN: 08858993. DOI: 10.1109/TPEL.2009.2022828.

[132] X. Lin, F. Feng, S. Duan, Y. Kang, and J. Chen, "The droop characteristic decoupling control of parallel connected UPS with no control interconnection," in *IEMDC 2003 - IEEE International Electric Machines and Drives Conference*, vol. 3, 2003. DOI: 10.1109/IEMDC.2003.1210693.

[133] H. Hanaoka, M. Nagai, and M. Yanagisawa, "Development of a Novel Parallel Redundant UPS," in *INTELEC, International Telecommunications Energy Conference (Proceedings)*, 2003.

[134] Y. Liu, J. Wang, N. Li, Y. Fu, and Y. Ji, "Enhanced load power sharing accuracy in droop-controlled DC microgrids with both mesh and radial configurations," *Energies*, vol. 8, no. 5, pp. 3591–3605, 2015, ISSN: 19961073. DOI: 10.3390/en8053591.

[135] J. Ma, X. Wang, J. Liu, and H. Gao, "An improved droop control method for voltage-source inverter parallel systems considering line impedance

differences," *Energies*, vol. 12, no. 6, 2019, ISSN: 19961073. DOI: 10.3390/en12061158.

[136] E. M. John, T. Larsson, and J. McDowall, "FACTS devices with battery-based energy storage - Extending the reach of traditional grid stability systems," *Proceedings of the IEEE Power Engineering Society Transmission and Distribution Conference*, pp. 1–6, 2012, ISSN: 21608555. DOI: 10.1109/TDC.2012.6281476.

[137] G. Tu, Y. Li, and J. Xiang, "Analysis, control and optimal placement of static synchronous compensator with/without battery energy storage," *Energies*, vol. 12, no. 24, 2019, ISSN: 19961073. DOI: 10.3390/en12244715.